2013

The Role of Nitric Oxide Dysregulation in Tumor Maintenance

Christopher Rabender
Virginia Commonwealth University

The Role of Nitric Oxide Synthase Dysregulation in Tumor Maintenance

A dissertation submitted in partial fulfillment of the requirements for the degree of Doctor of Philosophy at Virginia Commonwealth University.

by

Christopher S. Rabender

Bachelor of Science, Virginia Commonwealth University, 2003

Ross B. Mikkelsen, PhD

Professor and Vice Chair for Research, Department of Radiation Oncology

Virginia Commonwealth University

Richmond, Virginia

September 18, 2013

Acknowledgements

I would like to recognize a number of individuals who have supported me and contributed to my graduate education. First, I would like to thank my mentor, Dr. Ross Mikkelsen, for his guidance, time and willingness and patience to allow me to drive my own research. I am grateful for the education and experience obtained from his laboratory that has prepared me for my scientific career. I would also like to thank my committee member, Drs. Hamid Akbarali, Swati Deb, Dana Selley, and Vasily Yakovlev. I did not always walk away from our interactions feeling the best, but I did appreciate the conversations and the input into my research. I would like to especially thank Dr. Vasily Yakovlev who I have been working next to for 10 years. He has helped me immensely and has had to tolerate me through my ups and downs on a daily basis.

Thank you to the members of the Mikkelsen laboratory, both past and present: Scott Alexander, Dr. Rob Cardnell, Dr. Eric Howlett, and Asim Alam. I enjoyed my time in the lab with all of you and am forever grateful for all the help that was offered to me. I am especially appreciative of the way that we could interact socially and scientifically. We shared a lot of anxious moments working and a whole lot of laughs. I would like to thank Dr. Paul Graves who assisted me a great deal during my time as a laboratory technician and then early on in graduate school.

Thank you to all of my family and friends who without you this would not have been possible. I would like to thank my mom, Donna Rabender, for helping where I would allow her. I would like to thank my Aunt and Uncle, Sandra and Keith Hayashi, who helped me through some rough times growing up and always provided a positive influence. I would like to thank Mr. Kinder, Mr. Jim Crinkley and Mr. Levander Kelly who encouraged me as a young man and tried to bring out my best. Thank you to everyone who saw something in me and believed in me when I did not believe in myself. Thank you to everyone who never gave up on me. Thank you to all of my friends who encouraged me and supported me. I would like to extend a special thank you to Mrs. Jeannette Abelson-Goode for helping me to believe in myself and see that I have so much to offer. Finally, I would like to again thank Ross and his wife Linda Mikkelsen for everything they have done

Table of Contents

Page

ABBRREVIATIONS

8-Br-cGMP	8 Bromoguanosine 3’5’ cyclic monophosphate
AOM	Azoxymethane
BH2	dihydrobiopterin
BH4	tetrahydrobiopterin
cGMP	3,5 cyclic guanine mono phosphate
COX	Cyclooxygenase
CRC	Colorectal Cancer
DHFR	Dihydrofolate Reductase
DSS	Dextran Sodium Sulfate
EGFR	Epidermal Growth Factor Receptor
EMSA	Electromobility Shift Assay
eNOS	endothelial Nitric Oxide Synthase
ERK 1/2	Extracellular Regulated Kinase
FBS	Fetal Bovine Serrum
GSK3	Gylcogen Synthase Kinase 3
GSNO	S Nitrosoglutathione
GTP	Guanosine triphosphate
GTP-CHI	GTP cyclohydrolase I
HE	dihydroethidium

HE-OH	hydroxyethidium
HIF	Hypoxia Inducible Factor
HPLC	High Performance Liquid Chromatography
IBD	Inflammatory Bowel Disease
i.p.	intraperitoneal
IF	Immunofluorescence
IHC	Immunohistochemical
iNOS	inducible Nitric Oxide Synthase
IP	immunoprecipitate
IκB	Inhibitor of kappa B
JAK	Janus Kinases
LName	N-Nitro-L-Arginine Methyl Ester
L-NNA	L-NG-Nitroarginine; NG-nitro-L-Arginine
Luc	Luciferase
MAPK	Mitogen Activated Protein Kinase
MMTS	methylmethanethiosulfonate
MTX	Methotrexate
NADPH	Nicotinamide Adenine dinucleotide phosphate-oxidase
NAS	N-acetylserotonin
NFκB	Nuclear Factor kappa B
nNOS	neuronal Nitric Oxide Synthase
NO	Nitric Oxide
NOS	Nitric Oxide Synthase

NSAID	Non-Steroidal Anti-Inflammatory Drugs
O_2^-	Superoxide
ODQ	1H-[1,2,4]Oxadiazolo[4,3-a]quinoxal-in-1-one
$ONOO^-$	Peroxynitrite
PDE	Phosphodiesterase
Pen Step	Penicillin Streptomycin
PKG	cGMP dependent protein kinase
PTP	Protein Tyrosine Phosphatase
RNS	Reactive Nitrogen Species
ROS	Reactive Oxygen Species
SDS-Page	Sodium Dodecyl Sulfate Polyacrylamide Gel Electrophoresis
sGC	soluble guanylyl cyclase
SOD	Superoxide Dismutase
SP	Sepiapterin
STAT	Signal Transducer and Activator of Transcription
TGFβ	Transforming growth factor β
TLR	Toll Like Receptors
TNF	Tumor Necrosis Factor
VASP	Vasodilator-stimulated phosphoprotein
VEGF	Vascular endothelial growth factor

Abstract

THE ROLE OF NITRIC OXIDE SYNTHASE DYSREGULATION IN TUMOR MAINTENANCE

By Christopher S. Rabender, B.S.

A dissertation submitted in partial fulfillment of the requirements for the degree of Doctor of Philosophy at Virginia Commonwealth University

Virginia Commonwealth University, 2013

Advisor: Ross B. Mikkelsen, Ph.D.

Professor and Vice Chair for Research, Department of Radiation Oncology

The inflammatory nature of the tumor microenvironment provides a cytokine and chemokine rich proliferative environment. Much of the responsibility of this environment is due to the production of Reactive Oxygen Species (ROS). These studies examined

the proliferative rich tumor environment from a new perspective of Nitric Oxide Synthase (NOS) dysregulation. NOS's have the ability to become uncoupled and generate superoxide in lieu of nitric oxide (NO). A requirement of NOS for the production of NO is the cofactor tetrahydrobiopterin (BH4) and when it is missing NOS becomes uncoupled and turns into a peroxynitrite synthase. Here I demonstrate that NOS is uncoupled in tumor cells due to depleted BH4 levels. This uncoupling leads to decreased NO signaling and increased pro-inflammatory, pro-survival, signaling as a result of the increased generation of ROS/RNS from uncoupled NOS activity. I was able to recouple NOS through exogenous BH4 both *in vitro* and *in vivo,* reducing ROS/RNS and reestablishing NO signaling through cGMP protein associated kinase. Reduction of ROS/RNS resulted in the reduced activity of two major constitutively active transcription factors in breast cancer cells, NFκB and STAT3. In MCF-7 and MDA231 cells I found that increased NO-dependent PKG signaling led to tumor cell toxicity mediated by downregulation of β-catenin. Downregulation of β-catenin led to increased protein levels of p21 in MCF-7 and p27 in MDA 231cells, ultimately resulting in cell death. These results suggest that there is potential for BH4 as a therapeutic agent since exogenous dietary BH4 ameliorates chemically induced colitis, and reduced azoxymethane (AOM) induced colon and spontaneously developing mammary carcinogenesis.

Chapter 1

Background and Significance

Inflammation and cancer

The link between inflammation and cancer was proposed over a century ago when Virchow suggested that cancers tend to arise at sites of chronic inflammation [1]. It has been suggested that tumors are wounds that do not heal. Tissue injury is accompanied by enhancement of cell proliferation and inflammation, with both eventually subsiding. In the case of initiated cells, the inflammatory microenvironment rich in growth factors acts as the perfect host [2]. Several cancers have been shown to arise from sites of infection and inflammation. Colon cancer is the cancer most strongly associated with chronic inflammation. Inflammatory bowel disease, such as Crohn's and ulcerative colitis are linked to the formation of cancer. Hepatitis C in the liver is an underlying cause in many liver carcinomas. H. pylori infection has been linked to gastric cancer and HPV is a cause of nearly all cases of cervical cancer and is an important etiological factor in head and neck cancer [3, 4]

Cancer can be broken down into three stages: initiation, promotion, and progression. Sites of chronic inflammation play a role in tumor cell initiation[5]. These sites contain a variety of cells including, macrophages, activated fibroblasts, leukocytes

and other phagocytic cells, capable of inducing DNA damage in cells through the generation of Reactive Oxygen Species (ROS) and Reactive Nitrogen Species (RNS), such as peroxynitrite ($ONOO^-$), a mutagenic agent [6]. These toxic insults can occur through direct interaction with DNA or by modulation of proteins involved in DNA repair. It has been demonstrated that enhanced chromosomal instability occurs through inhibition of BRCA-1 (gene responsible for DNA repair) by RNS which reduces the ability of cells to repair DNA double stand breaks leading to error-prone repair and mutagenesis [7]. Tumor promotion and progression is stimulated in an environment rich in inflammatory cells. The tumor microenvironment is composed mainly of activated fibroblasts and infiltrating inflammatory cells. These cells secrete proteolytic enzymes, cytokines and chemokines which are mitogenic for neoplastic cells promoting not only tumor cell growth, but stimulating angiogenesis and enabling metastatic spread. Tumor associated macrophages (TAM's) comprise a large proportion of the inflammatory infiltrates in neoplastic tissues. Although these TAM's are there to kill neoplastic cells, they also produce many of the factors required for tumor proliferation [8]. Non-steroidal anti-inflammatory drugs (NSAIDs) have been shown to reduce the risk of developing and treating some cancers, including colon, lung and stomach and will be discussed more ahead [9, 10].

Nitric Oxide generation and signaling

Nitric Oxide Synthases (NOSs) are a group of calcium/calmodulin responsive enzymes (eNOS (NOS III), nNOS (NOSI), and iNOS (NOSII)) that catalyze the production of NO (and L-citrulline) through the oxidation of L-arginine [11]. The synthesis of NO occurs through NOS dimers and requires the substrate arginine along

with NADPH and molecular oxygen (O_2) as co-substrates. Tetrahydrobiopterin, FAD and FMN are required cofactors [12]. Both NOS I and NOS III are constitutively expressed in neural cells and endothelial cells respectively and are responsible for a low basal level of NO synthesis. NOS III is membrane associated and is constitutively expressed in endothelial cells and cardiac myocytes and is involved in maintaining vascular tone, platelet aggregation, angiogenesis and smooth muscle cell proliferation. NOS I is constitutively expressed in neurons and acts as a neurotransmitter in both the central and peripheral nervous system. In skeletal muscle NOS I is responsible for producing large amounts of NO during contraction of skeletal muscle [13]. NOS II is found in a variety of cell types including fibroblasts, macrophages, dendritic cells, epithelial cells, and some cancer cells. NOS II plays a role in host immunity and upon induction produces large amounts of NO, which in an inflammatory environment can react with O_2^- leading to cell toxicity [14]. A large focus of the current research focuses on NO and production of ROS and RNS that in normal cells would be toxic but in tumor cells stimulates pro-survival pathways due to dysregulation in these pathways.

NO generation and propagation of its signaling plays a major role in cardiovascular health. Regulation of blood pressure and vascular tone along with inhibition of platelet aggregation and leukocyte adhesion are the main cardioprotective effects. NO produced rapidly diffuses throughout cells and has many targets. The binding of NO to the heme moiety of soluble guanylate cyclase (sGC) is the main physiologically relevant target of NO. This binding results in the formation of 3,5-cyclic guanylate monophosphate (cGMP) from guanosine triphosphate (GTP). cGMP is the principle messenger involved in vasodilation, neurotransmission and platelet

aggregation. NO is the primary vasoregulator in mammalian cells and the generation of cGMP results in the subsequent activation of cGMP dependent protein kinase (PKG) leading to the phosphorylation of vasodilator-stimulated phosphoprotein (VASP) and the inositol 1,4,5-triphosphate receptor (IP3 receptor) resulting in vasodilation [15]. The binding of NO with sGC results in the formation of metal nitrosyls (Fe-NO) which are quite stable and occur rapidly. NO reacts with myoglobin and hemoglobin in the same manner along with cytochrome P450's [16]. DNA and lipid radicals are formed by the interaction of DNA and lipids with NO.

The cellular effects above are a direct result of the interaction of NO with a specific target, but NO can also have indirect effects. Indirect effects typically occur at higher concentrations. These effects occur when NO reacts with ROS, such as O_2^-, generated through normal cellular processes and form biologically active molecules known as RNS and will be discussed in the next section.

Under certain conditions NOS can become dysregulated and functions as a generator of O_2^- as well as NO when NOS becomes uncoupled due to limited availability of its cofactor BH4 or reduced substrate, arginine. When this occurs NOS becomes a generator of $ONOO^-$ resulting in a wide range of cell signaling implications. The uncoupling of NOS's is the focus of much of the following work and will therefore be discussed in much greater detail ahead.

Redox Signaling

ROS are chemically reactive molecules containing reactive oxygen derivatives. Historically ROS were viewed as the byproduct resulting from reactions involving

cellular oxygen metabolism and when they accumulated in cells they became toxic and had negative impacts on cells. Now, ROS are viewed and studied as relevant signaling molecules. ROS include radicals such as O_2^-, hydroxyl (•OH), and peroxyl (RO_2^-) that contain unpaired valence electrons. There are also non-radical compounds such as H_2O_2 and HOCl which have volatile O-O bonds.

Normal cellular metabolism results in the production of ROS due to the activity of the electron transport chain. Cells have their own antioxidant defense systems to combat damaging effects of ROS. Superoxide dismutases (SODs) catalyze the dismutation of superoxide into oxygen and H_2O_2. Cells then convert H_2O_2 to water by catalases, glutathione peroxidase and peroxiredoxins. Redox signaling by O_2^- is highly location specific as its lack of diffusibility and short half-life limit its range. On the other hand H_2O_2 mediated signaling is able to occur throughout the cell as it can diffuse easily and is relatively stable compared to radical species, and is generally believed to be the predominant intracellular redox signaling molecule [17, 18].

Production of ROS plays a major role in the induction of host defenses. NADPH oxidases (NOXs) are activated in the membranes of neutrophils during respiratory burst and was originally identified as a source of the microbial oxidants generated [19]. Platelets involved in wound repair release ROS to recruit additional platelets to the site of injury. As was discussed previously this process can become problematic. Overstimulation of these species is a hallmark of many diseases. NOX activity in arterial walls leads to macrophage recruitment causing them to adhere to the walls. If this inflammatory process remains unchecked it can lead to atherosclerosis.

As previously described, cancer cells exist in an inflammatory environment with high levels of ROS, which arise from TAM's, increased metabolic activity and mitochondrial malfunction. It has been demonstrated that ROS facilitates cancer cell survival through modulation of receptor tyrosine kinases (RTK's) required for cell proliferation [20]. Many of these signaling pathways manipulated by ROS are actually manipulated by RNS which has become synonymous with ROS. RNS are generated by reaction of ROS with NO. $ONOO^-$, produced from the reaction of NO with O_2^-, is a powerful oxidizer which can react with amino acids, metal containing compounds, nucleic acids and plays a major role in cellular injury. Cellular injury by $ONOO^-$ happens at levels of NO that approach SOD levels where NO outcompetes SOD for O_2^- and generates toxic amounts of $ONOO^-$. At lower concentrations of $ONOO^-$ it rearranges mostly to nitrite/nitrate and represents a cytoprotective mechanism [21].

Generation of RNS leads to altered cellular function through protein Tyr nitration and Cys S-nitrosylation or S-oxidation. Tyrosine nitration involves the incorporation of a nitro group ($-NO_2$) to the ring structure of tyrosine residues resulting in the formation of 3-nitrotyrosine. Biologically relevant protein Tyr nitration has been proposed to occur through several mechanisms: the generation of NO_2 radicals, reaction of NO with tyrosyl radicals, and through generation of $ONOO^-$ [22]. Recent work has validated the role of Tyr nitration and Cys S-nitrosylation as relevant cellular signaling mechanisms. Both processes are selective and reversible and these modifications can cause activation or inhibition of certain cellular pathways depending on the target [23, 24]. Nitration of Cytochrome C oxidase has been shown to inhibit mitochondrial respiration and our

studies demonstrate that nitration of IκBα was critical for the IR-induced activation of the transcription factor, NF-κB [25].

As previously stated, many of the RTK's and the phosphatases that regulate them are controlled by redox signaling. This occurs through reactive thiols on cysteine residues in the protein. Many of these cysteines are in the active sites of these kinases and phosphatases and their modification alters function. Cys S-nitrosylation occurs through direct interaction of NO with the thiol group of cysteines resulting in the formation of a nitrosothiol (S-N=O). Alternatively, formation of cysteine sulfenic acids in the presence of H_2O_2 has been demonstrated to regulate many of the proteins as well [26, 27]. A thorough review in the literature on redox regulation of receptors, such as the insulin receptor (IR), epidermal growth factor receptor (EGFR), and platelet-derived growth factor receptor (PDGFR) has been conducted [28]. There is much evidence that protein tyrosine phosphatases (PTPs) are regulated by this mechanism. Formation of sulfenic acid has been demonstrated at the catalytic center of PTPs through exogenous H_2O_2 or H_2O_2 generated by mitogenic cells. These PTPs are reactivated through reduction by GSH or reduced thioredoxin [29, 30]. SHP-1 and SHP-2 have been demonstrated by our laboratory and by others to be regulated by S-NO and sulfenic acid formation [31-33]. S-nitrosylation of the active site cysteine of Caspases has been shown to inhibit apoptosis in hepatocytes, endothelial cells, and tumor cells [34-36]. Figure 1.1 describes a cycle where inflammation begets inflammation and how this cycle is active in promoting tumor development

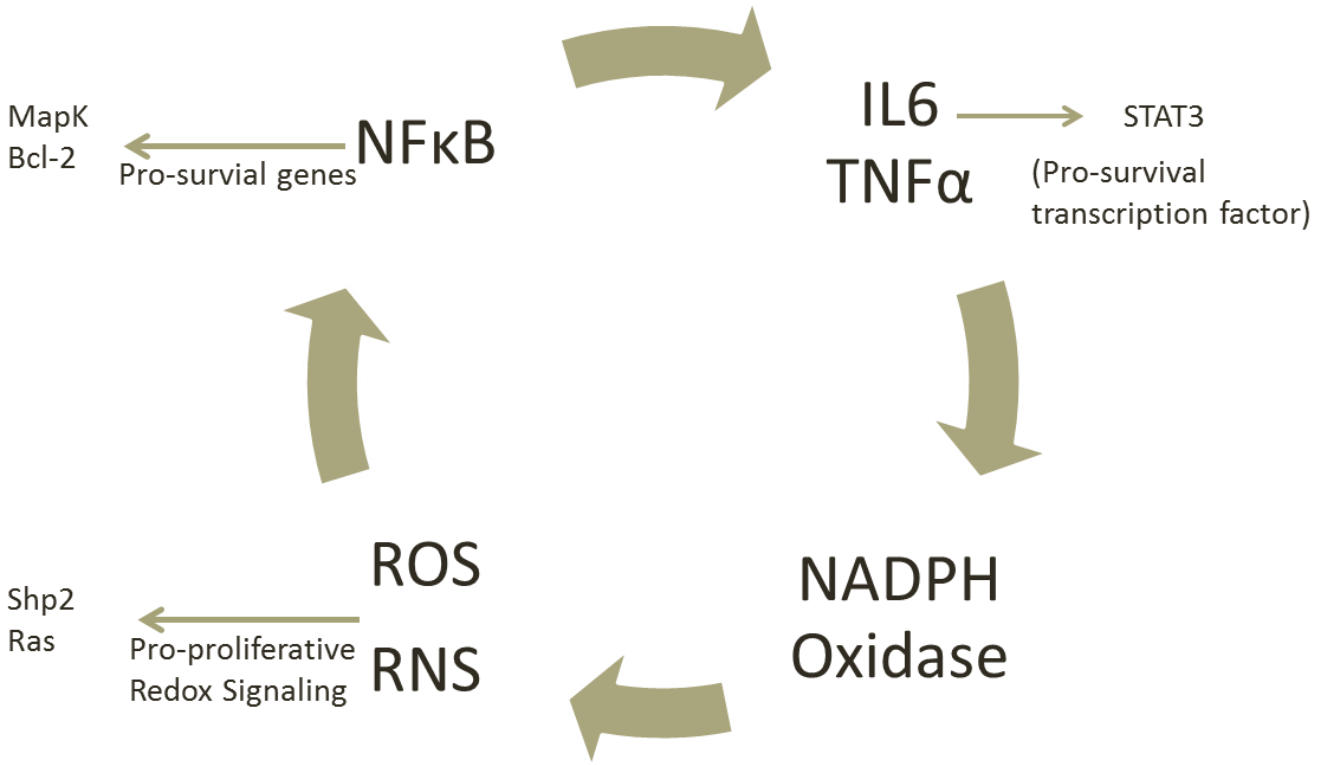

Figure 1.1 Chronic inflammation and tumor progression. Unchecked inflammation is a cycle of upregulation of pro-inflammatory/pro-survival transcription factors, NFκB, which then upregulate pro-inflammatory cytokines, leading to generation of ROS/RNS and if unchecked can keep cycling leading to a situation where inflammation begets inflammation. These activities are pro-proliferative in tumor cells whose signaling is aberrant.

Post-translational modifications on Cysteines can also be a marker for severe oxidative stress as persistent presence of H_2O_2 results in irreversible formation of sulfinic and sulfonic acids. There are many examples of redox signaling through nitration, s-nitrosylation and s-oxidation and these will be the focus of much of our work.

Nitirc Oxide as a cancer therapeutic

NO has been shown to play a role in both tumor initiation and progression. Agents that induce NO or NO donors have been used clinically in cardiovascular diseases and recently have been researched for use in treatment of malignancies. As a cancer therapeutic both anti-NO and NO-based anticancer treatments appear effective in several preclinical models. NO can promote apoptosis in some cells, whereas it inhibits apoptosis in other cells. This complexity is an indication of the importance of NO source (NO donors versus endogenous), location of that source, NO concentration, duration and cell type in understanding the cellular role of NO. Pro-growth effects of NO have been established in several tumor types. Tumor cells require a steady supply of oxygen, nutrients and growth factors which occurs through the production of NO from eNOS resulting in enhanced vascular relaxation and permeability. Tumor cells that are not receiving this steady supply of nutrients typically exists in hypoxic areas. Hypoxia exists within a tumor for a variety of reasons, including abnormal and insufficient vasculature leading to low intratumor blood flow. Hypoxia in a solid tumor leads to the stabilization and activation of hypoxia inducible factor-1 (HIF-1). Under normoxic conditions, HIF-1 is targeted for ubiquitination and subsequent proteasomal degradation, but activation during hypoxic conditions leads to the production of erythropoietin and vascular endothelial growth factor (VEGF) promoting tumor

vascularization [37]. Indeed, research has demonstrated that eNOS expression is up-regulated in solid tumor vessels resulting in enhanced angiogenesis and that this occurs through VEGF and HIF-1 expression [38, 39]. It has also been demonstrated that NO production results in the activation of COX-2 leading to increased prostaglandin PGE2 levels enhancing tumor vasculature permeability and facilitating angiogenesis [40]. This data would suggest that anti-NO treatments would be effective in containing tumor development and progression. Bevacizumab is an anti-VEGF monoclonal antibody approved for the treatment of colorectal, breast, lung and glioblastoma that works by inhibiting angiogenesis through inhibition of NO production[41]. Curcumin is another compound that has shown promise in reducing the expression of angiogenic factors by way of inhibiting the pro-inflammatory NFκB pathway resulting in decreased COX-2 and VEGF [42, 43]. By inhibiting NFκB signaling, curcumin decreases iNOS expression. Our laboratory has demonstrated that the NOS inhibitor L-NNA inhibits tumor growth alone and in combination with radiation in squamous carcinoma xenografts by decreasing tumor blood flow [44].

Effective anti-tumor possibilities have been demonstrated for NO inducers or NO donors as well, either as a single agent or in combination with other chemotherapeutics. Initial studies that lead to NO as having anti-tumor activity involved the observation that murine activated macrophages, that synthesized nitrite and nitrate, were cytotoxic to tumor cells [45]. Since that time NO donors have become a useful tool to study the anti-oncogenic effects in tumor biology. NO-NSAID's have shown promise as an anti-cancer agent. NO donating aspirin (NO-ASA) displayed marked ability as a chemopreventive in colon cancer cells both in vitro and in vivo [46, 47]. NO-ASA was shown to be an

effective releaser of NO and treatment of HCT116 and HT-29 colon cancer cells resulted in inhibition of growth [48]. The results showed that the NO released modified a number of cell signaling members key in tumor cell signaling, including NFκB, β-catenin and p53, all of which were shown to be S-nitrosylated. The S-nitrosylation of the p65 subunit of NFκB resulted in decreased DNA binding [49]. As will be discussed later, NFκB is a pro-inflammatory and pro-survival transcription factor that is constitutively active in many cancers.

The NO donating prodrug, O^2-(2,4-dintrophenyl) 1-[(4-ethoxycarbonyl)piperazin-1-yl]diazen-1-ium-1,2-diolate (JS-K) is another NO donating compound that has shown promise as an anti-oncogenic agent in leukemia, renal, prostate and brain cancer cells [50, 51]. Jurkat T-Acute Lymphoblastic Leukemia Cells treated with JS-K showed a concentration dependent decrease in proliferation through a mechanism involving the S-nitrosylation of β-catenin. β-catenin is a member of the Wnt signaling pathway and plays a role in cell proliferation through its regulation of Cyclin D1 (β-catenin will be discussed in more detail later) [52].

Tumor hypoxia has been shown to be a source of drug resistance in tumor cells, and it has been demonstrated that NO can be used as a chemosensitizing agent in combination with other chemotherapeutics or as a radiosensitizer in combination with radiotherapy. Exogenously administered NO donating drugs have been shown to reduce hypoxic conditions in tumors through an increase in tumor perfusion and that this increases the efficacy of other treatments. In a study using human prostate carcinoma (PC-3) cells, flank xenografts in athymic nude mice receiving both the NOdonor DETA/NONOate and cisplatin showed a substantial reduction in tumor volume

progression versus the drugs individually [53]. Studies in tissue culture cells, including MCF-7 and HT29-dx showed that administration of various NO donors (SNAP, SNP and GSNO) partially reversed doxorubicin resistance [54, 55]. It has also been demonstrated that SNP radiosensitized pancreatic cells by enhancing the formation of DNA strand breaks and, by an unknown mechanism, radiosensitizes glioma cells [56, 57].

There are several likely possibilities to this dual nature of NO in cancer therapeutics. Evidence has suggested that the level of NO produced plays a role in the effects seen. In general it has been shown that at low levels of NO (<100nM), cancer promoting pathways dominate, while at higher levels (>300nM), cytotoxic effects dominate [58]. Another factor that has to be taken into consideration is where in the cell the NO is being generated, and the fact that NO can have effects on the tumor cell and surrounding stromal cells resulting in different outcomes. Thus external donors of NO may have very different effects than endogenously generated NO. There are no definitive conclusions that can be made but there is enough evidence to warrant further consideration.

Scope of the dissertation

An area of research that has yet to be extended to cancer therapeutics is the coupling state of NOS in cancer cells. It has been established that tumor cells may originate and certainly thrive in inflammatory environments. Experiments were approached from a new perspective of NOS dysregulation and being able to manipulate a tumor cells response to its inflammatory environment. Studies in this dissertation

contributed to the elucidation of a novel role that NOS uncoupling plays in tumor cell proliferation and the potential mechanisms by which BH4 supplementation and NOS recoupling elicit antitumor effects. In Chapter 2, a series of experiments conducted in various tissue culture cells, flank tumor xenografts and normal tissue determined that the BH4:BH2 ratio is significantly reduced in tumor cells, resulting in increased NOS uncoupling. Several mechanisms including guanosine triphosphate cyclohydrolase I (GTP-CHI) overexpression, the rate-limiting enzyme in BH4 synthesis, and direct BH4 supplementation were used to overcome the reduced BH4:BH2 ratio and were shown to restore NOS coupling. By restoring NOS coupling we are able to manipulate the inflammatory environment in tumor cells and Chapter 3 examines the effects that increased NO produced through NOS recoupling has, with particular focus on signaling through the PKG and NFκB pathways. In Chapter 4 the therapeutic potential of BH4 supplementation was assessed by studying its effects on azoxymethane (AOM) induced colon cancer and Dextran sodium salt (DSS) induced colitis. We conclude that restoration of NOS coupling in tumor cells plays a role in cellular proliferation and is a potentially viable therapeutic tool. While we have established a role for PKG and NFκB in the antitumor effects of BH4 supplementation, experiments conducted in AOM induced colon cancers suggest that there may be other mechanisms involved.

Chapter 2

NOS is uncoupled in tumor cells in vitro and in vivo

NOS is uncoupled in inflammatory disease

Tetrahydrobiopterin is a necessary cofactor for the production of NO from NOS. Evidence has shown that NOS's can generate O_2^- under certain pathophysiological conditions and current research indicates that the level of BH4 is important in regulating the balance of O_2^- and NO produced by NOS. A BH4 molecule binds in the oxygenase domain of each NO synthase monomer resulting in two BH4 molecules in the active dimer. In conditions where BH4 levels are low, electron transfer in the active site of the enzyme becomes uncoupled from L-arginine oxidation resulting in the production of O_2^- instead of NO [59, 60]. The uncoupled enzyme therefore becomes a generator of $ONOO^-$, which is produced rapidly by the reaction of O_2^- with NO produced in the same area. The reaction of NO with O_2^- is six times faster than the reaction of O_2^- with SOD so $ONOO^-$ formation is favored. Figure 2.1 illustrates some of the cellular consequences of an uncoupled NOS. Cell signaling shifts from sGC activation and S-nitrosylation towards $ONOO^-$ and protein nitration.

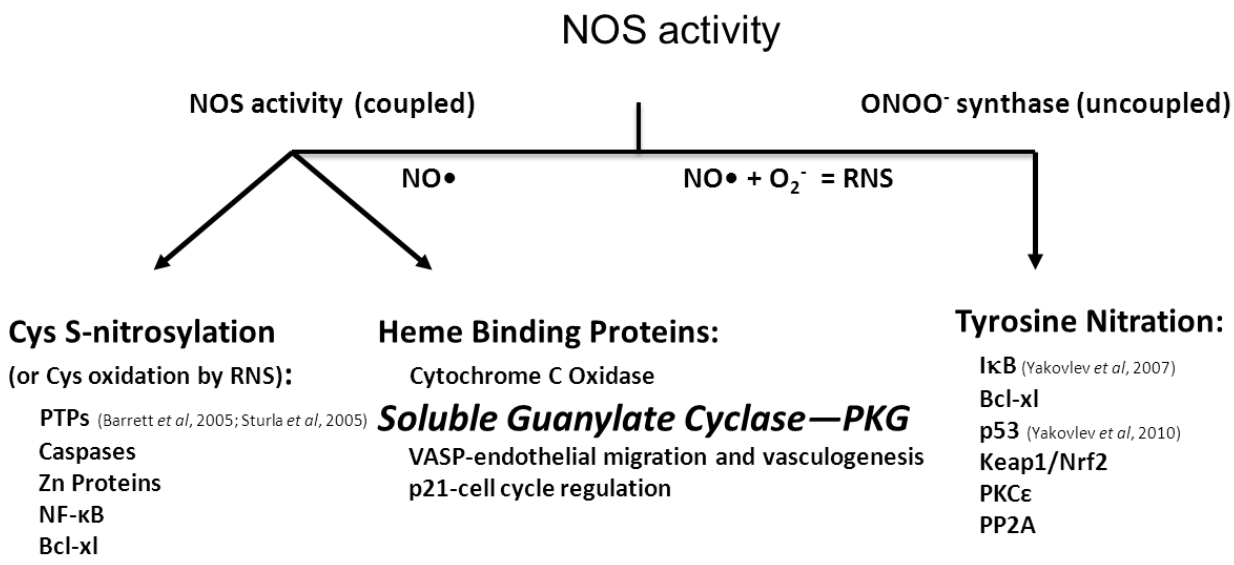

Figure 2.1 Cell signaling is influenced by the level of NOS coupling.

In inflammatory diseases such as diabetes, hypertension and atherosclerosis loss of NO production is a common feature. Until recently it was unclear how this was occurring as eNOS protein levels were still present at normal levels in the tissue endothelium. Initial studies determined that under these inflammatory conditions there is an increase in ROS such as O_2^-, H_2O_2, and hydroxyl radicals, that are able to react quickly with NO, reducing bioavailability. More recent experiments showed that under certain inflammatory conditions the cofactor BH4 is limiting and that this results in reduced NO bioavailability [61]. Low levels of BH4 can be a result of the low levels of GTPCH-I, the rate-limiting enzyme in the production of BH4, or through direct oxidation of BH4 to BH2 in the face of enhanced ROS [62, 63]. Evidence has shown that NOS's have an equal affinity for BH4 and BH2 but when BH2 is bound the NOS dimer is unstable and O_2^- production dominates [64]. In this situation eNOS is uncoupled and not only a victim of the inflammatory environment, but also becomes responsible for enhancing that environment.

Biopterin Metabolism

To further understand how BH4 is becoming limiting and how exogenous BH4 exerts its effects we must have an understanding of biopterin metabolism. BH4 was first discovered as a necessary cofactor of phenylalanine hydroxylases after it was determined that phenylketonuria, a disorder in converting phenylalanine to tyrosine, was caused by abnormal phenylalanine hydroxylase. It was discovered shortly after that BH4 and its precursors were also required for tyrosine hydroxylase and neuronal tryptophan hydroxylase, the rate limiting steps in the production of dopamine and serotonin respectively [65].

BH4 biosynthesis occurs via two mechanisms, the de novo synthesis and pterin salvage pathways. Figure 2.2 shows the reactions involved in generating BH4. On the right side is the de novo synthesis and is regulated by the availability of the rate limiting enzyme GTP-CH. The salvage pathway involves conversion of SP to 7,8BH2 by SR and subsequent conversion to BH4 by DHFR. Research has shown that BH4 does not accumulate to a great extent in tissue. Cells take up BH4 from extracellular fluid, utilize it and expel its oxidized form and the process is repeated as necessary [66].

Studies aimed at raising intracellular BH4 have shown the salvage pathway to be responsible for the accumulation of BH4 in cells. In a comparison of cellular uptake, SP was shown to elevate cellular BH4 concentration more effectively than BH4 and that the cellular increase was sensitive to methotrexate (MTX). Since MTX is an in inhibitor of dihydrofolate reductase (DHFR) it was later determined that BH4 was actually converted to BH2 before entering the cell and being converted back to BH4 by DHFR [66].

Hasegawa et al also showed that the BH4 accumulation with SP administration occurs more rapidly than with BH4 or BH2 as SP is readily transported into the cell where SR and DHFR catalyze the formation of BH4 and this BH4 is trapped in the cell due to the low permeability of the cell membrane. It was for these reasons that SP was used in the bulk of our studies examining BH4 effects [67].

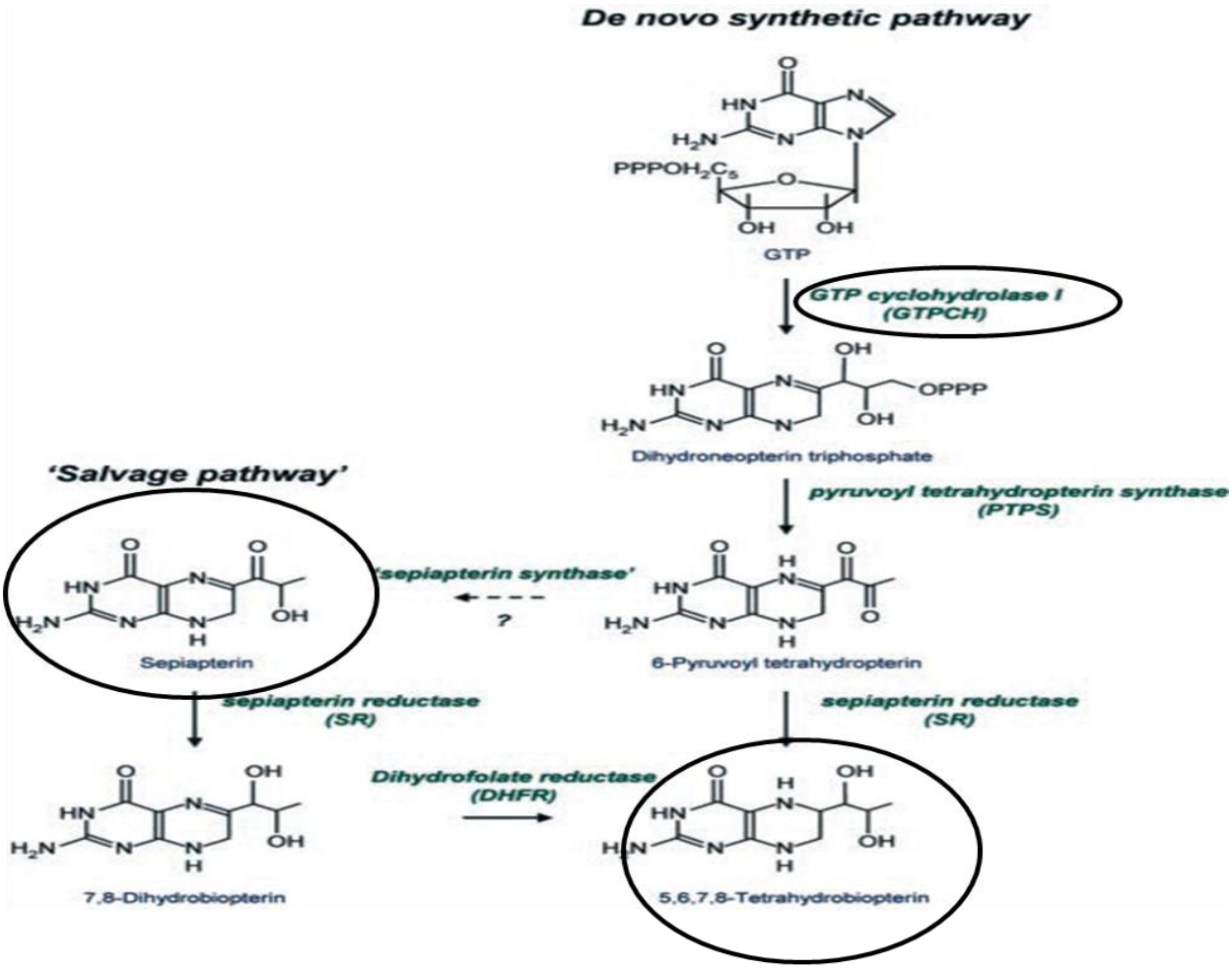

Figure 2.2. Modes of synthesis of BH4. The circled compounds are the mechanisms by which researchers have shown elevate cellular BH4 levels in tissue culture or in animals.

MATERIALS AND METHODS

Chemicals and Reagents

1.5mg, 60 day release pellets of 17β-estradiol were from Innovative Research of America (Sarasota, FL). Pterin (#11.903), L-Sepiapterin (#11.225), Biopterin (#11.203), 7,8 Dihydro-L-Biopterin (#11.206) , and (6R)-5,6,7,8-Tetrahydro-L-biopterin dihydrochloride (#11.212) were from Schircks Laboratories (Jona, Switzerland). Sodium Deoxycholate (D6750), Sodium Thiosulfate (S7026), Silver Nitrate (S1179), Potassium Carbonate (209619), 40% Formaldehyde (F8775), Ascorbic Acid (A5960), Potassium Iodide (P-4286), N_{ω} –Nitro-L-arginine (N5501), S-Nitrosoglutathione (N4148) and Iodine (20,777-2) were from Sigma Aldrich. Hydrochloric Acid (A144-212), Sodium Hydroxide (SS255-1), HPLC grade Methanol (A452-4), HPLC grade Water (W5-4), DMSO (D128), HPLC grade Acetonitrile (26827-0040), Trifluoroacetic Acid and Perchloric Acid (A229) were purchased from Fisher Scientific. Peroxynitrite (81565), Nitrotyrosine Affinity Sorbent (389549) and cGMP EIA kit (581021) were purchased from Cayman Chemical. PBS (10010-023) RPMI 1640 (11875-093), Trypsin EDTA (15400-054), Penicillin Streptomycin (15240-062), Lipofectamine (50470) and Plus Reagent (10964-021) for transfection were purchased from Invitrogen. Matrigel (356234) was purchased from BD Biosciences and dihydroethidium (D11347) was from Molecular Probes. Human GTP-CHI was generously provided by Dr. Paul Graves (VCU Department of Radiation Oncology). Nu/Nu mice were purchased from NCI.

For animal studies involving treatment with SP, stock solutions of 0.8mg/ml in H_2O were frozen at -20˚C. When ready to use they were thawed and 1ml was diluted to

40ml in animal drinking H_2O. For tissue culture studies involving SP we used tissue culture medium as the solvent to make a 1mM stock solution which could then be diluted as necessary. This solution was made fresh each time cells were to be treated.

Cell culture

Fadu and A431 cells were from ATCC (Manassas, VA) and MCF-7 and MDA231 were provided to us by Dr. David Gewirtz (VCU Department of Pharmacology and Toxicology). All cell lines were grown as monolayers in RPMI 1640 supplemented with 10% FBS and 50units/ml penicillin and streptomycin. Cells were incubated at 37˚C in 5% CO_2. Cells were passaged as necessary.

Mouse tumor xenografts

For Fadu, A431 and MDA231 cells the method was the same. Cells were trypsinized and counted. $1x10^6$ cells in 50µl PBS was injected into each flank of 8 week old Nu^-/ Nu^- mice from NCI. The mice for Fadu and A431 were male and we used female mice for the two breast tumor cell lines, MDA231 and MCF-7. The latency period for the different cell types varied from two weeks for Fadu and A431 to up to two months for MDA. To develop tumor xenografts for MCF-7 cells we had to use a different protocol. MCF-7 cells are estrogen responsive and in order for these cells to develop into a tumor the animal had to be implanted with an estrogen pellet the day before cells were to be injected. To do this we would make a small incision on the back of the mouse between the shoulder blades and insert a small 1.5mg 60 day release estrogen pellet under the skin before closing the incision and sealing it with super glue. The following day we would trypsinize and count cells. $2.5x10^6$ cells in a 50µl mixture of

PBS and matrigel were then injected into the flank of 8 week old female Nu^-/ Nu^- mice. The latency period for tumor development was similar to MDA.

MMTV neu mice that developed spontaneous mammary tumors were provided by Dr. Paul Fisher (VCU Dept. of Human and Molecular Genetics).

BH4 and BH2 measurements

A431, MCF-7 and MDA231 cells were plated at a density of $2x10^6$ cells/100mm dish and were allowed to adhere overnight. The next day cells would receive the indicated treatment and would then be placed back in the incubator for the duration of treatment. When the cells were ready to be harvested the dishes were washed in ice cold 1x PBS three times. After the final wash all PBS was removed and the cells were then lysed in 1ml of ice cold 0.1N HCl and placed in a 1.5ml microcentrifuge tube. The samples would sit on ice for 20min and then would be centrifuged for 20min at 13,200 RPM. The samples were divided into aliquots and placed either into a -80°C freezer or analyzed immediately for BH4 and BH2 content.

To analyze biopterin levels in tumors or other mouse tissue animals were euthanized with 20µl i.p. injection of euthasol. Once the animal was sacrificed we harvested the desired tissue and snap froze it in liquid nitrogen. The tissue was either placed in the -80°C freezer or immediately homogenized in 10 volumes of 0.1N HCl with a pestle and mortar kept on ice. The resulting tissue homogenate was centrifuged for 20min at max speed and the supernatant would be stored in aliquots at -80°C.

The protocol for HPLC analysis was adapted from Woolfe et al (1983). Three solutions were needed in order to perform the acid/alkaline oxidation: 2%I_2/3%KI in

0.1N HCl, 2%I_2/3%KI in 0.2N NaOH, and 2.5% Ascorbate in 0.4N $HClO_4^-$. 100µl of sample was incubated with 62.5µl of the HCl solution in one tube while another 100µl of sample was incubated with the NaOH solution for 1h at room temperature in the dark. After 1h, .5vol of the ascorbate solution was added to each tube and the samples centrifuged at 12,000 RPM for 10min. 50µl of the resulting supernatant from each sample was separated by HPLC on a Whatman RTF partisphere column using 5% methanol as the mobile phase at a flow rate of 1.0ml/min and fluorescent detection at 350/450nm.

To determine the BH4:BH2 ratio we compared the acidic and alkaline chromatograms for each sample. Under acidic conditions both BH4 and BH2 were converted to biopterin and eluted in one peak, while under alkaline conditions BH4 was converted to pterin and now eluted in a different peak. Comparing the areas under the curve we were then able to obtain the ratio of the two.

Determining cellular cGMP content

To make these measurements we took advantage of the fact that samples were to be harvested in 0.1N HCl, which allowed us to use some of the supernatant aliquots from the samples for BH4:BH2 analysis. We purchased a cGMP EIA kit from Cayman Chemical and followed the directions as described in the manual. The samples were not acetylated.

Superoxide quantification

We can measure O_2^- production in cells by measuring the interaction of O_2^- with exogenous dihydroethidium to form 2-hydroxyethidium. A protocol was adapted from

Zielonka et al to determine cellular concentrations of O_2^- in tissue culture [68]. $1x10^6$ cells were plated in 60mm dishes and placed in the incubator overnight to allow cells to adhere. Dishes were treated with SP according to the desired concentration and duration of incubation. 30 min prior to harvesting the cells, culture medium containing 10µM HE (5µl of 20mM HE in DMSO per 10ml of medium) was added to each dish. At this point three 1.5ml tubes for each sample were prepared: one empty tube to store an aliquot for protein determination, the second tube has 100µl of 0.2M $HClO_4$ in methanol and the third tube has 100µl of 1M phosphate buffer pH 2.6. To stop the reaction, medium was removed and the cells were washed with ice-cold 1x PBS three times. In the final wash 1ml of ice cold PBS was added to each dish and the cells scraped into a 1.5ml eppendorf tube. The cells were concentrated by centrifuging for 5 min at 1,000 RPM at 4˚C. The cells were lysed by adding 150µl of ice-cold PBS containing 0.1% of Triton X-100 to the cell pellet and trituration by drawing the mixture in and out of an insulin syringe ten times. The resulting lysate was clarified by centrifugation: 20 min x 12,000 RPM at 4˚C. To isolate the product, 2-hydroxyethidium, 100µl of the lysate supernatant was transferred into the tube containing 0.2M $HClO_4$ in methanol and vortexed for 10 seconds. The tubes were placed on ice for 1.5h to allow protein precipitation. Following this incubation, the protein precipitate was removed by centrifugation: 45 min x 13,200 RPM at 4˚C. 100µl of the resulting supernatant was added to the tube containing 1M phosphate buffer pH 2.6 and vortexed for 5 seconds. After a second centrifugation, 25 min x 13,200 at 4˚C, the supernatants were loaded into HPLC vials and kept on ice until placed into the HPLC.

Once samples were in the vials they were placed in the sample tray of the HPLC which was preset to 4˚C. We used a Whatman RTF partisphere C_{18} column to separate the samples. The column was equilibrated with 10% CH_3CN in water containing 0.1% TFA for 15 min before samples were injected. 50µl of sample was loaded onto the column and was separated by gradient elution using water containing 0.1% TFA (mobile phase A) and 99.9% CH_3CN with 0.1% TFA (mobile phase B) at a flow rate of 0.5ml/min. Table 1 is taken from Zielonka et al. and shows the gradient used for fluorescence detection of 2-hydroxyethidium at 510nm (excitation) and 595nm (emission). To determine sample concentration compare to standard curve produced from by injecting serially diluted standards.

Analysis of nitrated and S-nitrosylated of proteins

Cells were plated at a density of $2x10^6$/150mm dish. Cells were allowed to grow to 70% confluent and were then treated with SP for 6 hours or were left untreated. For nitration, dishes were washed 3x with ice cold 1X PBS and then cells were lysed in 1.0ml of ice cold buffer containing 50mM Tris pH 7.4, 150mM NaCl, and 1% NP-40. Lysates were cleared by centrifugation at 13,200 RPM for 20 min at 4˚C. As a positive control lysates were treated with 6µl of 150mM $ONOO^-$ by adding a droplet to the cap of the microcentrifuge tube and vortexing for 10s (not added directly to the tube due to the short half-life). Samples were then immunoprecipitated overnight at 4˚C with 10µl of Nitrotyrosine affinity sorbent. The samples were washed the following day twice with ice cold lysis buffer and once with ice cold 1X PBS. After removal of as much PBS as possible, 40µl of Llaemmli sample buffer was added and the samples were boiled for

5min. Samples were loaded and the proteins separated on a 10% SDS-Page gel. Proteins were visualized by silver stain.

To analyze cells for protein s-nitrosylation we plated and treated the cells in the same manner as for nitration. When the time came to lyse the cells, they were lysed in the dark in 450µl of RIPA buffer (50mM Hepes, 150mM NaCl, 1% Trition X-100, 0.1% SDS and 1% Sodium Deoxycholate). As a positive control one of the lysates was treated with GSNO. The biotin switch method was used for the detection of s-nitrosylated proteins. The beads were washed three times in wash buffer and the beads were boiled for 5min in laemmli sample buffer. Samples were then loaded and the proteins separated on a 10% SDS-Page gel. Proteins were visualized by silver stain.

Biotin Switch Method

This method was used to determine Cys s-nitrosylation. For total cellular s-nitrosylation, cells were grown to 80% confluent and then harvested. For analysis of a specific protein it was typically overexpressed. In MCF-7 cells, $1.2x10^6$ cells were plated and allowed to adhere overnight. The plasmid DNA encoding the protein(s) of interest was introduced the following day using Lipofectamine/Plus transfection reagents. 48 hours after transfection cells were treated and cell lysates were prepared at the designated time points in RIPA buffer. The resulting cell lysate was centrifuged for 5 min and the supernatant was mixed with blocking buffer (250mM Hepes pH 7.7, 1mM EDTA, 0.1mM neocuproine, 2.5% SDS, 20mM MMTS) to block all free sulfhydryls. The sample was then mixed with acetone to precipitate the proteins to

remove MMTS. The preceding steps are done under conditions of low light as to not create additional reactive Cys from exposure to UV. The pellet is resuspended in Hens buffer (25mM Hepes 7.7, 0.1 mM EDTA, 10µM neocuproine, 1% SDS) to which is added biotin-HPDP and ascorbate to a final concentration of 1mM. Samples incubate for 1 hour at room temperature. Proteins are again precipitated with acetone to remove excess biotin. Proteins are resuspended in neutralization buffer (20mM Hepes, 100 mM NaCl, 1mM EDTA, 0.5% Triton X-100) and the biotin labeled proteins are purified on streptavidin-agarose beads overnight, washed the following day with wash buffer (neutralization buffer with 600mM NaCl) and then eluted in sample buffer containing β-mercaptoethanol. The samples were then resolved by SDS-Page. Western blots are probed with streptavidin for total s-nitrosylation or with antibodies for specific proteins.

Silver Stain Protocol

The gel is fixed 10% methanol and 10% acetic acid for 30min and subsequently washed four times in water, at least 5min per wash. Gels are incubated in sodium thiosulfate (1 pellet per 500ml of water) for 90 seconds exactly saving 20ml of this solution for use later. The gelis then quickly washed three times three with water (fill dish then dump, repeat). A silver nitrate solution (0.9g of silver nitrate in 500ml of water) is then added and the gel is stained for 10min. The gel should turn slightly yellow. After 10min, the gel is washed three times quickly with water. Developer solution (10g of potassium carbonate, 20ml of sodium thiosulfate from above, and 250µl of 40% formaldehyde in 500ml of water) is added and staining of the gel is followed. When the staining reaches a satisfactory level, the reaction is stopped by the addition of

destain (10% methanol and 5% acetic acid) and the gel is washed two to three times in water.

RESULTS

NOS is uncoupled in tumor cells

The consequences of NOS dysregulation have been discussed thoroughly in the previous sections. Here we examined whether or not tumor cells have an uncoupled NOS in tissue culture cells and mouse tumor models. We were able to do this through examining the hallmarks of NOS uncoupling: decreased BH4:BH2 compared to normal tissue and increased O_2^- in lieu of NO leading to increased Tyr nitration. Preliminary experiments focused on the ability of $ONOO^-$ to oxidize BH4 to BH2 as this is a mechanism by which cellular BH4 levels are manipulated during inflammation. To accomplish this we harvested the kidney, heart and colon of several C57BL/6 mice and treated a portion of the resulting organ homogenate with 10µl of 140µM $ONOO^-$ (final concentration 1.4 µM). The amount of BH4 and BH2 in the tissues was measured by acidic/alkaline oxidation to either biopterin or pterin using HPLC as described. Figure 2.3 shows a decrease in the BH4:BH2 ratio from 9.1:1 in normal tissue to 1.7:1 in tissue treated with $ONOO^-$ (only the data from the colon are shown but the other tissues were similar). This data demonstrates that a major product of an inflammatory environment, $ONOO^-$, is able to oxidize BH4 to BH2, which is consistent with our model of BH4 in the tumor microenvironment, and that we are able to measure this change

To determine the extent of NOS uncoupling in tumor cells we compared the BH4:BH2 ratios of normal tissues to several cell lines of interest, both *in vitro* and

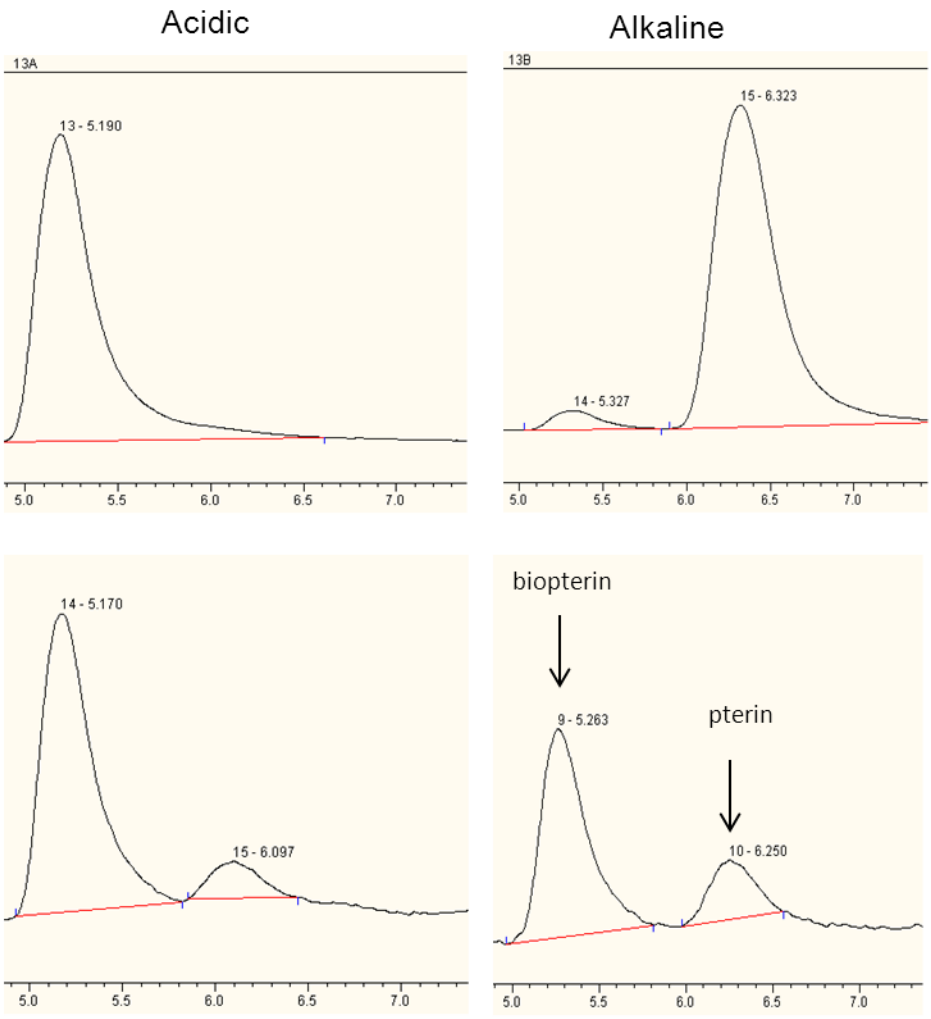

Figure 2.3 BH4/BH2 measurements in colon by acidic alkaline oxidation. Top panes are control colons while the bottom panes are control colons treated with $ONOO^-$. Under acidic conditions BH4 and BH2 are converted to biopterin while under alkaline conditions BH2 remains biopterin while BH4 is coverted to pterin. The ratio of BH4:BH2 changes from 9.1:1 to 1.7:1 after treatment with $ONOO^-$.

in vivo. Tumor cells were evaluated in several different ways to assess BH4:BH2. We grew them as a monolayer in tissue culture dishes, as flank xenografts in mice, or we analyzed spontaneously derived tumors. Figure 2.4 shows that in each tumor cell line we tested, whether in tissue culture or as a tumor, the BH4:BH2 ratio was significantly lower than in normal tissue, with MCF-7 cells being the most aberrant. With ratios in some of these cell lines significantly below 1, the main activity of NOS in these cells is as a peroxynitrite synthase. If we look again at Figure 2.2, we see several approaches (the circled items) that have the potential to elevate cellular BH4 and we wanted to determine whether these compounds could be effective in elevating BH4:BH2 in the tumor cell lines we were investigating. We can take the genetic approach and overexpress GTP-CHI, the rate-limiting enzyme in BH4 biosynthesis. We can use SP exogenously, which is taken up by cells and converted to BH4 through SR and DHFR, or we can give direct administration of BH4. Figure 2.4 shows the effect of adding SP or BH4 to the drinking water of mice or treating tissue culture cells with SP, BH4 or overexpressing GTP-CHI. Animals were treated for 24 hours and tissue culture cells were incubated for 6 hours. The BH4:BH2 ratio is significantly increased with each compound with SP having the greatest effect in both tissue culture and mice. In our studies as well as by others it has been shown that the most effective route for enhancing the BH4:BH2 ratio is through exogenous SP, which is why it is the compound of choice in the bulk of our studies [66].

SP enhances NOS coupling in tumor cells

Normal Tissue	BH4:BH2	In vitro	BH4:BH2	BH4:BH2 +50μMSP	In vivo	BH4:BH2	BH4:BH2 +1mg/kg/ml
Colon	9.1 ±0.6	**A431**	0.30±0.5	2.06±0.6	**Fadu**	0.83±0.17	2.6±0.34
Lung	11.1±2.4	**MCF-7**	0.17±0.085	10.1±0.4	**MCF-7**	1.05±0.15	7.9±0.2
Liver	8.3±0.8	**MDA231**	0.98±0.1	5.8±0.2	**MDA231**	1.4±0.28	6.4±0.39
Kidney	13.4±1.2	**MCF-7 +GTPCH**	3.6±0.19		**MMTV neu**	1.2±0.47	3.9±0.24

Figure 2.4. BH4:BH2 ratio. BH4:BH2 ratio was measured by HPLC in normal tissue from Nu^{-}/Nu^{-} mice, various tissue culture cells and flank tumor xenografts from the indicated cell. In all cases the ratio of BH4:BH2 is lower in tumor tissue and we are able to elevate it with exogenous agents that generate BH4 in cells. N=3 and data is reported as the mean +/- SEM.

We determined that NOS is uncoupled in a variety of tumor cells and that we are able to manipulate the BH4:BH2 ratio in these cells. To assess whether or not enhancing BH4:BH2 had an actual effect on the product from the oxidation of L-Arginine we monitored two key cellular components: cGMP formation and O_2^- generation. cGMP is formed from the interaction of NO with its main target in cells, sGC. In our experiments we used cGMP formation as an indirect method for measuring NO generation. To assess O_2^- generation we monitored the oxidation of diyhdroethidium to either hydroxy or dihydroxyethidium. The product formed here has been shown to be due to the interaction of dihydroethidium with O_2^- as it was not formed by reaction with other oxidants (H_2O_2 or $ONOO^-$) [66]. To gain an understanding of the time required for SP to recouple NOS in tumor cells, MCF-7 cells were treated with 20μM SP and harvested at various time points post treatment followed by determination of the BH4:BH2: ratio (Figure 2.5). What we found was that the ratio began to elevate around 3 hours with a maximum level achieved at 6hrs and maintained until roughly 18hrs. We had now determined the window in which all future experiments would be conducted, as maximum BH4:BH2 ratio directly correlates to maximum NOS coupling.

Experiments that followed determined if during this time period there was enhanced cGMP formation. Earlier studies used a concentration of SP from the literature that was shown to be effective in mediating aberrant NO production from NOS, but we decided to examine cGMP formation over a range of concentrations. In Figure 2.6 we show that 6 hours after treatment cGMP increased in a concentration dependent manner in both MCF-7 and MDA 231 cells (only the data for MCF-7 cells is shown as

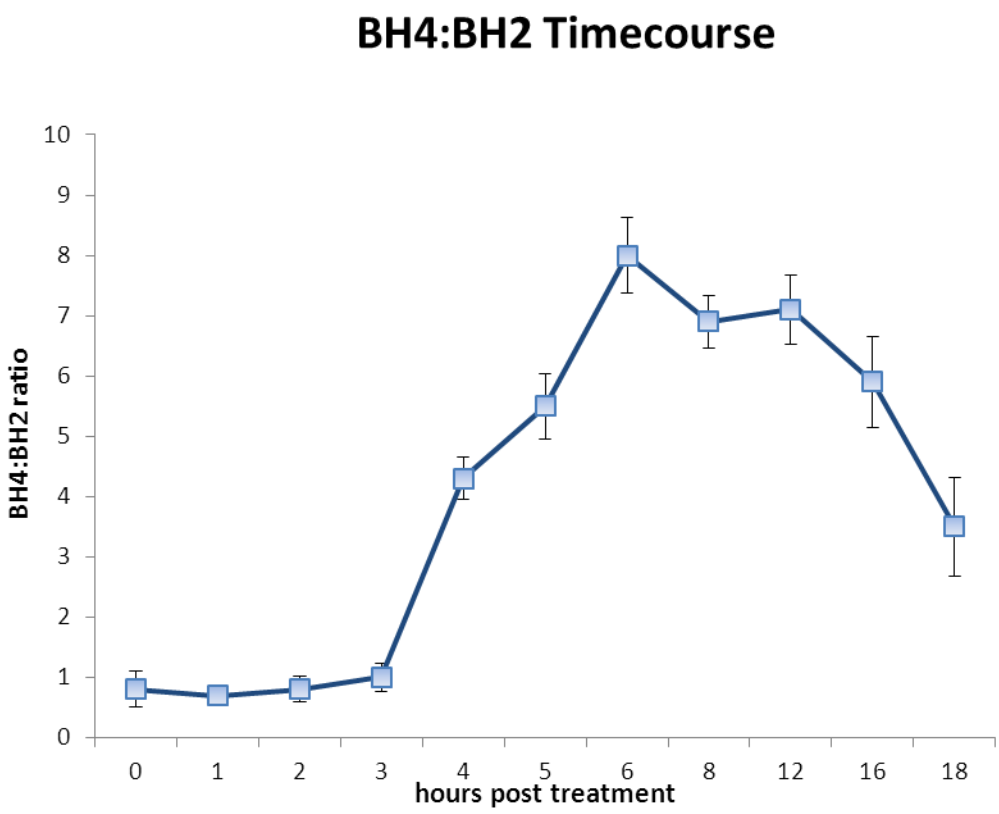

Figure 2.5 BH4:BH2 ratio in MCF-7 cells. The ratio of BH4:BH2 was measured at various points post treatment with 20μM SP. Results are reported as the mean ± SEM. N=3

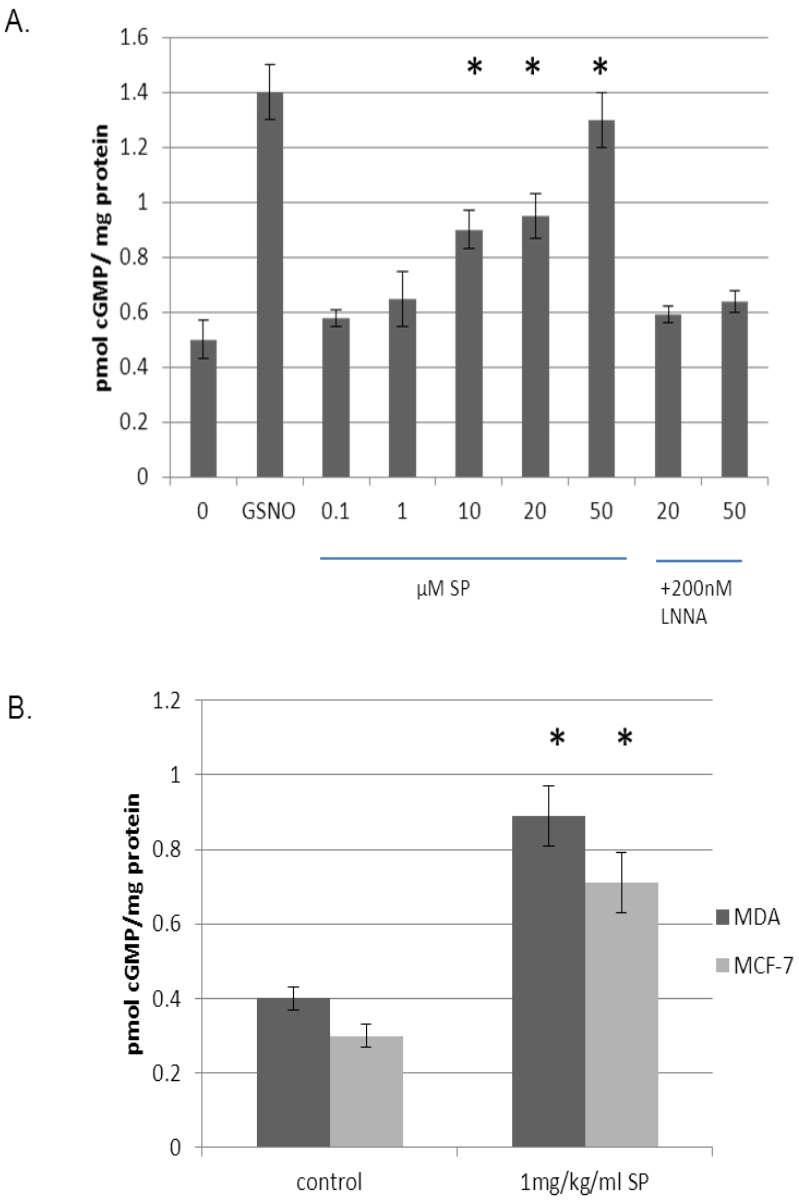

Figure 2.6 cGMP formation. (A) cGMP formation, an indirect measurement of NO production, was assayed by ELISA and showed increased cGMP formation in a dose dependent manner in tissue culture cells. Treatment of MCF-7 cells with 200nM L-NNA abrogated the effect. N=3, *p<0.05 by one-way anova with dunnett's post hoc. (B) Nu/Nu mice with flank tumor xenografts showed a significant increase in cGMP formation after 1mg/kg of SP in the drinking water. Data reported as mean +/- SEM. * p<0.01 by unpaired student t-test, N=4.

the results were extremely similar). We also measured the effect of SP on cGMP in flank tumor xenografts of these cells and found that after 48 hours of SP in the drinking water there was a significant increase in cGMP. We decided to wait for 48 hours to harvest the flank tumor due to the animals receiving SP via drinking water to make sure that they had time to ingest it and reach a steady level (Figure 2.6). We pretreated cells with the non-selective NOS inhibitor, LNNA (200nM), to confirm the role of NOS in the changes of cGMP with exogenous SP. The rationale is that by enhancing NOS coupling, NO production will increase and since sGC is one of the main interactions with NO, the level of cGMP should increase. Pretreatment of cells resulted in nearly complete reversal of the effects SP had, confirming that SP acts by enhancing the BH4:BH2 ratio thereby stimulating NOS coupling and NO generation.

To assess cellular O_2^- production from NOS we used the same doses and time point (6hr) to harvest cells. Figure 2.7 shows a dose dependent decrease in O_2^- from NOS in MCF7 and MDA231 cells. Since NOS uncoupling is generating some of this O_2^- the NOS inhibitor L-NNA treatment should block the portion that is being generated by NOS and we do see O_2^- blocked in the presence of 200nM L-NNA.

SP changes the balance of signaling from nitration to s-nitrosylation

Now that we were seeing more NOS coupling we wanted to determine if there was an overall decrease in total cellular Tyr nitration and if that led to a concomitant increase in Cys s-nitrosylation. Figure 2.8 shows that treating cells with 20μM SP for 6h

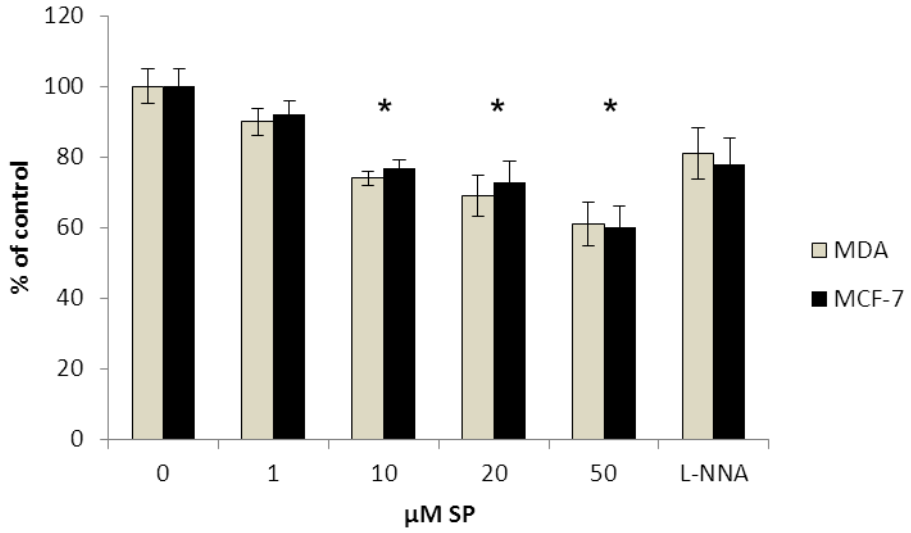

Figure 2.7 Superoxide measurements in MCF-7 and MDA231. Superoxide production in cells was shown to decrease with increasing doses of SP. Cells were incubated with 10 µM HE for 30min and then HE-OH formation was measured by HPLC. Plotted as mean ± SEM. N=3, *p<0.05 by one-way anova with dunnett's post hoc.

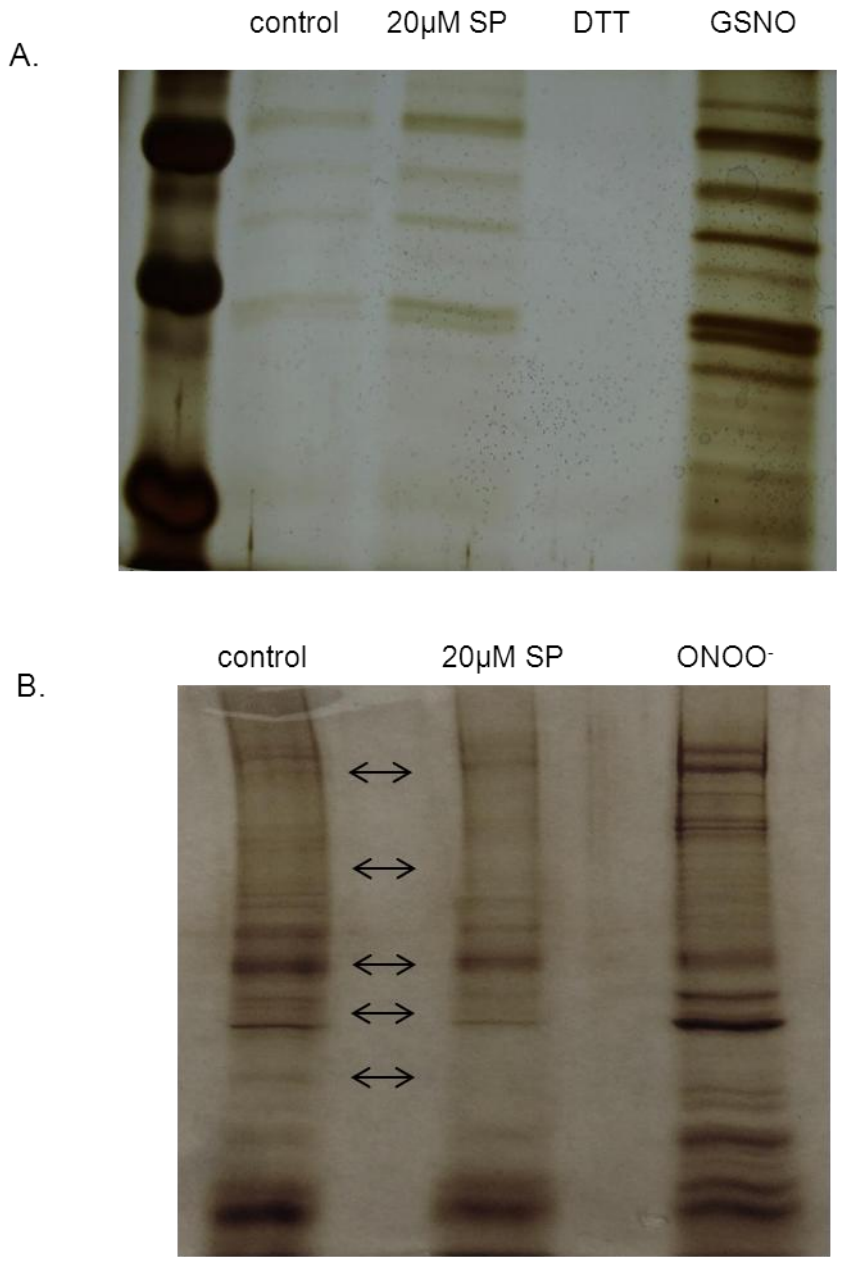

Figure 2.8. Nitration and S-nitrosylation in tumor cells. (A) s-nitrosylation in total cell lysate determined by the biotin switch method . (B) Total protein nitration

results in decreased overall protein Tyr nitration and that 20μM SP enhanced formation of S-nitrosothiols in a variety of proteins. Without a specific target in mind we decided to examine overall nitration and S-nitrosylation by purifying the proteins based on the post translational modification and then separating them on a gel and silver staining the gel. This only showed us modifications on very abundant proteins, but was sufficient to establish the trend of moving from nitration to S-nitrosylation.

DISCUSSION

In view of the importance of BH4 in NOS function and its known sensitivity to oxidative stress and NOS's role in redox signaling we hypothesized that: (i) BH4 depletion in tumor cells contributes to promotion of the inflammatory tumor micro environment through NOS uncoupling and, (ii) that exogenous BH4 would be effective in reducing this. Due to BH4 being a requirement for NOS production of NO and that BH2 has an equal affinity for NOS, we examined the BH4:BH2 ratio in tumor cells and found that they were reduced when compared to normal tissues resulting in O_2^- production from NOS in lieu of NO. Exogenous BH4 raised intracellular BH4:BH2 ratios increasing NOS coupling as measured by increased cGMP formation and decreased O_2^- generation. Figure 2.9 summarizes what we have shown experimentally.

A fully coupled NOS is the result of a stable homodimer with BH4 as the cofactor. NOS dimers that are formed with BH4 have been demonstrated to be stable in 2% SDS at temperatures below 30°C while NOS dimers without BH4 as the cofactor are not [69]. The extent to which exogenous SP stabilizes the NOS dimer could be measured and

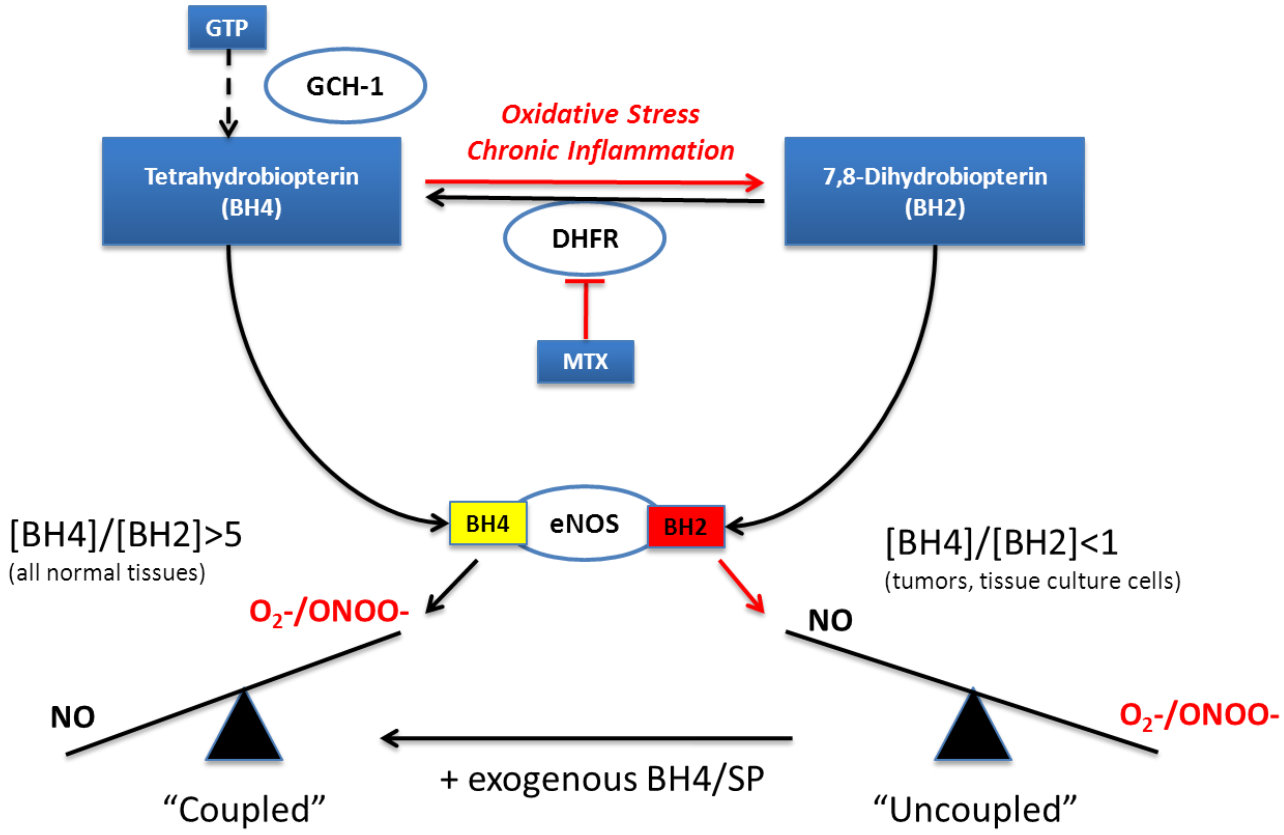

Figure 2.9 NOS uncoupling in tumor cells

would provide additional evidence of fully recoupling NOS activity, but we feel the evidence clearly demonstrates NOS uncoupling and manipulation of uncoupling by SP.

The extent to which O_2^- decreased in the presence of SP was surprising and may be explained by free radical scavenging by NO. NO produced from the coupled enzyme can scavenge O_2^- from mitochondrial respiration or NOX activity to form $ONOO^-$. The formation of hydroxyethidium is a product specific to oxidation by O_2^- and not $ONOO^-$ so NO scavenging would reduce the amount of O_2^- detected. Free radical scavenging by NO may also explain the difference between O_2^- produced in the presence of SP and after treatment with L-NNA. We would expect NOS inhibition to limit O_2^- production to the extent that SP did as we are eliminating the same sources of O_2^-. We therefore attribute some of the reduction of O_2^- in the presence of SP to scavenging by the increased NO production from a coupled NOS reacting with cellular O_2^-.

We demonstrated a trend that overall cellular nitration goes down and S-nitrosylation goes up, but that may not always be the case. By enhancing NOS coupling we increase the amount of NO generated in cells, increasing the diffusion distance of NO. It is possible that individual proteins may be nitrated to a greater extent, especially those proteins associated with mitochondria and NADPH oxidases.

Potential limitations to these experiments are that the tumor xenografts are generated in immune deficient mice. Given that the innate immune system contributes to tumor progression through mechanisms discussed earlier and that response is partially mediated by NOS there is a possibility that the extent of BH4 depletion may have been greater as there would have been an active immune response. This would

lead to a higher degree of NOS uncoupling in the immunocompetent animals. There is also a key piece of information that is undetermined by these studies. Are the effects of exogenous BH4 in animals due to effects on the surrounding stromal cells reducing the inflammatory environment, on the tumor cells themselves or both?

It was initially demonstrated that eNOS effects on tumorigenesis were due to activity in endothelial cells, but as discussed in the introduction, eNOS activity in tumor cells plays a vital role in maintaining tumor through redox activation of key signaling proteins [70]. Lim et al described how tumor maintenance is mediated by eNOS and demonstrated that S-nitrosylation of Ras proteins was critical for PI3K-AKT regulation of tumor cell proliferation [71]. When they inhibited eNOS they blocked tumor initiation and maintenance. Their experiments did not determine the level of total S-nitrosylation of eNOS in their cells and given what we know about this post-translational modification it is highly unlikely that just S-nitrosylation is responsible for the oncogenic effects they demonstrated. We discussed earlier that in an inflammatory environment proteins can be modified by nitration, S-nitrosylation and S-oxidation. Given that NOS is intimately involved in redox signaling, we believe that the contribution of an uncoupled NOS contributes greatly to what they have shown. Our findings underscore the importance that a decreased BH4:BH2 ratio may have in tumor cells. We are able to manipulate how tumor cells respond to an inflammatory insult through exogenous BH4 to maintain NOS coupling. These findings also point to a need for further understanding of the role of NOS uncoupling in the redox state in tumor cells.

Chapter 3:

Modulation of Critical Signaling Pathways in Breast Cancer Cells

INTRODUCTION

In chapter 2 we clearly demonstrated that NOS is uncoupled in tumor cells and that the extent of uncoupling can be manipulated by exogenous compounds. The focus of this chapter is the investigation of the consequences of NOS recoupling and the signaling pathways manipulated through this process, with particular focus on several of the constitutively active pathways that play a role in breast cancer cells: β-catenin, NFκB and STAT3. That we altered cellular ROS/RNS, the expectation is that signaling through redox sensitive proteins will be altered. Both NFκB and STAT3 are redox regulated. The role of PKG is thoroughly investigated as increasing NO results in increased cGMP which should lead to an active PKG. Figure 3.1 is a schematic of the pathways being investigated and how we believed the recoupling of NOS would affect them.

cGMP Dependent Protein Kinases and Their Role in Cancer

As discussed in the introduction the main target for NO in cells and the target with the highest affinity is the heme binding domain of sGC. This stimulates a rapid

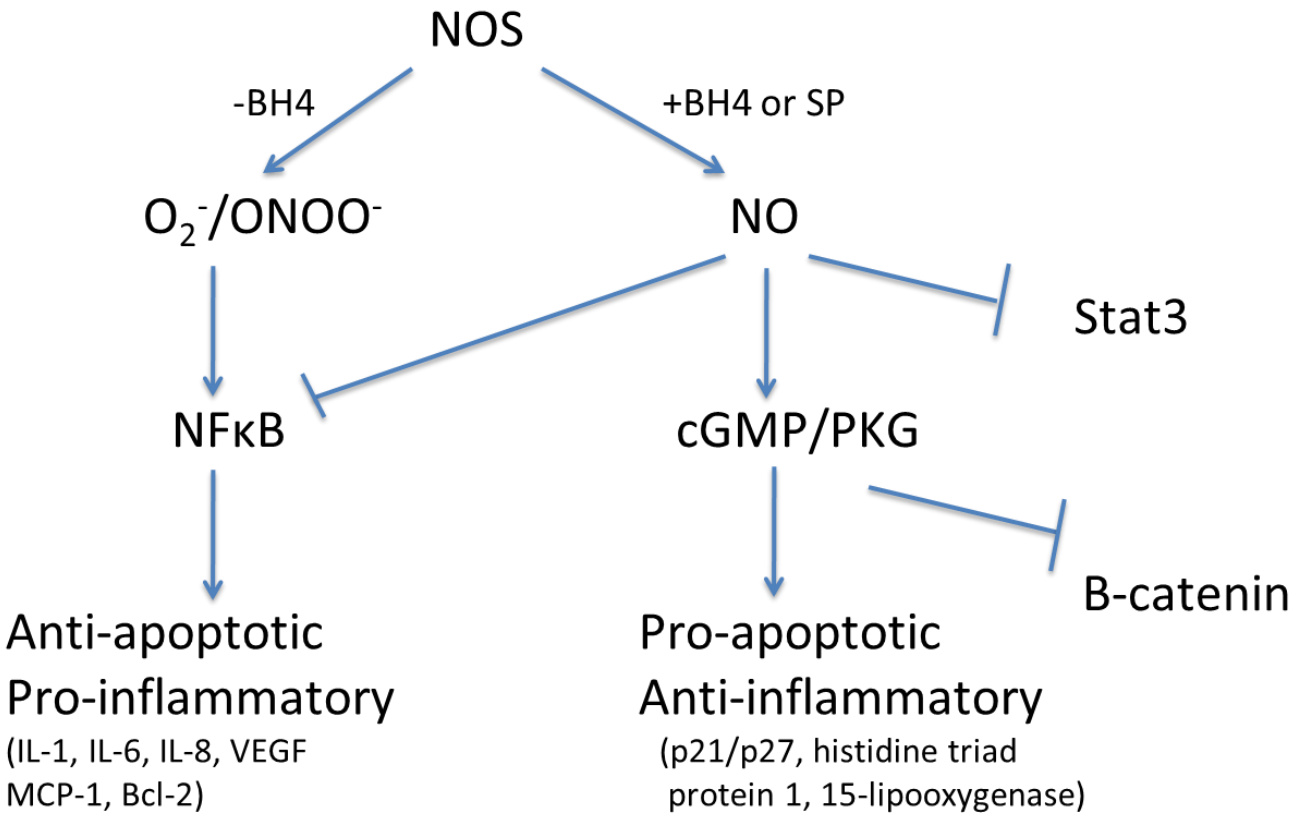

Figure 3.1 BH4:BH2 ratio determines signaling outcome. Uncoupled NOS leads to pro-survival signaling and upon NOS recoupling we are able to manipulate many of these pathways in an anti-proliferative fashion.

increase in cGMP and activation of cGMP dependent PKG, a serine/threonine kinase. There are two types of PKG encoded by different genes, types I and II. Type I can be alternatively spliced to form PKGIα and PKGIβ that differ only in the amino-terminal 89 and 104 residues and their affinity for cGMP (α is ten times more sensitive to cGMP than β). PKGI is usually associated with the cytoplasm whereas PKGII, with a myristylated N terminus, is generally associated with the plasma membrane. PKGI has been studied extensively while the function of PKGII remains more a mystery. PKGII has been shown to be expressed highly in the intestinal mucosa and in the brain. In the intestine it has been demonstrated to play a role in Cl^- and Na^+ transport [72]. Although PKGI distribution appears to be ubiquitous, expression levels vary in different tissues. It has been detected in high concentrations in VSMC's and platelets and lower concentrations in vascular endothelium and cardiomyocytes. A major function of PKG as a vasoregulator was described previously, but PKG is known to have many other functions. Evidence for the activity of PKG has been demonstrated in modulating the activity of stress and growth regulated MAPK, p38 and ERK respectively. PKG directly phosphorylates p38 leading to ATF-2 dependent gene expression and phosphorylates Raf uncoupling Ras-Raf interaction and preventing ERK1/2 activation [73, 74]. PKG regulates the activity of c-fos, JunB, p21, NFκB and has been shown to directly regulate the CRE sites of the cyclin D1 promoter [75, 76].

Much of the evidence for the role of PKG in tumor cells comes from exogenous expression as there is considerable data showing loss of endogenous PKG expression in cultured cells [77]. Not only do tumor cells lose PKG as they are passaged, but a comprehensive examination using cDNA arrays showed that PKGI expression was

found to decrease in tumor cells compared with normal cells [78]. Some tumor cells have lost PKG entirely and this appears to be a mechanism by which the cells avoid apoptosis. To study PKG function in tumor cells, IB Weinstein's group constructed several PKG mutants and determined that when introduced into SW480 colon cancer cells, PKGIβ inhibited colony formation and induced apoptosis. If they overexpressed the dominant negative mutant, the effect was lost [79].

An alternative approach to stimulating cGMP production through exogenous activators of sGC is through inhibition of PDE's that break down cGMP. It has been shown that metastatic breast, colon and lung cancers have increased levels of PDE 2 and/or PDE 5 compared to normal tissue [80]. Exisulind , sulindac sulfone (a metabolite of the NSAID sulindac), has been shown to have proapoptotic effects in SW480 and HT29 cells by inhibiting PDE's leading to elevated cGMP [81, 82].

Anti-angiogenic effects of PKG have also been demonstrated in SW620 tumor xenografts. SW620 cells expressing an exogenous PKG produced smaller, more apoptotic tumors and further examination determined that the parental cell line led to tumors that were more highly vascularized compared to those overexpressing PKG. It was observed that VEGF expression in the SW620 cells overexpressing PKG was significantly reduced compared to "normal" SW620 cells [83].

The exact mechanism of how PKG leads to growth arrest and apoptosis is still under investigation. Several researchers have examined this apoptotic effect of PKG and have demonstrated that it can occur through sustained activation of JNK1, induction of p21/waf1, a decrease in β-catenin, a decrease in cyclin D1, and through activation of

caspases [79, 84-86]. Taken together, the above data suggest that by increasing PKG activity through recoupling of NOS, tumor cells can be driven in an anti-proliferative direction.

β-*catenin*

β-catenin plays a significant role in both normal mammary development and in tumorigenesis. β-catenin interacts with cadherins at the plasma membrane in cell-cell adhesion complexes which function to maintain epithelial integrity. Its central role in this complex allows it to regulate cell growth and adhesion between cells. The location of β-catenin within a cell and its expression are often abnormal in breast tumors. Increased cytoplasmic and nuclear β-catenin levels in breast tumors correlate with poor prognosis and are seen in about 40% of breast tumors [87-90].

The most well defined pathway for β-catenin stabilization is through canonical Wnt signaling (Figure 3.2). Wnt ligands prevent the destruction of β-catenin resulting in cytoplasmic accumulation and subsequent translocation into the nucleus where it is recruited by and associates with TCF/Lef DNA binding proteins (group of transcription factors involved in Wnt signaling) resulting in cell-context specific gene expression, to include c-Myc, cyclin D1, and c-Jun [91].

Research has shown that retroviral insertion of active Wnt-1 was sufficient to induce mammary tumors and follow up studies have demonstrated similar results in transgenic animals expressing Wnt1, Wnt3 and Wnt10b [92-94]. Several human breast tumor cell lines and patient tumor samples have been found to over express Wnt ligand and dishevelled (a phosphoprotein downstream of Wnt receptors) has been shown to

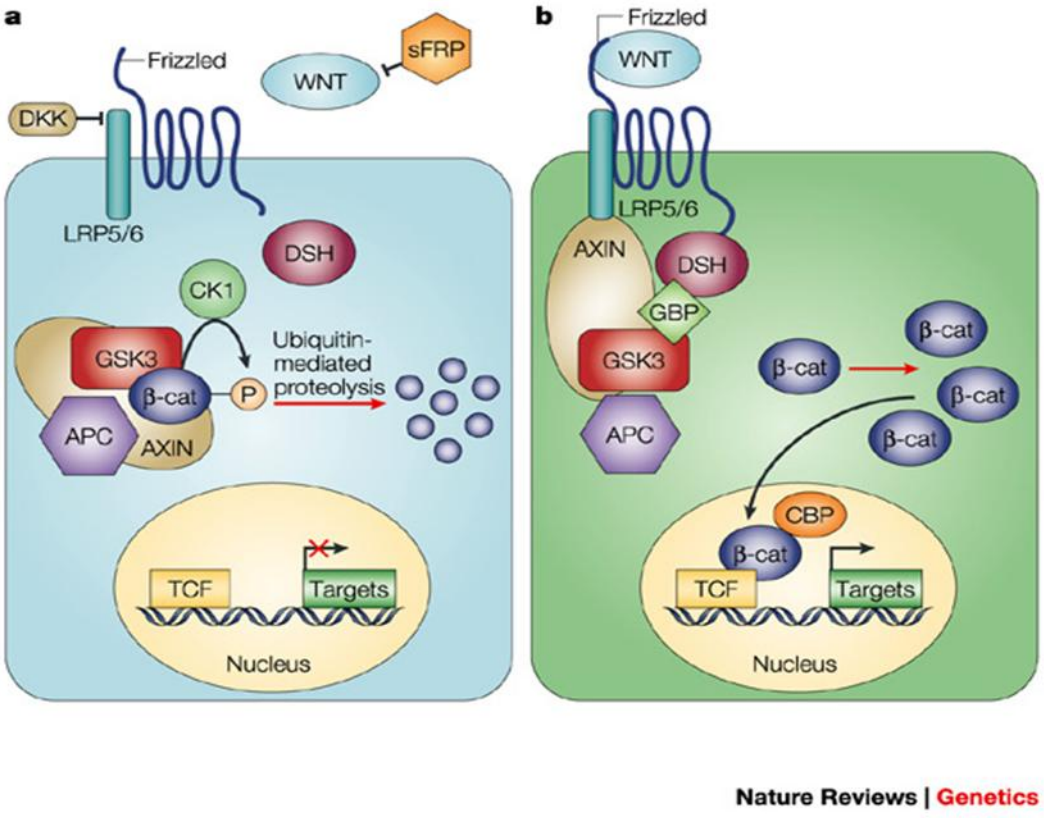

Figure 3.2 Canonical Wnt Signaling. (a) Absent ligand, β-catenin remains in complex with APC and GSK3β resulting in its phosphorylation and subsequent degradation. (b) Ligand bound receptor results in inhibition GSK3β and β-catenin is then able to accumulate and move into the nucleus activating transcription of targeted genes. Figure provided by Nature Reviews, Moon 2004.

be upregulated in up to half of breast cancers, both promoting β-catenin signaling [95-98].

β-catenin regulation by PKG has been studied extensively in colon tumorigenesis as members of the Wnt family control renewal of the luminal epithelium at the crypt base [99]. APC is a tumor suppressor gene that is often mutated in colon cancer. As shown in figure 3.2, β-catenin associates with APC in a complex with GSK3β and phosphorylation of β-catenin by GSK3β leads to its degradation, regulating cellular proliferation. Research has demonstrated that many colorectal tumors contain an APC that is unable to bind β-catenin, leading to enhanced β-catenin signaling even in the absence of Wnt [100].

Downregulation of β-catenin signaling by PKG has been studied extensively in colon tumorigenesis; however inhibition of its signaling plays a role in limiting tumor growth in other cancers as well. Induction of p21/waf1 in gastric carcinomas was due to loss of β-catenin signaling and resulted in apoptosis [101]. In MDA231 xenografts, the inhibitory effect of naringin was found to occur through modulation of p21/waf1 and suvrvivin by inactivation of β-catenin [102].

Given that β-catenin plays a role in mammary tumorigenesis and due to the possibility of increasing a known modulator of its signaling, PKG, we decided to examine the effects on β-catenin signaling in breast tumor cells after treatment with SP.

Nuclear Factor Kappa B

The NFκB family of transcription factors are mediators of the immune and inflammatory response in cells as a result of injury or infection. NFκB exists as homo or

heterodimers of five family members including p50/p105, p52/p100, c-Rel, RelB, and p65 (RelA), and in unstimulated cells these proteins are sequestered in the cytosol by their inhibitor proteins, the IκB proteins. The classical pathway for NFκB activation involves activation of IKK's through ligand binding to Toll Like Receptors and cytokine receptors such as TNFR. Active IKK's phosphorylate IκB causing its dissociation from the NFκB dimer resulting in translocation of the dimer to the nucleus and transcription of corresponding genes. The physiological response in the cell due to activation of NFκB can be any of an inflammatory response, an immune response, a cell survival response or a cell proliferation response.

NFκB plays a major role in the interaction between the immune system and cancer cells and its actions help to shape the tumor microenvironment. This environment is rich in inflammatory cells and ROS [103]. An area of great interest to our lab has been the regulation of NFκB by ROS/RNS. The activation of NFκB can lead to increased NO production in cells through increased eNOS transcription and through stimulation of NOSII [104]. NO, in turn, has been shown to regulate NFκB activity in a negative feedback manner by directly modulating the activity of some family members resulting in the inhibition of NFκB signaling. Tyrosine nitration of p65 has been shown to inactivate NFκB signaling in HEK293 cells [105]. S-nitrosylation of p65 inhibits NFκB dependent gene transcription in cytokine stimulated A549 cells [106]. Under conditions of shear stress, the p50 subunit has been shown to be s-nitrosylated inhibiting the binding of the p65/p50 heterodimer to DNA. NO-donating aspirin in colon cancer cells s-nitrosylates the p65 subunit and this results in decreased binding of the heterodimer to DNA as well [49]. This data further implicates NO in modulating the inflammatory

state of the cell. Our lab demonstrated that low level NO production results in tyrosine nitration of IκBα results in dissociation from the NFκB dimer resulting in translocation of the p65/p50 complex into the nucleus [25]. NFκB is also regulated by a variety of post translational modifications (e.g. phosphorylation and acetylation) that regulate its nuclear localization, DNA binding, oligomerization, interactions with coactivators and corepressors, that may also be ROS sensitive [107].

Evidence has shown that many breast tumors express a constitutively active NFκB, leading to enhanced tumor progression via activation of pro-survival pathways, angiogenesis pathways, and cell proliferative pathways, which have been shown to occur through several mechanisms, including upregulation of Bcl-2 and activation of MAP kinases. Several NO donating drugs (nitric oxide-donating aspirin, NO-ASA) have shown positive results as cancer prevention agents. The mechanism by which this occurs has been shown to be through S-nitrosylation of proteins, including p53, p65 and β-catenin in HCT116 cells. The importance of NFκB as a therapeutic target in cancer is further appreciated by the fact that current chemotherapeutics and radiotherapy can lead to its activation. It has therefore been postulated that this enhanced NFκB activity contributes to the development of resistance to these modes of treatment. In light of this there has been substantial research aimed at the use of NFκB inhibitors as sensitizers for therapy. Bortezomib is an inhibitor of IκB degradation and therefore blocks NFκB activity. This drug showed great promise in pre-clinical studies as an adjuvant to other chemotherapeutics, but turned out to be ineffective and caused significant toxicities [108]. Off target effects can be a major drawback to NFκB targeted

therapies as they are involved in a wide array of signaling pathways. Here we examined NFκB activity from the novel perspective of NOS dysregulation.

STAT3

Signal Transducers and Activators of Transcription (STATs) are a family of cytoplasmic proteins that participate in normal cellular responses to cytokines and growth factors. When receptors such as EGFR, PDGFR, fibroblast growth factor receptor (FGFR), and granulocyte colony-stimulating factor receptor (GCSFR) are activated it sets off a tyrosine phosphorylation cascade. There are several ways in which this can occur. Receptors like EGFR, once bound by ligand, dimerize and auto-phosphorylate tyrosine residues which other proteins, like STATs, are able to interact with through their phophotyrosine binding SH2 domains. Another well characterized mode of STAT activation involves the recruitment of Janus kinases (JAKs) to activated receptors. JAKs, which have tyrosine kinase activity bind to the activated receptor and phosphorylate tyrosine residues on the receptor creating sites for interaction with STATs SH2 domains. The recruitment of STAT to the receptor and subsequent phosphorylation on Tyr 705 results in STAT dimerization and translocation to the nucleus stimulating transcription of the responsive genes. Recently however, it has been shown that unphosphorylated STAT3 is still capable of dimerization and transcriptional activities[109]. STAT3 is constitutively activated in approximately half of primary breast tumors where it plays important roles in survival, drug resistance, and angiogenesis. Constitutive activation of STAT3 has been demonstrated to occur through hyperactivation of JAK's and Src kinase (Burke WM 2001). Previous studies have demonstrated that downregulation of STAT3 results in decreased tumorigenicity in

several breast cancer cell lines in vitro and in vivo [110, 111]. Introduction of anti-sense or dominant negative STAT3 leads to apoptosis in several human tumor cell lines and knockdown of STAT3 by RNA interference inhibits the induction of breast tumors in immunocompetent mice [112]. Identification of STAT3 as being constitutively active led to a push for the development of small molecule inhibitors which have exhibited anti-tumor potential. FLLL31 and FLLL32 bind selectively to JAK2 and the STAT3 SH2 domain and have been shown to be effective inhibitors of STAT3 phosphorylation and DNA binding activity [22].

Given that STAT3 is upregulated in many breast tumors, blockade of STAT3 signaling results in decreased tumorigenesis, and that activation of STAT3 comes from receptor tyrsosine kinases that have been shown to be regulated by ROS, investigation of STAT3 after treatment of breast tumor cells with SP seemed logical.

MATERIALS AND METHODS

Chemicals and Reagents

KT5823 (10010965) and ODQ (81410) were purchased from Cayman Chemical. NAC (A1824), 8-Br-cGMP (B1381), Trypsin (T9201), Collagenase (C0130), and DNase (D4527) was from Sigma. Propidium Iodide (51-66211E) was from BD Pharmingen (Franklin Lakes, NJ). The luciferase based reporter construct of NFκB (pNFκB–Luc) was purchased from Clontech (Mountain View, CA). The TCF/LEF reporter construct was from Addgene (plasmid 12456) and was provided to them by Randal Moon. NPH4 (11.309) was purchased from Schircks Labs. 1% Casein in TBS was from BioRad (161-0782). LucLite luciferase reporter gene assay kit was from Perkin Elmer (Waltham,

MA). WST-1 (05015944001) reagent was from Roche (Indianapolis, IN). STAT3 IRDye 700 labeled oligonucleotides (829-07922) and Odyssey EMSA Buffer Kit (829-07910) were form Li-Cor (Lincoln, NE). 10X TBE (EC-860) was purchased from National Diagnostics (Atlanta, GA).

The following primary antibodies were used: anti-Bcl-2 (sc-7382), pVASP (sc-23507) and actin (sc-1616) were from Santa Cruz Biotechnology (Dallas, TX). Anti-p65 (4764), anti-p50 (3035), anti-p21 (2947), anti-cyclin D1 (2978), anti-JNK1/SAPK (4668), anti-pGSK3β (9323) and anti-Stat3 (9131) were from Cell Signaling Technology (Danvers, MA). Ant- c-Myc EZview affinity gel (E6654) was from Sigma Aldrich (St Louis, MO). Anti-PKG (KAP-PK002) was from Stressgen (Ann Arbor, MI). Anti-Nitrotyrosine (06-284) was from Millipore Corp (Billerica, MA). Anti-β-Catenin (610153) was from BD Tansduction Laboratories (Franklin Lakes, NJ). The secondary antibodies used were IR conjugated and designed for use on the Li-Cor Odyssey Infrared Imager: anti-rabbit 800 (611-132-003), and anti-goat 700 (605-730-002), were from Rockland Immunochemical (Gilbertsville, PA).

Luciferase Reporter Gene Assay

NFκB: MCF-7 cells were plated at a density of $1.2x10^6$ cells/60mm dish and the cells were allowed to incubate overnight to adhere. We then transfected the cells with NFκB-Luc or according to the Lipofectamine/Plus protocol from Invitrogen. We then treated the cells for 4 hours with SP after which the old medium containing the SP was removed and new medium was added.

TCF/LEF: MCF-7 cells were plated at a density of $2x10^5$ cells/60mm dish and were allowed to incubate for 6 hours to adhere. The cells were to be transfected with the TCF/LEF construct 24 hours before harvesting so we had to treat cells with SP accordingly. That meant that 48 hours before we transfected the cells we treated the 72 hour time point with SP. All cells were placed in fresh 10% medium after transfection. The cells were washed in ice cold PBS and harvested in the lysis buffer provided in the kit. We followed the protocol in the kit exactly.

P50 and P65 s-nitrosylation

We plated MCF-7 cells at a density of $1.2x10^6$ cells/60mm dish and allowed them to incubate overnight to adhere. The cells were then transfected with both p65 and p50 plasmids according to the Lipofectamine/Plus protocol from Invitrogen. Following transfection the cells were treated with the dose of SP and for the duration indicated. S-nitrosylated p65 and p50 was determined by the Biotin Switch Method described in detail in Chapter 1. Once the s-nitrosylated proteins were isolated, SDS-Page electrophoresis was used to separate the proteins and western blotting was used to determine protein levels.

IκBα nitration

We plated cells at a density of $1.2x10^6$ cells/60mm dish and were allowed to incubate overnight to adhere. Cells were transfected with a Myc tagged IκBα plasmid according to the Lipofectamine/Plus protocol from Invitrogen. Once cells had been treated with the dose of SP and for the duration indicated they were washed three times in ice cold 1X PBS and lysed in buffer containing 50mM Tris pH 7.4, 150mM NaCl, 1%

NP40, and a 1X concentration of phosphatase and protease inhibitors. Samples were centrifuged for 20min at 13,200 at 4˚C and the supernatant was transferred to a clean 1.5ml eppendorf tube. Myc-IκBα was then immunopurified with anti c-Myc overnight at 4˚C. The beads were washed twice in ice cold lysis buffer and once in ice cold 1X PBS. All of the PBS was removed and the beads were boiled in 35µl of laemmli sample buffer. The sample was then resolved on a 10% SDS-Page gel and after transfer the resulting membrane was probed for anti-nitrotyrosine.

Growing cells as Spheroids

5ml of 1% agarose in RPMI without FBS or Pen/Strep was used to coat the bottom of 100mm petri dishes and placed in the incubator to solidify. During that time the cells were trypsinized and counted. MCF-7 cells were plated at a density of $1.5x10^5$ cells/ml of medium on top of the agarose layer (10ml/dish). The dishes were placed on a rocker in the incubator and allowed to grow for three days before they were used in experiments. To harvest the spheroids the medium containing the floating spheroids was removed from the dish and centrifuged at 1,000 RPM for 5min. The supernatant was removed from the top of the cell pellet and then the cells were resuspended in 5ml of ice-cold PBS to wash. The wash step was repeated twice. After removing all of the PBS from the wash steps, the cells were lysed in laemmli sample buffer, sonicated and then boiled for 5min.

Western Blot Analysis

Protein was extracted from flash frozen tumors using a pestle and mortar in 20 ml/g tumor RIPA lysis buffer (50 mM Hepes pH 7.4, 150 mM NaCl, 1% Triton X-100, 1%

sodium deoxycholate, 0.1% SDS, 5 mM EDTA) and processed under reducing conditions. Alternatively tissue culture cells were harvested in 1X Laemmli sample buffer. Proteins were resolved by SDS-polyacrylamide gel electrophoresis and transferred to nitro-cellulose membranes. Membranes were incubated with the primary antibody of interest overnight at 4°C. Blots were developed using IR 700 or IR 800 conjugated secondary antibodies (Rockland Immunochemicals, Gilbertsville, PA) diluted 1:10,000 and imaged/analyzed using the Odyssey Licor system.

Cell Survival Assay (WST and Clonogenic Assay

WST-1: Cells were washed, trypsinized and counted. This assay is performed in a 96 well plate and samples are plated in triplicate. $1x10^3$ cells/well in 200µl of medium were plated and allowed to incubate overnight to adhere. When we were ready to determine cell viability 4µl of WST-1 reagent was added to the well and allowed to incubate for 3 hours before. The formazan that is formed by metabolically active cells is then quantified by spectrophotometer at 420-480nm. For our experiments involving SP treated cells, if the treatment was for longer than 24 hours, new SP was put on the cells every day until the end of the treatment period.

Clonogenic Assay: cells were trypsinized and plated in 10cm dishes. 200 cells were plated in the control dishes while 500 cells were plated in the treatment groups. Dishes were treated with varying concentrations of SP 16 hours after plating. When the colony size reached 50 cells, cells were fixed in -20˚C methanol, stained with 0.5% crystal violet and counted.

Ex-vivo Clonogenic Assay: Tumors were harvested and minced into small pieces with a scalpel in medium without serum. The pieces were washed twice in medium and then the pieces were agitated in medium containing 0.08% collagenase and 0.5% Trypsin for 40min at 37˚C. DNase to 0.06% was added to the medium and the cells were strained through a .70µM cell strainer. The resulting single cell suspension was counted, excluding RBC's, and plated at several concentrations. The plating efficiency of this type of experiment is very poor so we plate many more cells than we would for the tissue culture assay. We plated 2k, 5k, 10k, and 20k cells per 100mm dish. The dishes were fixed and stained as above when colonies reached approximately 50 cells.

Nuclear Preps

The cells were plated in 100mm dishes and treated accordingly. When they were ready to be harvested they were washed twice with ice cold PBS. Cells were then scraped into 1ml PBS and transferred to a microcentrifuge tube and centrifuged for 5min at 2500 RPM at 4˚C. The cell pellet was resuspended in 1ml of PBS and centrifuged for 5min at 2500 RPM. The supernatant was completely removed after this rinse. 3x pellet volume of ice cold solution I (10mM Tris-HCl pH7.5, 25mM KCl, 2mM Mg Acetate, 1mM DTT, protease inhibitors), about 150µl, was added to the pellet to resuspend. The slurry was then centrifuged for 3min at 3500 RPM and the resulting supernatant was discarded. Again we added 3x volume of solution I to resuspend the pellet and then incubated the tube on ice for 10min. The cells were then homogenized ten times with a 27G1/2 needle. The homogenate was then centrifuged 5min at 3500 RPM with the resulting pellet containing the nuclei. The cell pellet was resuspended in

150µl of Solution II (10mM Tris-HCl pH 7.5, 400mM KCl, 2mM Mg Acetate, 20% Glycerol, 1mM DTT, protease inhibitors) and incubated on ice for 10min after which it was centrifuged for 5min at 12000 RPM. The supernatant is the nuclear extract. Aliquot and store at -80°C.

EMSA

We purchased the EMSA buffer kit and the IRDye 700 labeled oligos from Li-Cor and followed the general protocol. A 5% TBE native acrylamide gel in 0.5X TBE was pre-run for 30min at 70V (while the binding reactions are being prepared). 20µl reactions were set up in the following order: H_2O, 2µl 10X binding buffer, 2µl of 25mM DTT/2.5% Tween 20, 1µl of 1µg/µl Poly (dIdC), 1µl of 1% NP-40, 1µl of 100mM $MgCl_2$, 1µl of IRDye oligo, and 5µg of nuclear extract. The tubes were mixed and incubated in the dark at room temperature for 20min. 2µl of 10X orange loading dye was added to each reaction tube and samples were loaded on to the gel and separated at 70V. The gel box was covered to keep it in the dark and the gel was visualized using the Li-Cor Inrared imager after 1hr.

Flow Cytometry

Cells were plated at a density of $2.5x10^5$ cells/100mm dish and allowed to adhere overnight. We wanted to plate at a density where the cells would be 50-60% confluent on the day we harvested. Cells were treated accordingly with SP on the days leading up to harvest. When we were ready to harvest cells we washed the dishes with PBS, trypsinized and counted the cells. The cells were centrifuged and then resuspended in PBS at 10^6/ml. 1ml of cells was centrifuged and the supernatant was removed. The

pellet was resuspended in 0.5ml of PBS and vortexed at high speed in order to achieve a single cell suspension. While vortexing 4.5ml of -20°C 70% ethanol was added dropwise into the cell suspension. The cell suspension was vortexed for an additional minute after the addition of all of the ethanol. The cells could be stored overnight at 4°C or stained. To stain the cells they were first centrifuged and then resuspended in PBS. This process was repeated twice. The cell pellet was then resuspended in 1ml of propidium iodide/RNase staining solution (To 10ml of 0.1% Triton-X/PBS add 2mg of DNase-free RNase A and 0.2ml of propidium iodide stock (1mg/ml). Cells were stained for a minimum of 1 hour and then analyzed for cell cycle by the Massey Cancer Center Flow Cytometry Shared Resource Core.

Flank Tumor Xenografts

See Chapter 2. For tumor volume measurements N= number of animals, n= number of tumors.

Biotin Switch

See Chapter 2

RESULTS

MCF-7 and MDA231 contain PKG that is activated by treatment with SP

The main signaling pathway activated as a result of NO production is binding to sGC and subsequent activation of PKG. First we determined whether or not our cells expressed PKG and secondly determined if the activity changed in the presence of SP. Western blot analysis of PKGI in MCF-7 and MDA231 cells confirmed the expression of

PKGIβ (Figure 3.3A). The phosphorylation of VASP has been identified as a useful marker for cGMP induced cell death due to increased PKG activity and so we measured pVASP as a marker for activity in our cells after treatment with SP [113]. We had difficulty detecting endogenous pVASP so we transfected VASP into MCF-7 cells and treated them 24 hours after transfection with SP. Western blot analysis of the cell lysate showed a 10-fold increase in pVASP 6 hours after treatment with 50μM SP (Figure 3.3B). Having determined PKG activity is increased in our cell lines as a result of recoupling NOS we wanted to examine some of the downstream targets.

Activation of PKG results in decreased β-catenin signaling

We described in the introduction how a reduction in Cyclin D1, β-catenin signaling and an increase in p21/waf1 has been observed in colon cancer cells upon induction of PKG activity and are responsible for the cytotoxic effects seen in colon cancer cells. Since we determined that we were getting PKG activity in our cells after SP treatment we looked for changes in the levels of these proteins. Western blot analysis of β-catenin confirms that protein levels decline over time when cells are treated with SP both in MCF-7 and MDA231 cells, and that this effect is reversed when we treat cells with KT5823 in conjunction with SP (Figure 3.4A). KT5823 is a potent, selective, cell permeable inhibitor of PKG (IC_{50} 20nM *in vitro*) and should therefore block the effects of SP if the actions are through PKG. Western blot analysis of tumor cell homogenates also confirmed that we lose β-catenin protein in flank tumor xenografts of MCF-7 cells (Figure 3.4B). To confirm that we were getting decreased β-catenin signaling at the level of transcription we used a Luc TCF/LEF reporter construct. When we transfected the luciferase reporter construct into MCF7 cells we were able to see

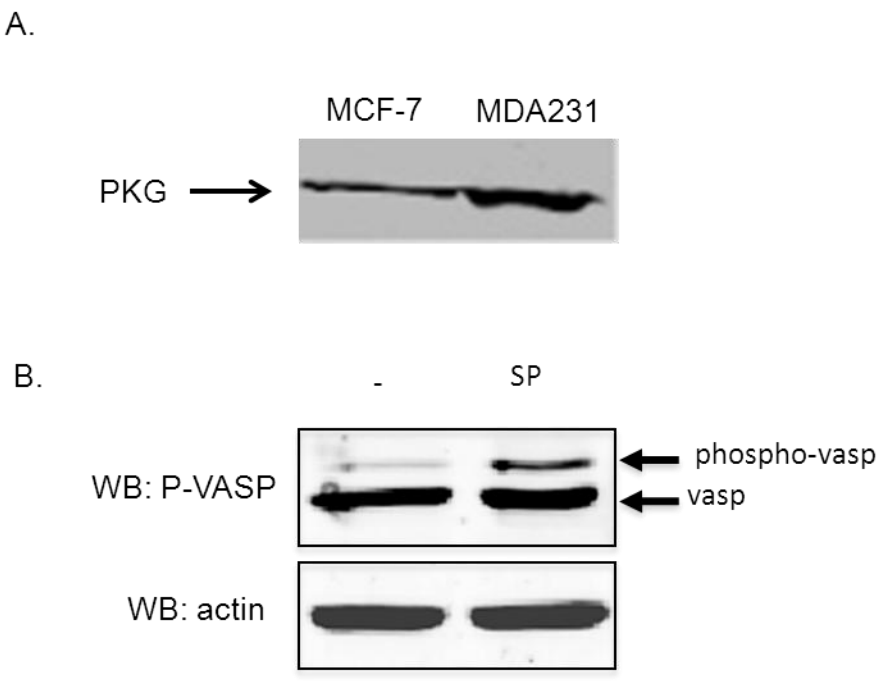

Figure 3.3 Activation of PKG after treatment with SP. (A) MCF-7 and MDA231 cell lysates were separated by SDS-Page and western blot analysis confirmed PKG expression in both cell lines. (B) MCF-7 cells overexpressing VASP were treated with 50μM SP for 6h resulting in a 10-fold increase in VASP phosphorylation.

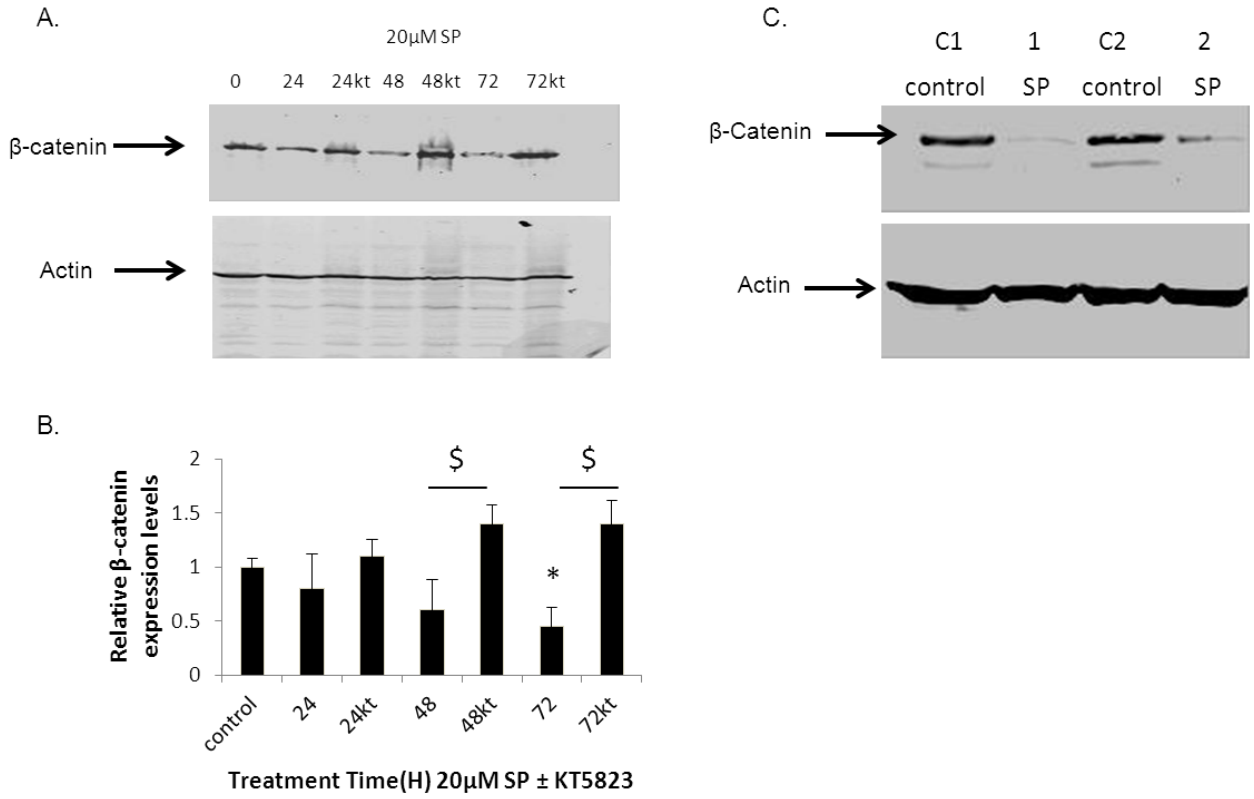

Figure 3.4 β-catenin protein levels significantly reduced in MCF-7 cells treated with SP both *in vitro and in vivo*. (A) Western blot analysis of β-catenin shows that protein levels decrease after treatment with SP and the decrease is blocked by 1μM KT5823. (B) Densitometry of western blot. *, $ $p<0.05$ by two-way anova. N=3 (C) β-catenin protein levels in tumor homogenates from MCF-7 flank xenografts after 48 hours of 1mg/kg/ml SP in the drinking water. 4 animals, 2 per group.

decreased β-catenin signaling in SP treated cells that was also reversed by KT5823 (Figure 3.5). We used 100μM 8-Br-cGMP, a cGMP analogue that is resistant to PDE's, as a positive control. We were unable to conduct this experiment in MDA231 cells as the transfection efficiency was too poor.

When we examined signaling downstream of β-catenin we saw increased p21 protein levels in MCF-7 cells, abolished by KT5823, but did not see any changes in cyclinD1 protein levels (Figure 3.6). In our analysis of MDA231 cells we saw that there were no changes in p21 but we did detect increased p27 protein levels at 24, 48 and 72 hours post SP treatment. Several other groups had analyzed cell cycle distribution in cells after PKG activation and shown G1 arrest, which was mainly though loss of cyclin D1 protein. We did not see loss of cyclin D1 but we did see changes in p21 and p27 and as both play a role in cell cycle progression we examined our cells by flow cytometry to determine if cells were arresting at some point in the cell cycle which could help explain the cytotoxic effects. We found that neither MCF-7 nor MDA231 cells showed any significant changes in cell cycle distribution when treated with SP (Figure 3.7).

Sepiapterin reduces NF-κB activity

Previous studies have demonstrated that when the p50 or p65 subunit of NF-κB is S-nitrosylated there is decreased binding of the complex to DNA. Our initial experiments tested whether SP had an effect on the level of S-nitrosylated p50 and/or p65 in our cells. MCF-7 cells were co-transfected with WT p65 and p50 and on the following day treated with varying concentrations of SP for 6h. The cells were harvested

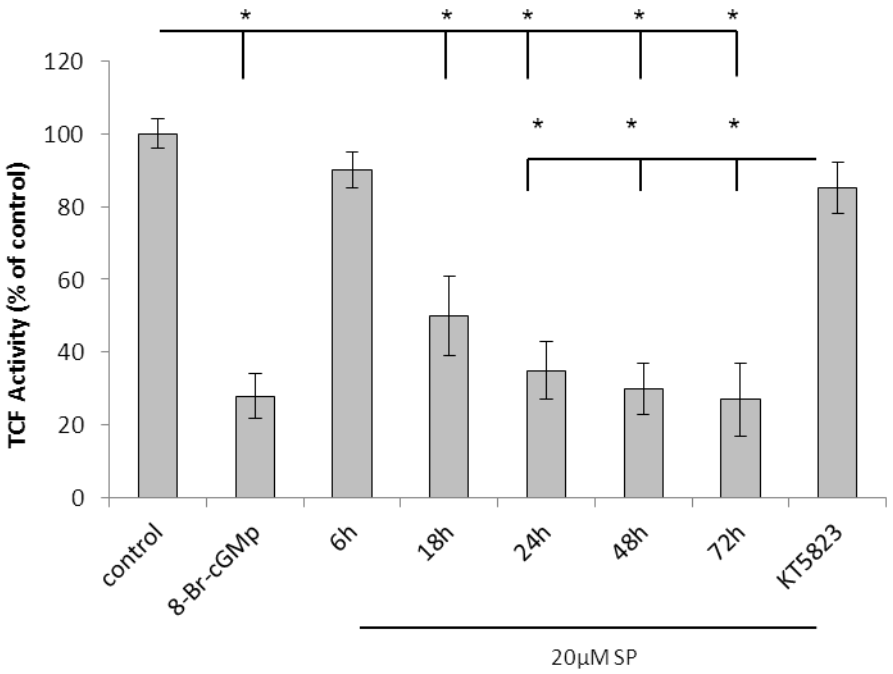

Figure 3.5 TCF activity decreased in MCF-7 cells treated with 20μM SP. The relative inhibition of TCF activity by SP at different times is expressed as % of control. Luciferase activity was measured at 24 hours post transfection. The PDE resistant cGMP analogue, 8-Br-cGMP, was used at 100μM as a positive control. Results are reported as means ± SEM. N=3, * $p<.05$ by one-way anova with dunnett's post hoc.

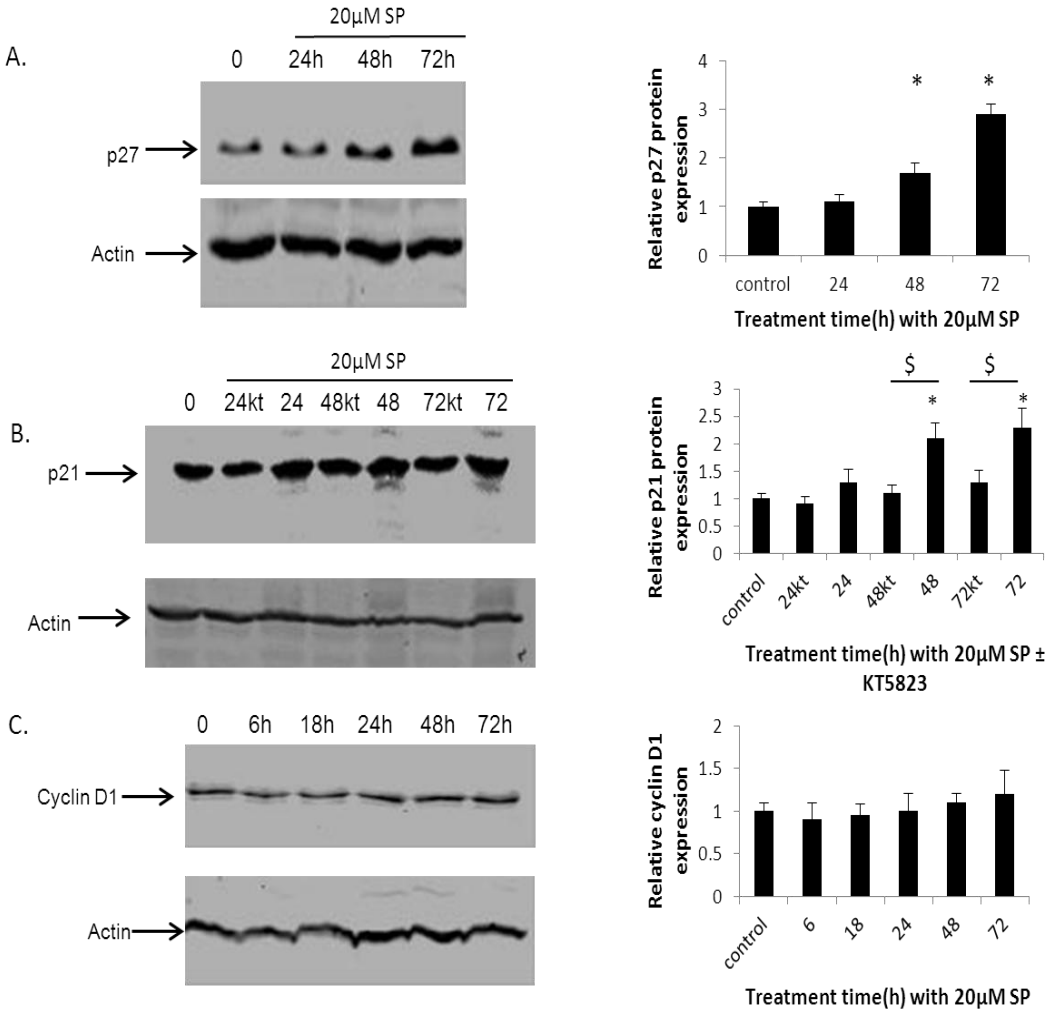

Figure 3.6 Downstream β-catenin targets. (A) p27 in MDA231 cells increases 3 fold after 72h with SP. * $p<0.05$ by one way anova with dunnett's post hoc, N=3 (B) p21 levels in MCF-7 cells increase 2-fold after 72h with SP and is blocked by treatment with 1μM KT5823t. *, $ $p<0.05$ by two way anova, N=3. (C) Cylcin D1 expression in either cell line did not respond to treatment with 20μM SP (Data shown for MCF-7 cells).

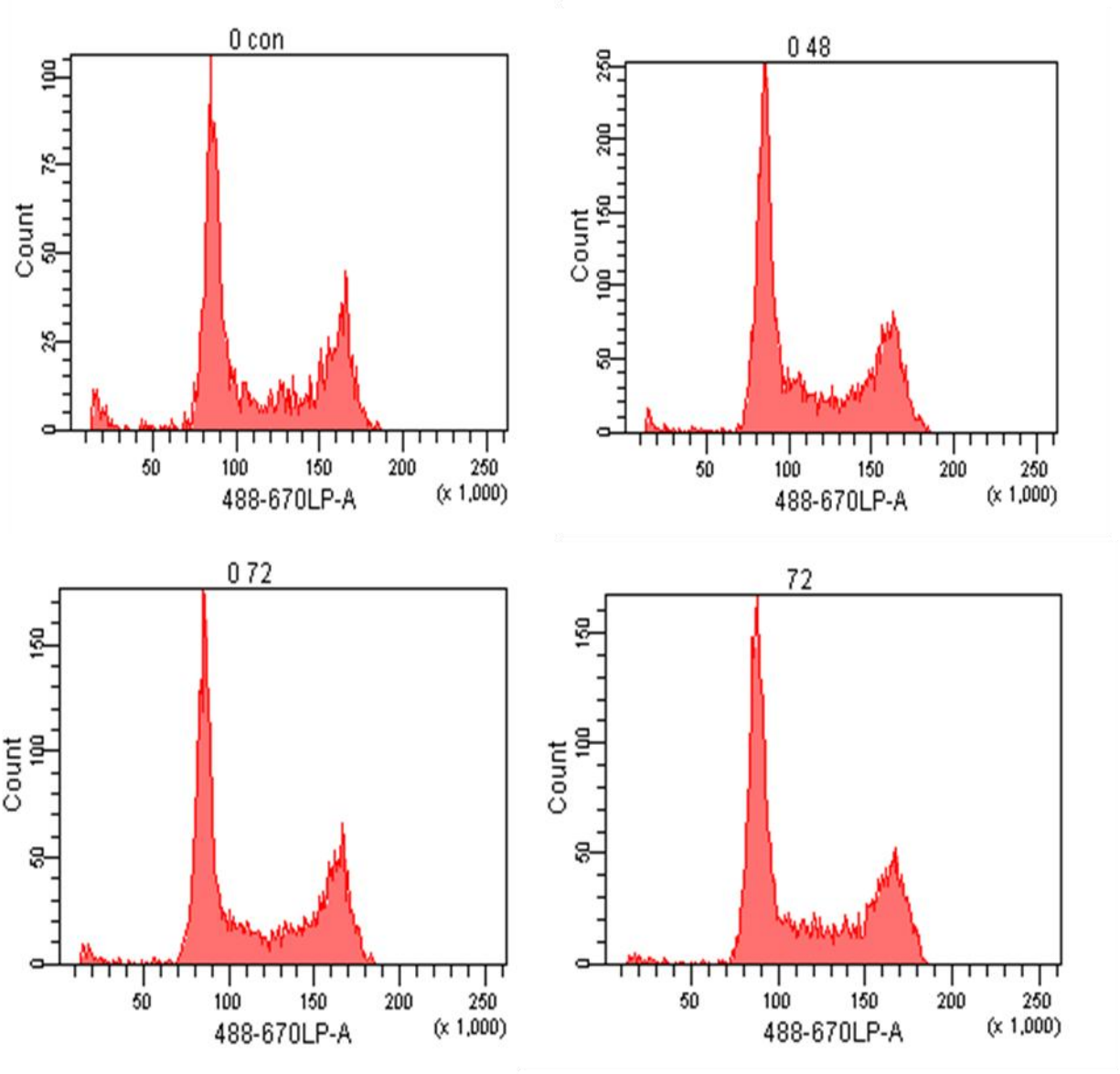

Figure 3.7 Cell cycle analysis of MCF-7 cells. MCF-7 cells were treated with SP for 48 and 72 hours ± 1μM KT. The results show that there was no significant change in cell cycle distribution with SP alone or with SP+KT. The results for MDA231 were similar and so the data is not shown

in RIPA buffer and analyzed for S-nitrosylated p65 and p50 by the biotin switch method described in methods. The results showed a dose dependent increase in S-nitrosylated p65, but we were unable to detect any S-nitrosylated p50 (Figure 3.8A). To determine if the increased p65 S-nitrosylation had any effect on NFκB activity we transfected a luciferase based NFκB reporter construct into MCF-7 cells and treated them with a range of SP concentrations. Treating cells with SP resulted in a dose dependent decrease in NF-κB luciferase activity with a maximal inhibition of 40% at 50μM (Figure 3.8B).

To verify that the S-nitrosylation of p65 was responsible for the decreased NFκB activity measured by luciferase assay we constructed a p65 plasmid with a C38S mutation. This Cysteine was demonstrated to be S-nitrosylated in previous studies and p65 C38S has been shown to bind to DNA and activate transcription [114]. We co-transfected MCF-7 cells with the luciferase based NFκB reporter construct and the mutant p65 and 24 hours later we treated the cells with SP. We determined by measuring the NFκB luciferase activity that the p65 C38S mutant treated with SP behaved like untreated cells (Figure 3.9). These data indicated that the S-nitrosylation of p65 due to recoupling of NOS decreased NFκB activity. One mechanism by which NFκB exhibits its anti-apoptotic activities is through upregulation of Bcl-2. Now that we had demonstrated decreased NFκB activity in tumor cells after treatment of SP we wanted to assess the effects on some of the downstream targets. We homogenized several tumors and by western blot determined that Bcl-2 was expressed in substantially lower amounts in tumors treated with SP than in untreated tumors (Figure 3.10).

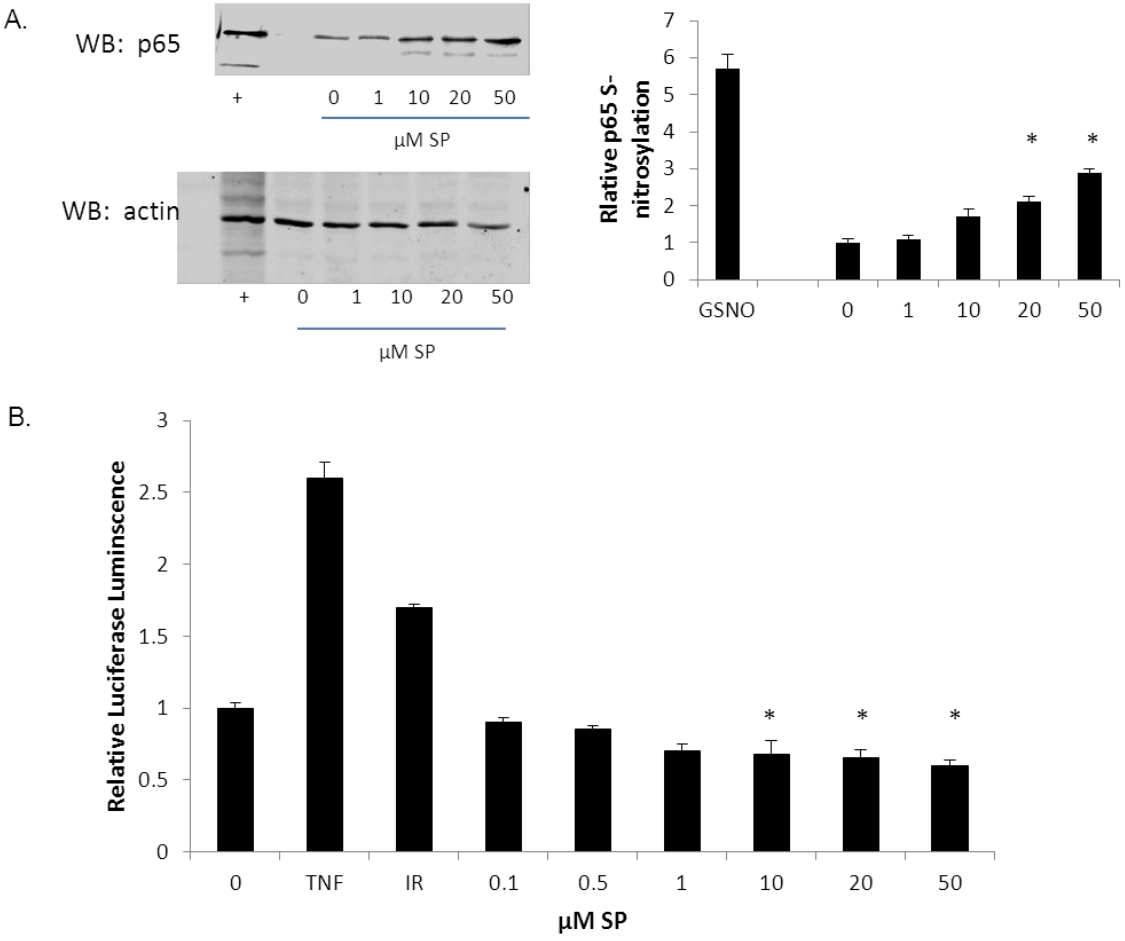

Figure 3.8 SP induces s-nitrosylation of p65 and reduces NFκB activity. (A) MCF-7 cells were treated as indicated with SP for 6h and were analyzed for s-nitrosylation by the biotin switch method. GSNO was added to the cells as a positive control (B) MCF-7 cells were transfected with a Luciferase based reporter construct and treated with SP for 6 hours. The results show a significant decrease in NFκB binding to DNA. Values shown are the means +/- SEM. N=3. * $p<0.05$ by one-way anova with dunnette's post hoc.

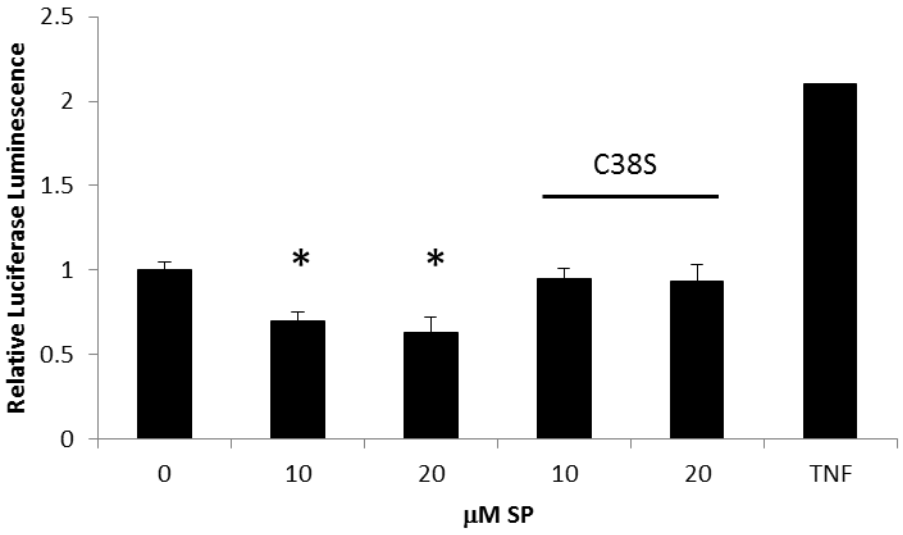

Figure 3.9 SP has no effect on p65 C38S activity. MCF-7 cells were co-transfected with a NFκB Luciferase based reporter construct and p65 C38S mutant. Cells were treated with SP for 6 hours. The results show a significant decrease in NFκB binding to DNA with SP which is abolished by p65 C38S. Values shown are the means +/- SEM. N=3. * $p<.05$ determined by Student's t test.

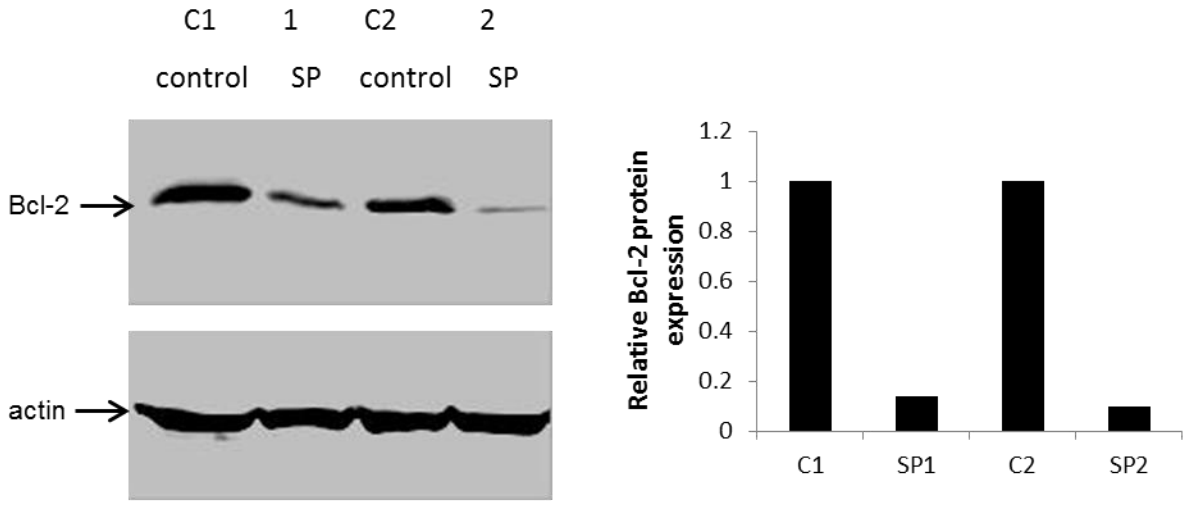

Figure 3.10 SP causes a reduction in Bcl-2 in MCF-7 flank tumor xenografts. Animals were given 1mg/kg of SP for 48h in their drinking water. Following excision, tumors were snap frozen in liquid nitrogen and then homogenized in RIPA buffer (50mM Hepes pH 7.5, 150mM NaCl, 1% Triton-X 100, 0.1% SDS, 0.05% DOC). Western blot analysis of Bcl-2 in SP treated animals showed decreased protein levels compared to control animals.

Sepiapterin reduces STAT3 nuclear translocation in MCF-7 cells

STAT3 is another transcription factor known to be constitutively activated in breast tumor cells and has been shown to be manipulated by ROS so we treated MCF-7 cells with 20μM SP for 24, 48 and 72 hours and assessed the level of STAT activation in two ways: phosphorylation of Tyr705 and nuclear translocation. Western blot analysis of pSTAT3 showed a decrease in phosphorylation at all time points examined post treatment (Figure 3.11A). As the result was only marginal we then decided to prepare nuclear extracts to examine the level of STAT3 in the nucleus. The gel shift clearly indicates that DNA binding of STAT3 is reduced in cells that had been treated with SP (Figure 3.11B). Putting this in the context of the rest of our data shows that recoupling of NOS leads to downregulation of STAT3 signaling.

SP inhibits cell growth both in vitro and in mouse tumor xenografts

Discussed in detail previously, PC3 cells react in a pro-proliferative manner when given BH4 and NO donors can have a pro or anti-apoptotic effect depending on a number of factors. The above studies show that we are able to manipulate the activity of several important pro-survival transcription factors and now we wanted to determine the effects of SP on cell proliferation. We first performed a WST assay to determine the effects of SP on metabolically active cells. In cells receiving a 50μM does of SP we saw a growth inhibitory effect in MDA-231 cells and a cell death effect in MCF-7 cells (Figure 3.12).

Carrying our tissue culture studies a step further we used a clonogenic assay to determine actual cell death. Figure 3.13A shows that in single cells plated and treated

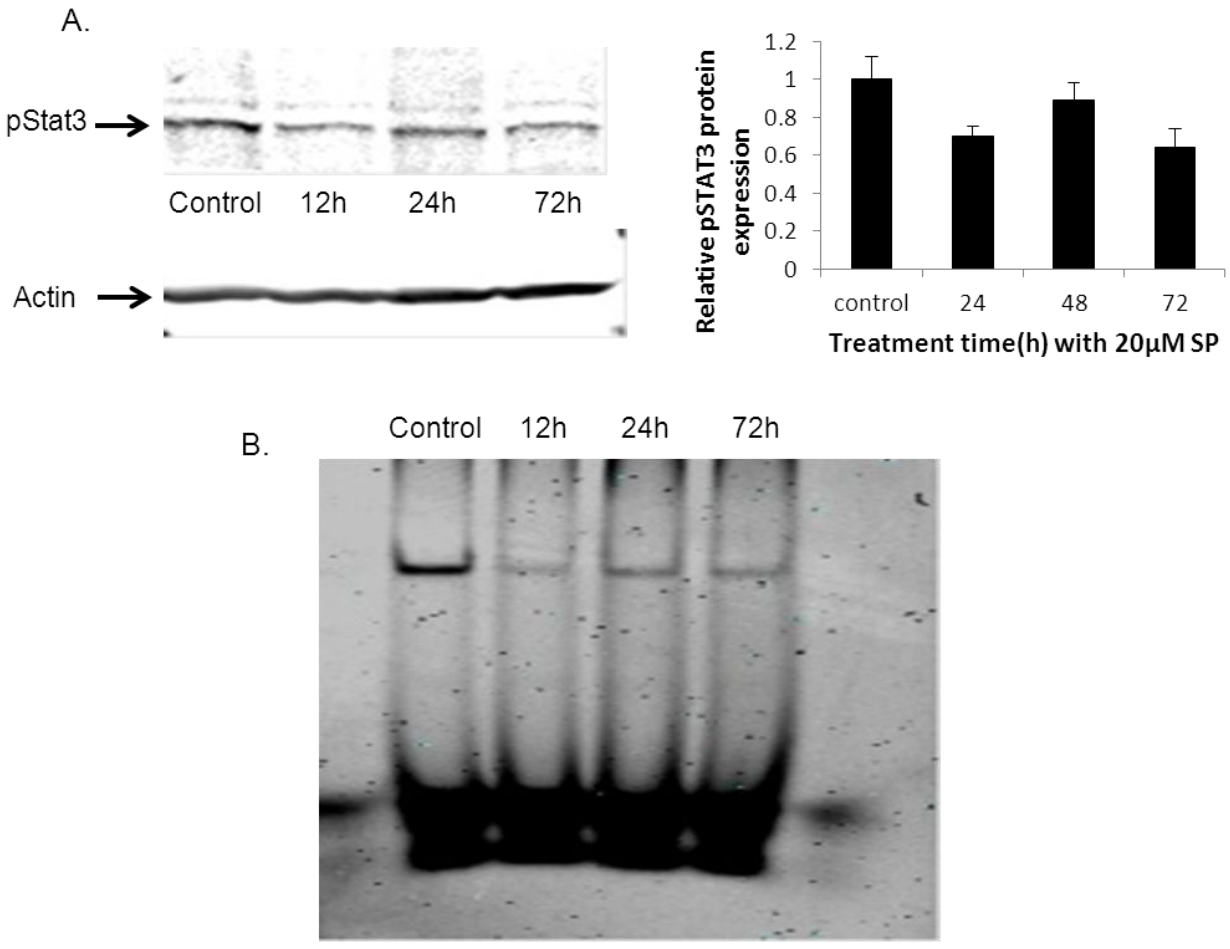

Figure 3.11 SP reduces pSTAT3 and STAT3 translocation to the nucleus. (A) Treatment of MCF-7 cells with 20μM SP results in decreased pStat3 Tyr705. Data present as the mean ± SEM, N=2. (B) Nuclear preparations of MCF7 cells treated with 20μM show decreased Stat3 translocation into the nucleus at the indicated times.

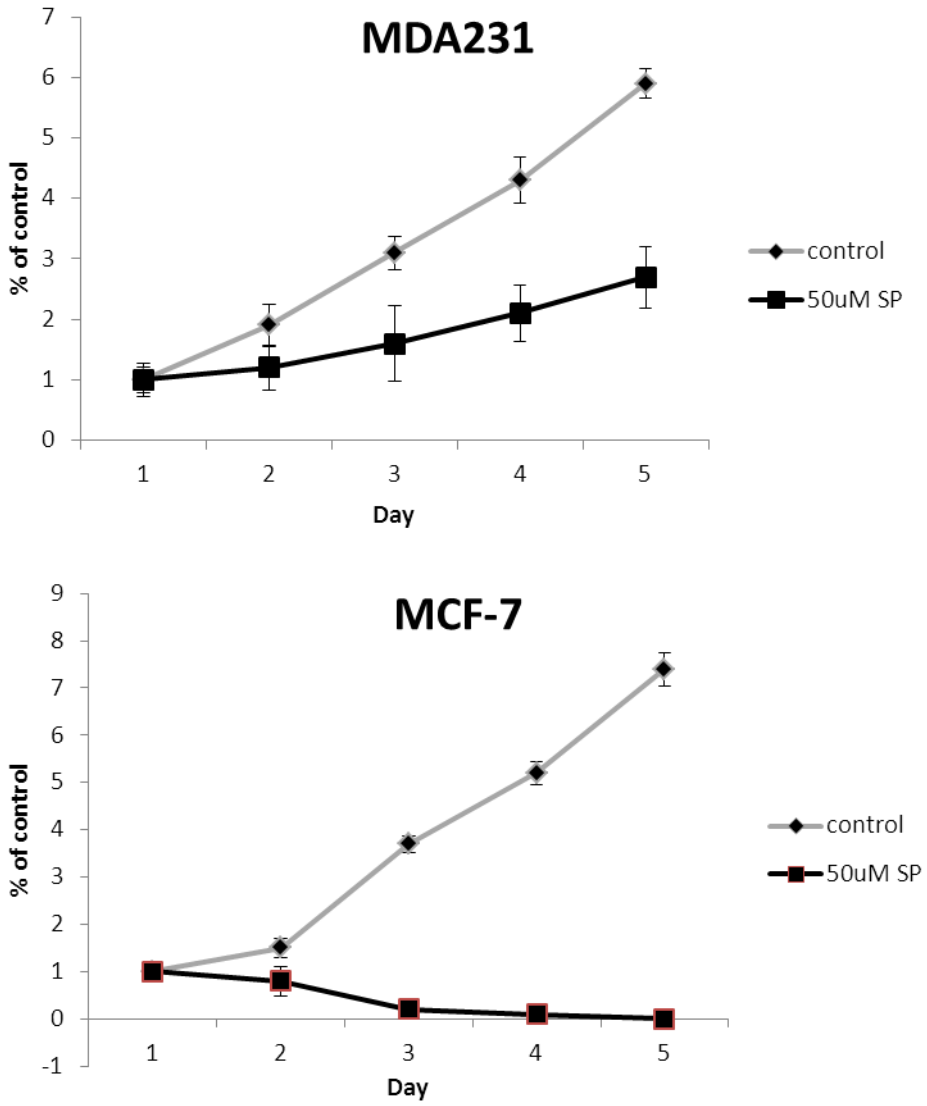

Figure 3.12 Cell metabolic activity. MDA231 and MCF-7 cells treated with 50μM SP display decreased metabolic activity as measured by WST-1. Cells were treated with fresh SP each day and incubated with WST reagent for 3h before measuring activity. Data presented as the mean ± SEM. N=3

with SP we saw a concentration dependent decrease in MCF7 and MDA231 tumor cell survival. Several key controls were included in these experiments, LNNA, NPH4, N-Acetylserotonin (NAS) and KT5823. Treating cells with 200nM LNNA to block NOS activity in these cells completely eliminated the toxicity of SP which confirms that SP is working through NOS. NPH4 has the same ability as BH4 to be reduced but will not bind to NOS, and in our experiments controls for anti-inflammatory effects. If BH4 were just having an anti-inflammatory effect then we should see the same results in the clonogenic assay in cells treated with NPH4. The results obtained determined that the effect of BH4 is through NOS and not due to BH4 as an anti-inflammatory as NPH4 had no effects on cell viability. These data also showed that KT5823 significantly restored cell viability (Figure 3.13B).

Both MDA231 and MCF7 cells can be grown as xenografts in nu/nu mice (called nude mice due to their lack of hair). Nude mice have a genetic mutation that causes deteriorated or absent thymus resulting in an inhibited immune system, and have no rejection response to tissue xenografts. We injected cells into the flanks of the mice and waited for the tumor to reach a palpable volume. We treated some of the animals for 48 hours with 1mg/kg/ml of SP in their drinking water and then harvested the tumors and plated them for an ex-vivo clonogenic assay. To be certain that SP was not having off target effects we gave the animals NAS in conjunction with SP. NAS is a sepiapterin reductase inhibitor which blocks SPs conversion to BH4. Figure 3.14 shows that when animals bearing MDA231 flank xenografts are treated with 1mg/kg/ml of SP for 48 hours that there was a significant decrease in clonogenicity which was blocked by a 10mg/kg i.p. injection of NAS. From both our tissue culture and ex-vivo clonogenic data we

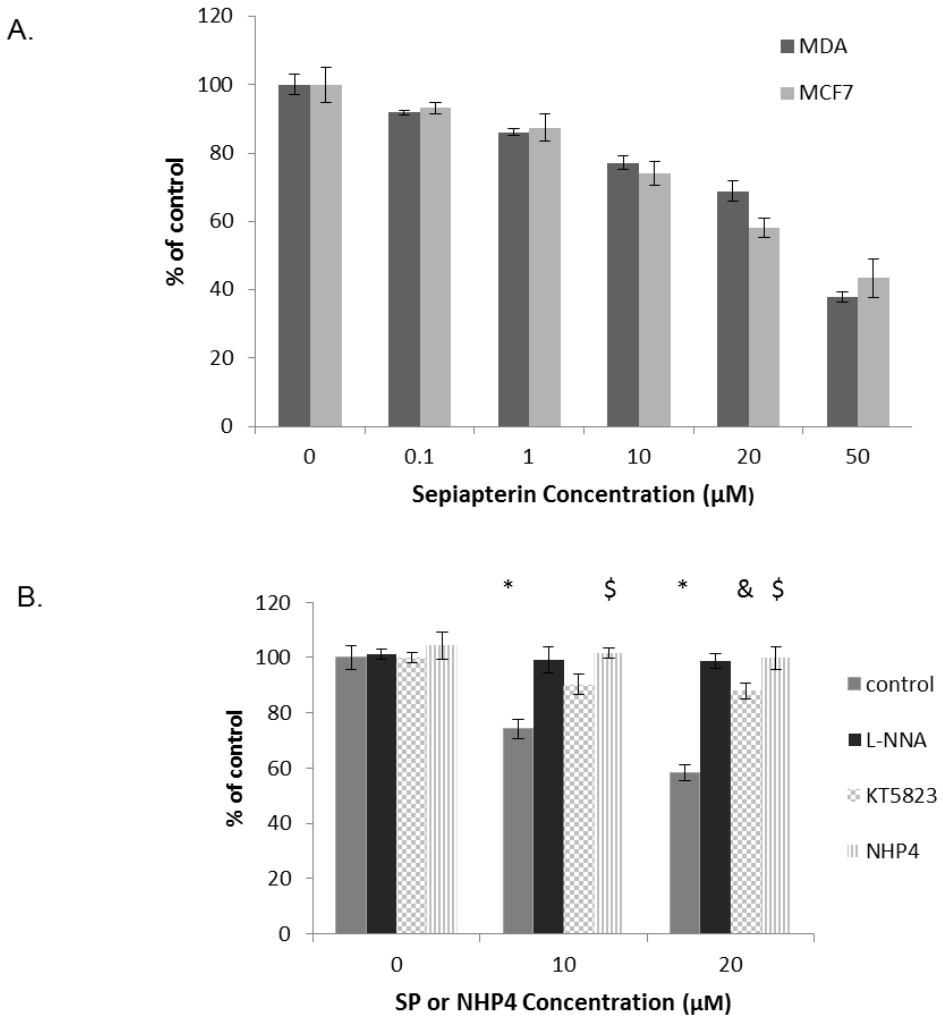

Figure 3.13 SP reduces cell survival. (A) Does response to SP in MCF-7 and MDA231 cells. (B) We chose 2 doses of SP and then used the PKG inhibitor KT5823 (1µm) and 200nM L-NNA to inhibit the effects of SP on the indicated cell lines. We also used 10µM and 20µM NHP4 to insure the effect of SP was not due to anti-inflammatory actions. *p<0.05 (SP to control), & p<0.05 (SP to KT5823), $ p<0.05 (SP to NHP4) by one-way anova, N=3. Data shown for MCF-7 (data for MDA231 were similar).

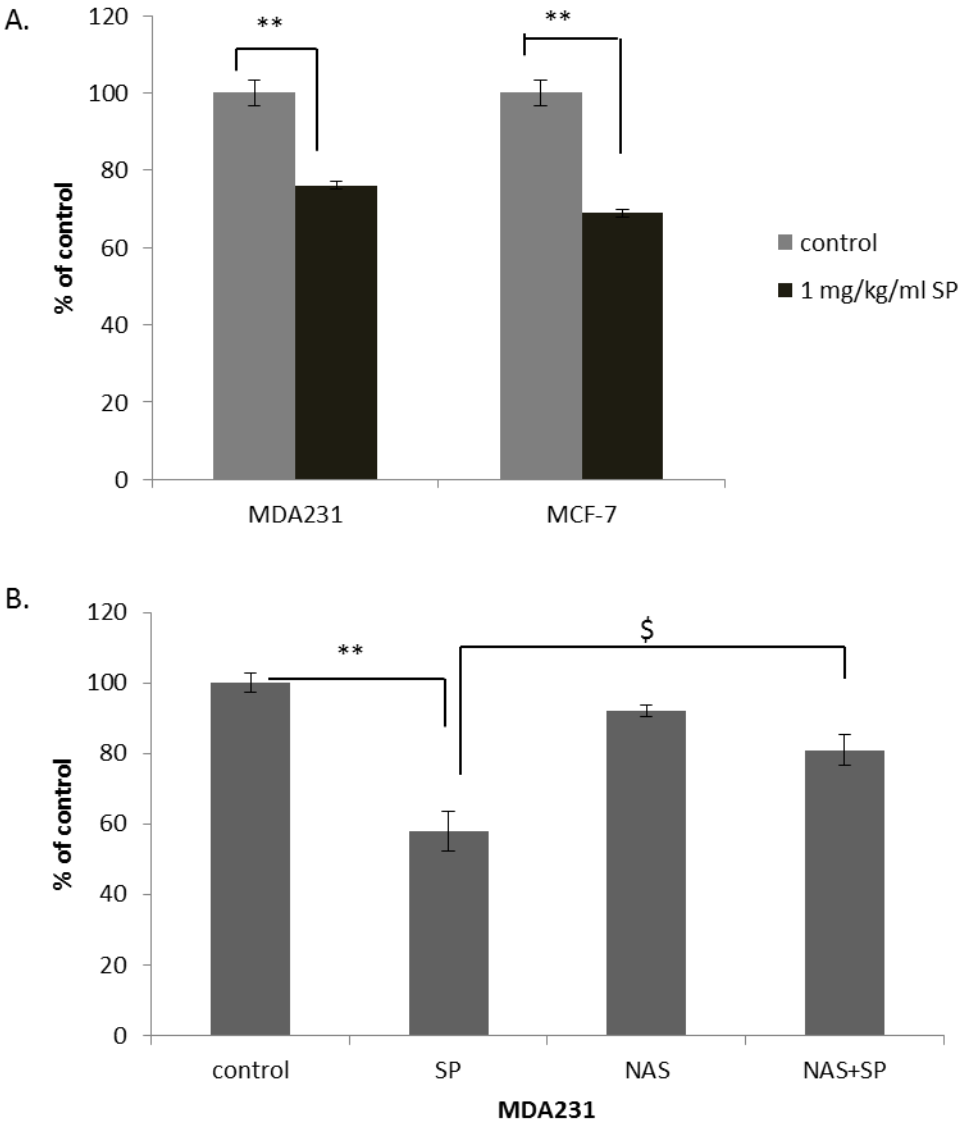

Figure 3.14 *In vivo* analysis of SP on cell survival. (A) 1mg/kg/ml SP for 48 hours in flank tumor xenografts significantly decreases tumor cell survival measured by ex-vivo clonogenic assay. (B) Animals bearing MDA231 flank xenografts given i.p. 10mg/kg NAS, a SR inhibitor, showed a significant reduction in the cytotoxic effects of SP as measured by ex-vivo clonogenic assay. Reported as the mean +/- SEM. N=. $ p<.05, ** p<.01 as measured by t test.

concluded that the cytotoxic effects of SP are mediated through recoupling of NOS and at least partially through PKG.

Having determined that SP exerted a cytotoxic effect on tumor cells grown as flank xenografts, we then wanted to assess the effects of SP on tumor growth over an extended period of time so we generated MDA231 flank xenografts and allowed them to grow unhindered until they reached approximately 150mm^3 in volume. The animals were then divided into two groups: control and SP treated. We measured the tumor volumes of the animal every 2 days until we had to sacrifice the animals as a result of the tumors getting too large. We saw that there was a significant delay in tumor growth in animals with SP in their drinking water versus control animals (Figure 3.15).

Signaling in MCF-7 cells

We had variable results when we used cell monolayers in assessing β-catenin protein levels and therefore we decided to grow our MCF-7 cells as spheroids. Growing cells as spheroids has the advantage of the cell growing in three dimensions instead of two, potentially changing how it interacts with neighboring cells. MCF-7 cells are amenable to growing as spheroids and the process is described in the methods section.

Discussion

SP, through recoupling of NOS, stimulates the catalytic activity of NOS as an NO synthase and reestablishes sGC signaling while at the same time moving the cellular environment away from pro-proliferative and inflammatory to anti-inflammatory and pro-death. Here we showed that treatment of MCF-7 and MDA231 cells with SP, whether in tissue culture or in mice, resulted in decreased clonogenicity. This effect is mediated at

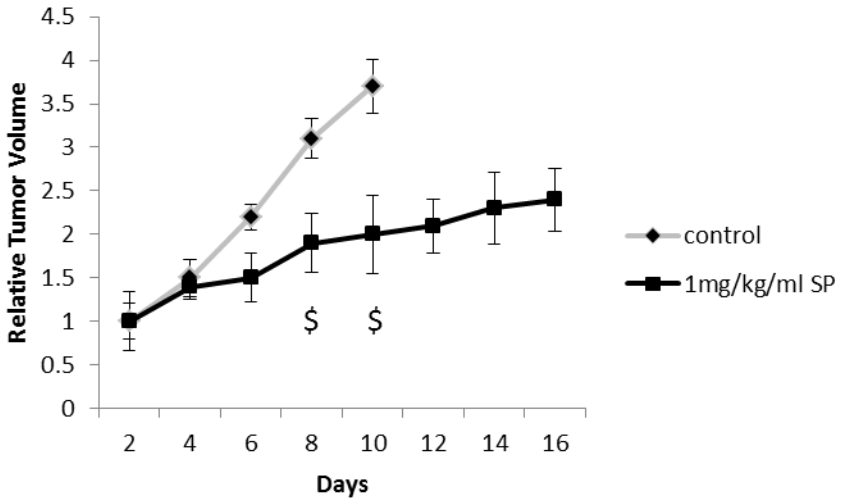

Figure 3.15 SP reduces the rate of xenograft growth. Relative volumes of control and SP treated tumors. Data presented as mean relative volume± SEM. For control tumors N=4, n=6. For SP treated tumors N=4, n=7 $ $p<0.05$ as measured by one-way anova with dunnett's post hoc.

least in part by PKG signaling through β-catenin and also through redox manipulation of two very important transcription factors in breast cancer, STAT3 and NFκB.

Studies have shown that MDA231 cells express all three NOS isoforms, but there are conflicting reports on MCF-7 cells. Some reports have shown all three, some NOSI and NOSIII, and others just NOSIII (Mathews, NE 2001 Nakatani K 2004 Fiszman G I 2007). We did not evaluate NOS expression in our cell lines but the literature has shown that BH4 has equal affinity for the three isofroms. Studies of the binding site interactions of BH4 and NOS in crystallized structures showed similar interactions between all three isoforms and they suggest that any difference in affinities of BH4 for NOS would be minimal and be as a result of changes in the hydrophobic interactions at the binding site (Kotsonis P 2001). This data suggest that as long as cells express NOS, regardless of the isoform, that SP should effectively alleviate uncoupling.

The experiments with NPH4 (Figure 3.13) are important to our findings. SP is not acting like just another anti-inflammatory. NPH4 and NAS clearly show that the effects of SP are as a direct result of modulation of BH4 levels which has an impact on the product of NOS catalytic activity. What we have shown through treatment of cells with SP is that we have a direct impact on the NOS catalytic cycle and cellular metabolism.

β-catenin downregulation

We examined several possible mechanisms for the downregulation of β-catenin signaling. GSK3β resides in complex with β-catenin and when GSK3β is dephosporylated on Ser9, an inhibitory phosphorylation, it is then able to phosphorylate

β-catenin on Ser33, Ser34, and Thr43 targeting it for ubiquitination and proteosomal degradation. The inhibitory GSK3β ser9 phosphorylation is due to pAKT signaling as seen in figure 3.2 and western blot analysis of pAKT and pβGSK3 in the breast tumor cell lines we studied demonstrated there is no change in phosphorylation or protein level in either protein after treatment with SP, indicating a different mechanism (data not shown).

Several other potential mechanism of β-catenin downregulation remained unexplored in our cell lines. There has been some evidence that PKG can directly phosphorylate β-catenin leading to its degradation [115]. The PKG inhibitor KT5823 blocks the downregulation of β-catenin and future studies could elucidate the role of PKG on phosphorylation of β-catenin through western blot of phosphorylation sites combined with mutation analysis. A mechanism that may be involved, as we do not see complete restoration of β-catenin signaling in the presence of KT5823, is the s-nitrosylation of β-catenin. Previous studies have demonstrated that β-catenin can be s-nitrosylated resulting in loss of function [116]. It is also possible that loss of β-catenin is occurring in response to STAT3 downregulation. Analysis of the gene promoter of β-catenin shows multiple STAT3 binding sites and it has been shown that loss of pSTAT3 results in loss of β-catenin [117].

p21 and p27 upregulation

The role that p21/waf1 plays in the cytotoxic effects of SP needs to be examined further. p21 prevents cancer cell growth due to its ability to transiently or permanently stop proliferation. p21 accumulation contributes to maintenance of the arrest at G_1-S

and G_2-M through inhibition of cyclin dependent kinases that regulate these cell cycle transitions. It was initially identified to be transcriptionally upregulated by p53 in response to DNA damage and is an integral part of the p53-mediated growth-arrest pathway [118]. More recent studies have shown that p21 can also be induced by various transcription factors and subsequently mediate growth arrest, senescence and apoptosis in a p53 independent manner [119, 120]. p21 and p27 have similar functions but their mechanisms of induction and regulation are distinct. While studies have shown both G_1 and G_2 to be regulated by p21, p27 has only been demonstrated to be involved in the G_1/S phase transition [121].

As discussed, p21 can exert its inhibitory effects throughout the cell cycle as well as being involved in other modes of cell signaling (Figure 3.16). A large proportion of the data on p21 shows that it inhibits the cell cycle during the G_1 phase, that it has other actions may eplain our FACS analysis. These data showed that we were not enhancing the G_1 population, at least in the timeframe we were looking at, 0-72 hours. We only examined the cell cycle out to 72 hours but recently we have discovered that some researchers are seeing G_1 arrest after 5 days even though p21 has been upregulated 3 days prior [122]. Our future studies will examine carry treatment of SP out further to determine if we see G_1 arrest at later time points.

Our future studies will examine the mode of cell death. The cells were not undergoing apoptosis, at least out to 72 hours, as the sub G_1 population remained the same. To further rule out apoptosis in these cells we looked at PARP and Caspase 3 cleavage at up to 72 hours. We saw no changes in cleavage of either protein after treatment with SP (data not shown). Experiments now focus on determining if our cells

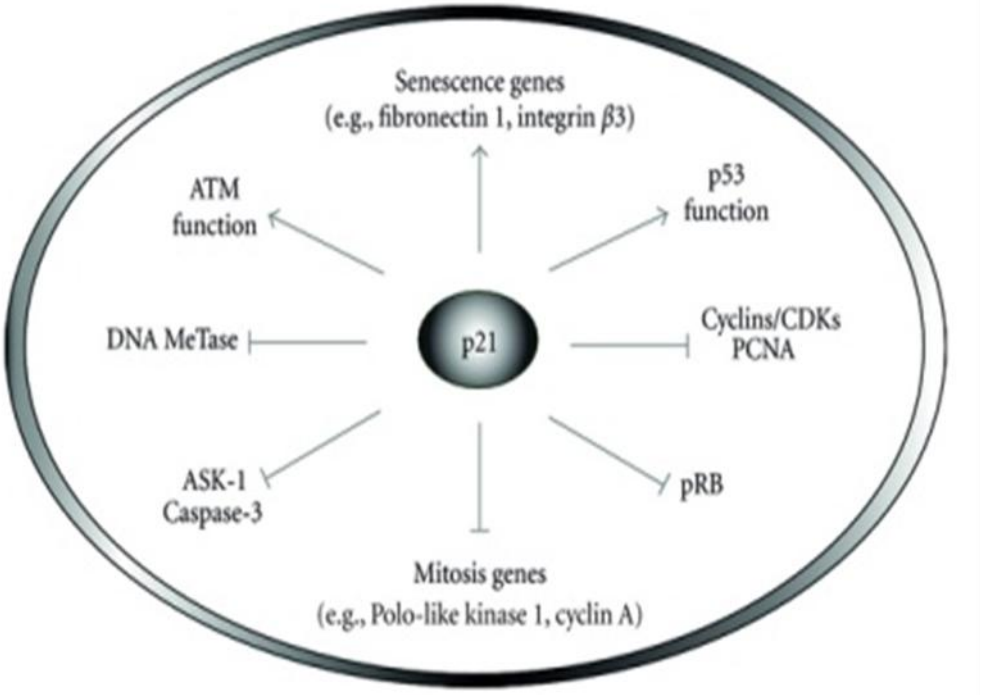

Figure 3.16 p21. p21 has the ability to regulate cells in a variety of ways.

are undergoing senescence. p21/waf1 not only regulates cell cycle progression but is also involved in regulating cellular senescence and may be a possible explanation for the effects seen in our cells after treatment with SP [123].

Inhibition of NFκB promoter binding

NFκB constitutive activation is a hallmark of various types of tumors and inhibition of its activity remains a hot topic. The activation of NFκB is inherently complex, given the multitude of signaling pathways and crosstalk. Although we have shown that NFκB activity is reduced in MCF-7 cells after treatment with SP the transcriptional outcome is still not understood. We were able to show that Bcl-2 is downregulated in MCF-7 xenografts but we are not sure of the mechanism.

We showed that we could manipulate p65 and therefore could reduce NFκB DNA binding but we had also hoped to show that NOS uncoupling resulted in NFκB activity being regulated by nitration as well. As described previously, our laboratory had demonstrated a mechanism by which NFκB became transcriptionally active following nitration of IκBα. The hypothesis was that by changing the redox environment of the cell we could switch from one activating post-translational modification to an inactivating post-translational modification, but attempts to manipulate the nitration of IκBα with SP have been unsuccessful so far.

Inhibition of STAT3 translocation to the nucleus

We show that SP decreased pSTAT3 and reduced the amount of STAT3 in the nucleus. Future studies will determine the role of changing the redox state of the cell on STAT3 activity. Changing the redox state of the cell potentially alters the activity of

RTK's through changes in PTP's activity. It has been demonstrated that PKG can activate SHP2 and this is a mechanism that could be potentially involved in the down regulation of STAT3 in our cells. JAKs, which are responsible for STAT3 activation, are highly redox sensitive and have been shown to be NO sensitive and to be activated to various degrees based on the level of oxidants in the cell [124]. There are four cysteines in the catalytic domain of JAK2 that have shown the potential to regulate activity [125].

Other considerations

Our studies have focused on manipulating the BH4 levels to restore the sanctity of NOS. As we discussed in the introduction NO signaling is ubiquitous and is concentration and context dependent. There have been other groups who examine NO signaling from an inhibitory side. Pickert et al. examined the effects that inhibition of GTP-CH had on angiogenesis and tumor growth. They demonstrated that shRNA mediated knockdown and pharmacological inhibition of GTP-CH resulted in decreased angiogenesis and tumor cell death [126]. Several concerns arise when reviewing the data. The first is that the concentration of the SR inhibitor used is 1mM all the way up to 50mM which is extremely high and would tend to suggest having several off target effects. There is an important point that we believe is missed and that our results help to shed some light on. That NOS is uncoupled in these cells and that by inhibiting GTP-CH we don't know what is happening to the BH4:BH2 ratio. They never look at the ratio. Taking another look at the data, the shGCH1 was only mildly effective in knocking down protein levels of GTP-CH. Lastly, the colony forming assay showing that shGCH1

inhibits colony formation is insignificant and we would suggest that the effects seen in the animals are through an undetermined mechanism.

The results seen in the two different cell lines were extremely similar except for the WST assay. There are several differences between MCF-7 and MDA231 cells. MDA231 cells are ER-negative and highly invasive while MCF-7 cells are ER-positive and weakly invasive. MDA231 are p53 mutant at 280K while MCF-7 cells are p53 WT, suggesting a potentially p53 independent mechanism of action. The WST-1 alludes to different mechanisms of action of SP on cell metabolism between the two cell lines. After 3 days of SP treatment the MCF-7 cells had all been arrested or killed off and this was a much greater effect than what we saw in the clonogenic assay. The only difference in the way we treated the cells was that in the clonogenic assay the cells only receive one dose of SP whereas in the WST assay the cells received fresh SP every day. Future studies should consider taking a look at concentration of NO generated in the cell, different dosing regimens and the role of p53 plays in the cytotoxic effects observed.

We used the clonogenic assay as the ultimate determinant of cell fate as studies measuring the tumor volume are difficult to assess. Cells may be dying but the tumor may swell due to poor lymphatics resulting in fluid accumulation. When we consider the tumor volume measurements, some of the animals developed tumors faster than others and this led to differences in the tumor size at the beginning of treatment. Closer examination of the data suggest that we may have seen an enhanced effect on tumor cell proliferation had we started some of the animals on SP when the tumors were smaller. The animals whose tumors were smaller seemed to have a greater response

in terms of reduction in tumor growth with SP. Studies in the next section and future studies will focus on issues like this and some of the other potential therapeutic uses of SP.

A big piece to the puzzle that was never determined was whether the effect of SP was due to actions on the stromal cells, the tumor cells, or both. Studies have shown that BH4 promotes tumor angiogenesis, however these studies were conducted on the stromal cells and not on the immortalized tumor cells [127]. Further studies are needed to determine the full effects of BH4 supplementation on cancer cells in the context of a "normal" tumor environment: immune cells, vascular cells and tumor cells all interacting.

Chapter 4:

The Therapeutic Potential of Tetrahydrobiopterin

Introduction

The focus of this chapter is on potential uses of BH4/SP as a therapeutic agent in the treatment of colitis induced colorectal cancer. Previous chapters have demonstrated how NOS is uncoupled in tumor cells and that exogenous SP helps to eliminate the encouragement to proliferate by the tumor microenvironment. The theme has been the same from the beginning: Tumor cells are supported by their pro-inflammatory, pro-proliferative environment which not only contributes to NOS uncoupling but creates a cycle by which NOS then exacerbates it. This chapter will detail the effects of SP in animal work we performed with DSS induced colitis and AOM generated colon tumorigenesis.

Role of tetrahydrobiopterin in NOS recoupling and inflammatory disease

Superoxide generation by eNOS has been demonstrated in several inflammatory disease states, including atherosclerosis, hypertension and diabetes [128-130]. Several mechanisms are employed to enhance BH4:BH2 ratios in cells to alleviate this. BH4 supplementation has been shown to be effective in reducing NOS uncoupling and improving endothelial dysfunction in hypercholesterolemia, diabetes, hypertension, coronary artery disease and heart failure [131-133]. BH4 has also been shown to reverse endothelial dysfunction in post-ischemic tissues.

The development of the hph-1 mouse deficient in GTP-CH has been used to study the human condition known as DOPA responsive dystonia which is characterized by low levels of BH4, catecholamines, and serotonin with low levels of tyrosine hydroxylase protein ([134]. These animals also exhibit hyperphenylaninemia.

The hph-1 mouse has been a useful tool for studying BH4 deficiency in cardiovascular disease and pulmonary hypertension. Pulmonary hypertension is characterized by vascular remodeling and vasoconstriction and loss of NO bioavailability has been demonstrated. The hph-1 mouse was used as a model of pulmonary hypertension as it had normal eNOS levels but reduced NO and the BH4 deficiency caused pulmonary hypertension. What Khoo et al. showed was that in hph-1 mice augmented by overexpression of GTPCH, BH4 deficiency was reduced and pulmonary hypertension prevented [135]. The hph-1 mouse could prove a useful tool in study NOS dysregulation in our lab.

DSS induced colitis and AOM induced colon cancer

As discussed, inflammation provides initiating and promoting stimuli and mediators, generating a tumor-prone environment. In this animal model, DSS provides the inflammatory environment while a single exposure to AOM provides the initiating event. In combination the latency period for tumor development is dramatically reduced In colon tumorigenesis inflammatory bowel disease (IBD) is one of three high risk conditions for the development of colorectal cancer (CRC), the others being familial adenomatous polyposis coli (APC) and hereditary non-polyposis CRC. A hallmark of inflammation and oxidative stress is increased nitration of proteins, and enhancement in the expression of iNOS in epithelial and invading inflammatory cells results is likely the

cause [136, 137]. It has been demonstrated in colitis that motility is affected by nitration and inhibition of the $Ca_V1.2$ calcium channel of colonic smooth muscle cells [138]. ROS/RNS scavengers and inhibitors of NOS have been shown to attenuate chemically induced IBD. Another study demonstrated that dietary supplementation with nitrite ameliorated DSS-induced colitis ([139].

We have demonstrated the role of NOS uncoupling in inflammation and the effects it has on the tumor environment. NFκB is intertwined in the inflammatory response and β-catenin is associated with colon cell proliferation as described earlier so we decided to determine the effects on DSS induced colitis and AOM induced tumorigenesis in the presence of SP.

Rob Cardnell, PhD and Ross Mikkelsen, PhD contributed to the following

METHODS

Mouse model of colitis:

Short-term colitis was induced by the addition of 2.5% dextran sodium sulfate (DSS; USB Corporation, Cleveland OH) to the drinking water of 5-6-week-old C57 BL/6 male mice for a period of 7 days. Mice designated for SP (Schircks Laboratories, Switzerland) treatment received 4mg/100ml SP in their drinking water continually starting 3 days before DSS treatment. All animals were monitored daily for weight, stool consistency and the presence of blood in the excreta. Disease activity index (DAI) was determined by combining scores for weight loss, stool consistency and bloody excreta as follows: Weight loss (0: <1%, 1: 1-5%, 2: 5-10%, 3:10-15%, 4: >15%); Stool consistency (0: normal, 2: loose, 4: diarrhea); Blood in excreta (0: normal; 2: reddish, 4: bloody). Long-term colitis/carcinogenesis was induced by the I.P. injection of AOM

(10mg/kg) seven days prior to the onset of DSS treatment; three week long courses of DSS were given as above separated by 2 weeks of DSS-free water. Animals were sacrificed 3 weeks after the final DSS treatment, 77 days after AOM treatment. Mice designated for SP treatment received 4mg/100ml SP in their drinking water continually starting 3 days before DSS treatment. All animals were monitored daily for weight, stool consistency and the presence of blood in the excreta. All procedures were approved by the Institutional Animal Care and Use Committee of Virginia Commonwealth University and conformed to the guidelines established by the National Institutes of Health, protocol numbers AM10080 and AM10185.

BH4/BH2 analysis:

See Chapter 2

cGMP ELISA:

See Chapter 2

Isometric Tension Recording:

Approximately 1.5-cm strips of distal colon were suspended in the longitudinal direction in an organ bath containing 15 ml of Krebs solution (118 mM NaCl, 4.6 mM KCl, 1.3 mM NaH_2PO4, 1.2 mM $MgSO_4$, 25 mM $NaHCO_3$, 11 mM glucose, and 2.5 mM $CaCl_2$), bubbled continuously with carbogen (95% O2 and 5% CO2) at 37°C under a resting tension of 1 g and equilibrated for a period of 1 h. Isometric contractions were recorded by a force transducer (model GR-FT03;Radnoti, Monrovia, CA) connected to a personal computer using Acknowledge 382 software program (BIOPAC Systems, Santa Barbara, CA). After equilibration in Krebs solution, tissues were incubated for 30 min in Ca^{2+}-free high-potassium solution (80 mM) in which equimolar NaCl was replaced by

KCl containing 0.1 mM EGTA and changed every 15 min. Cumulative dose-dependent contraction responses to $CaCl_2$ (10 μM to 10 mM) were performed in distal colon strips depolarized by Calcium-free high-K^+ (80 mM)-physiological saline solution (without EGTA). The cumulative concentration–dependent increases in tissue tension by $CaCl_2$ was analyzed among tissue strips isolated from control, DSS, DSS with SP and SP alone treated groups of mice. Experiments performed by Gracious Ross, PhD.

Histopathology

Colons were excised from animals, flushed with PBS, cut longitudinally, rolled into "swiss rolls" and immediately flash frozen in liquid N_2. Frozen swiss rolls were embedded in OCT and cryosections prepared.

For macrophage detection, frozen sections were fixed in ice-cold acetone for 10 min. After serum blocking for 60 min, the sections were stained with primary mAb for F4/80 (5 mg/mL, AbD Serotec) overnight at 4^{o}C, followed by incubation with Alexa594-labeled donkey anti-rat secondary IgG (Invitrogen) at RT for 1 hour. A negative staining control was performed by incubation with isotype control Abs.

For Hematoxylin and Eosin (H&E) staining, cryosections (20 μm) were fixed in 4% paraformaldehyde, submerged in Modified Mayer's Hematoxylin (Richard Allan Scientific), destained in acid ethanol, stained with eosin, dehydrated and mounted with permount. Images were captured using the Ariol Digital Pathology Platform.

Gene expression analysis

Colons were excised, flushed with PBS and flash frozen using liquid N_2. mRNA was extracted using the Qiagen RNase Mini Kit per the manufacturer's instructions. cDNAs were generated using the Invitrogen SuperScript III First-Strand Synthesis

System for RT-PCR per the manufacturer's instructions using 1ug total RNA per reaction and Oligo$(dT)_{20}$ primers. For quantitative PCR analysis, transcription profiles of IL-17α, IL-1β, and IL-6 were assessed on an ABI prism 7900HT Sequence Detection System using TaqMan Universal PCR Master Mix (Applied Biosystems, Foster City, CA). Primers and FAM-labeled probe sets were obtained as pre-developed assay reagents from Applied Biosystems: IL-17α, Mm00439618_m1, IL-1β, Mm01336189_m1, IL-6, Mm99999064_m1. The PCR was started with 2 min at 50 °C and an initial 10 min denaturation at 94 °C, followed by a total of 40 cycles of 15 sec denaturation at 94 °C, and 1 min of annealing and elongation at 60 °C. All measurements were performed in triplicate wells and repeated three times. Gene expression was quantified relative to the expression of the housekeeping gene β-actin, and normalized to that measured in control cells by standard 2(-ΔΔCT) calculation.

Statistics

For contraction measurements, data from different groups were analyzed by two way-ANOVA followed by Bonferroni's post-test. $P \leq 0.05$ was considered significant. For all other experiments, data are shown as mean +/-SEM with P values calculated by student's t-test.

RESULTS

SP treatment ameliorates DSS-induced colitis

To determine the effect of SP upon experimental colitis animals were placed in four groups drinking water containing DSS, SP, DSS and SP or untreated water and were monitored for the development of colitis. Colitis was measured by daily recordings

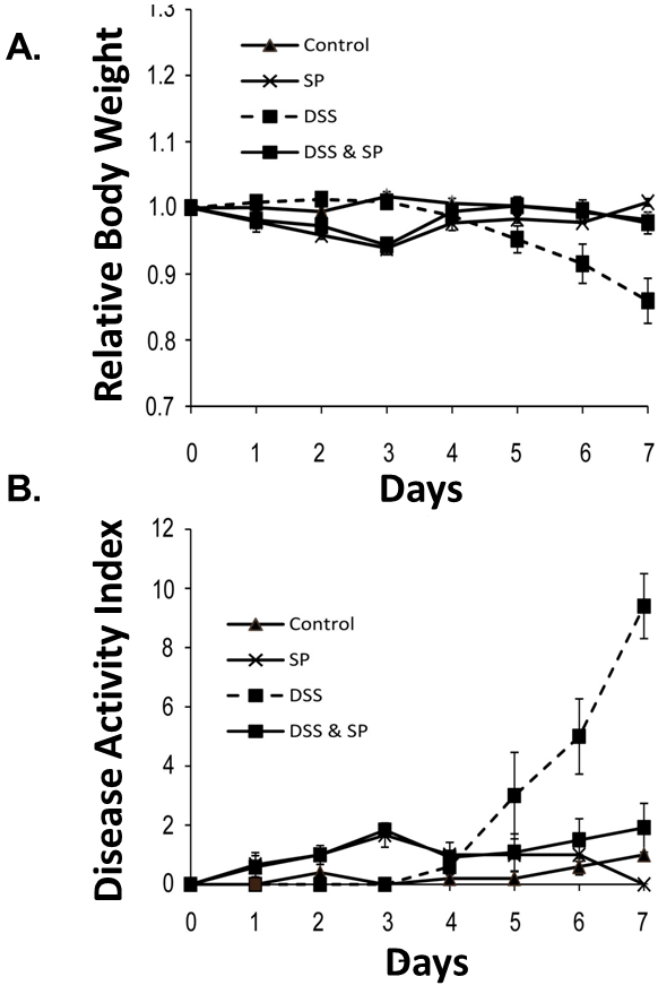

Figure 4.1. Disease activity in mice with experimental colitis. Disease activity in animals receiving 2.5% DSS in their drinking water was significantly reduced in animals that also received 4mg/100ml SP in their drinking water. Attenuated disease was observed as measured both by animal weight (A) and disease activity index (B). Data presented as mean ± SEM, n=5 per group.

of weight, stool consistency, and the presence of blood in the excreta. As shown in Figure 4.1A, by day 7 animals receiving DSS have lost 14% of their starting body weight. The weight loss in DSS treated animals was prevented by the addition of SP to the drinking water. Similarly, the disease activity index (Figure 4.1B) was significantly increased in only the DSS treated animals at day 7. The development of DSS-induced colitis and its partial mitigation by co-treatment with SP was also monitored by H&E staining of frozen sections of colons from treated animals. As shown in Figure 4.2, a loss of villi and crypts is observed in the DSS alone treated colon and co-treatment with SP mostly mitigates this change in colonic morphology. Separation of the muscle and muscularis mucosae is predominantly observed in both the DSS-treated colons but was also observed to some degree in SP colons indicating mild colitis in DSS with SP colons that is not detected by assessment of the disease activity index.

Reduced calcium-induced contraction in murine colitis is restored by SP

Cumulative addition of $CaCl_2$ induced a concentration-dependent contraction in both control and inflamed (DSS treated) distal colon depolarized by Ca^{2+}-free high potassium (80 mM) physiological saline solution. DSS treatment significantly ($P \leq 0.01$) reduced the overall calcium-induced contraction curve (Figure 4.3A, B & C), as analyzed by two-way ANOVA ($F(1,28)=8.30$). In vivo treatment of SP reversed the reduced $CaCl_2$-contraction in the DSS treated group (Figure 4.3B & E) without affecting the contractility in the control group (Figure 4.3D) (DSS plus SP, $F(1,28)=26.65$; SP, $F(1,28)=0.42$, two–way ANOVA, n=3 per group). The efficacy of $CaCl_2$ is significantly ($P \leq 0.001$) enhanced by SP treatment in the DSS treated group, unlike in otherwise untreated animals.

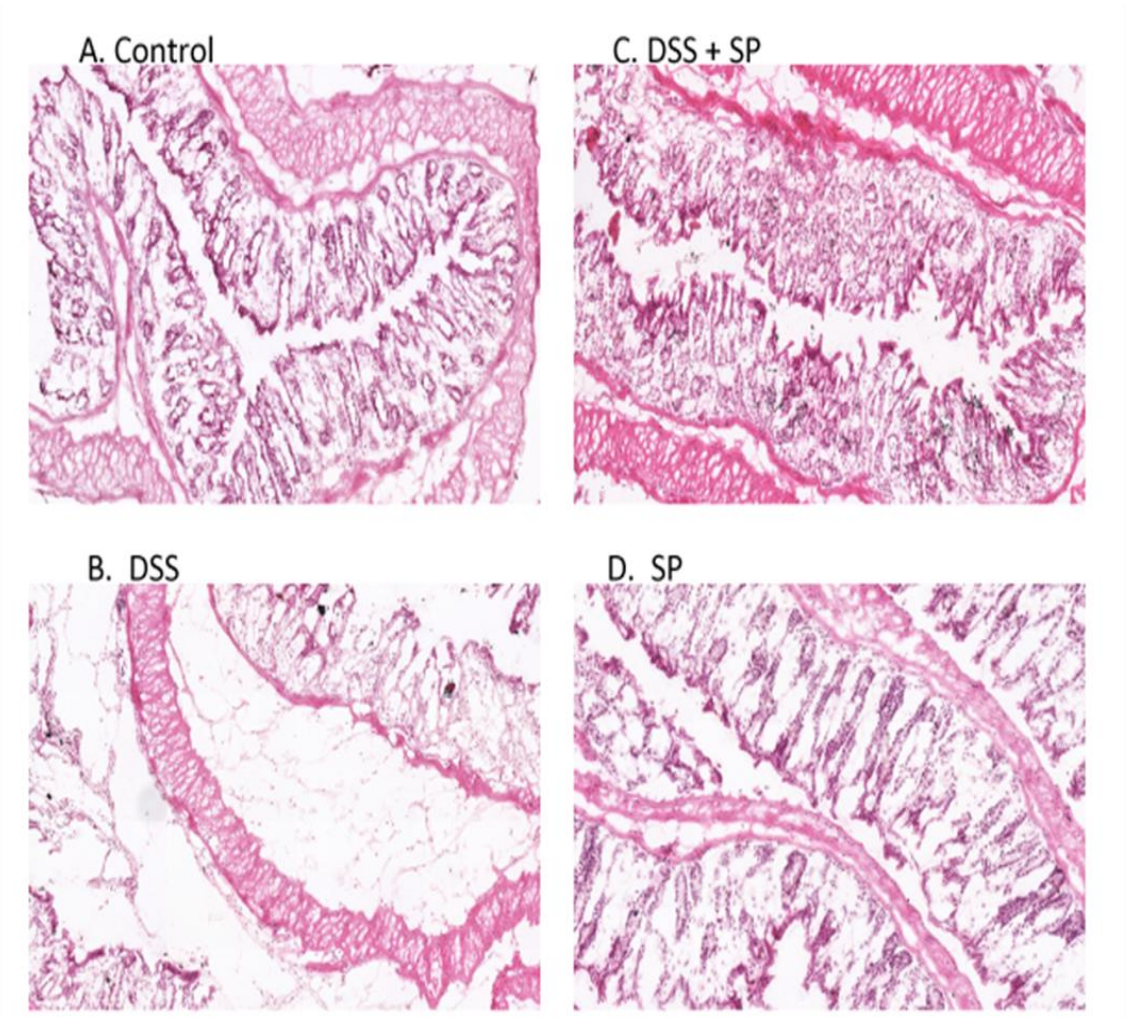

Figure 4.2. H&E staining of colons from control and treated mice. H&E stained frozen sections of colon "swiss rolls". Swiss roll preparations allow the visualization of the whole colon distal (D) to proximal (P) in a single section. Note Typical overview images (A) and 20X magnification (B).

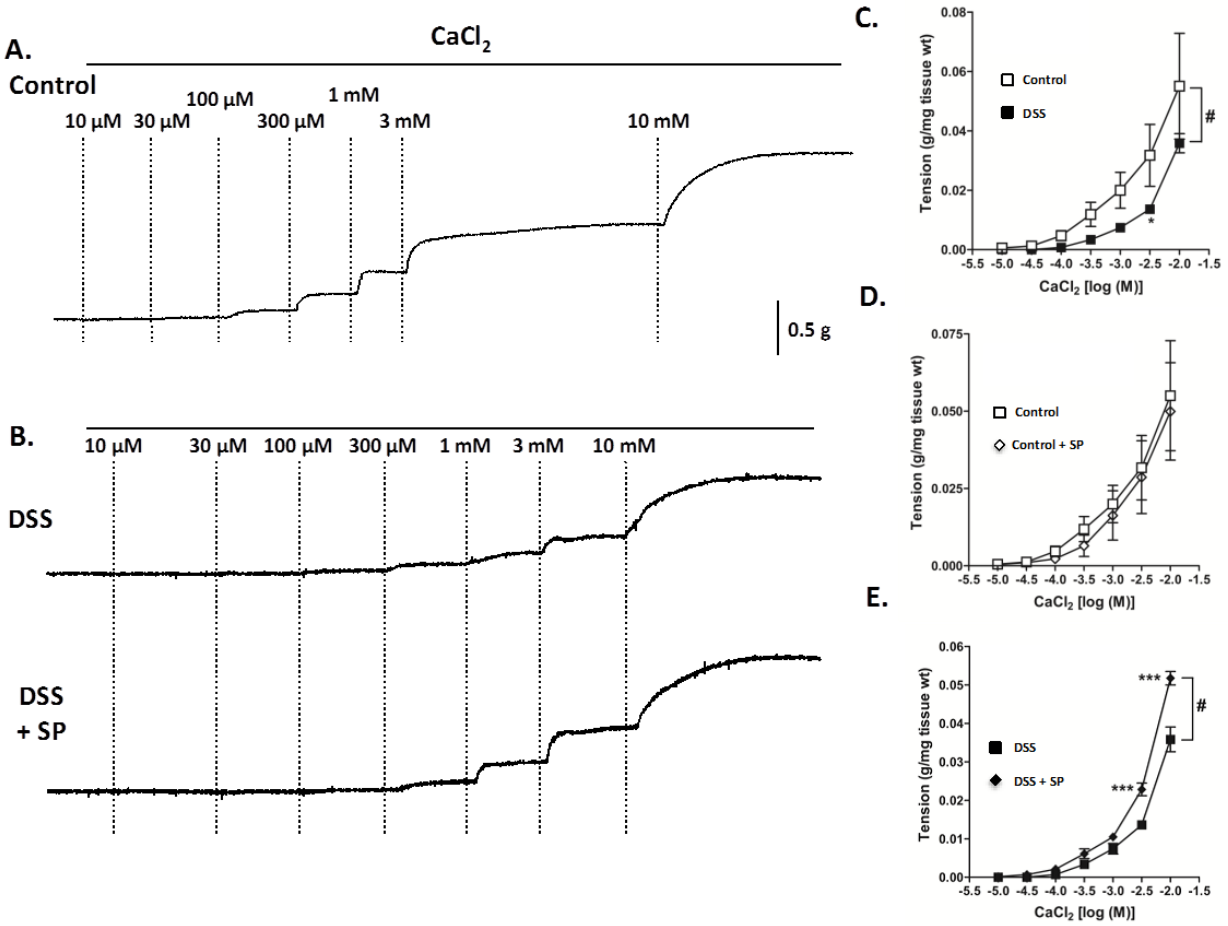

Figure 4.3. Colon contractility in DSS-induced colitis. Representative isometric tension recording of $CaCl_2$–induced concentration–dependent contraction of distal colon tissue strips from A) control, B) DSS and DSS with SP treated mice. Right panel displays graphical representation and comparison of concentration–dependent $CaCl_2$ –induced increase in tension of colon muscle strips: C) control vs DSS, D) Control vs SP, and E) DSS vs DSS and SP. Note that inflammation decreased the contraction while treatment with SP increased the $CaCl_2$–induced contraction in inflamed tissues. Data are expressed as mean ± SEM, and analyzed by Two-Way ANOVA followed by Bonferroni post test, n=3 per group.

The DSS-induced inflammatory response is reduced by SP treatment

DSS treatment is known to elicit an inflammatory response that includes the recruitment of infiltrating immune cells such as macrophages. As SP treatment is expected to be anti-inflammatory we stained colon sections for the presence of macrophages. The top row of images of Figure 4.4 (F4/80 plus DAPI) show that infiltration of inflammatory macrophages is observed throughout the length of the mouse colon after DSS treatment and this is mostly reversed by inclusion of SP in the drinking water of mice. Higher magnifications are also shown in the lower rows of images. These results confirm that DSS treatment elicits an inflammatory response and that it is at least partially reversible with SP. To determine how SP treatment reduced macrophage recruitment in DSS-treated colons, gene expression analysis was performed to determine the expression of pro- and anti-inflammatory cytokines. As shown in Figure 4.5, DSS treatment elicited significant increases in the expression of mRNA for the pro-inflammatory cytokines IL-1β, IL-6 and IL-17A. This increased cytokine expression is blocked by the addition of SP to the drinking water. We also assayed for the anti-inflammatory cytokine IL-37 since this cytokine has been shown to protect the mouse colon from DSS induced colitis [140]. However, IL-37 expression was not detected in any of the colon samples tested. The observed changes in cytokine expression indicate that SP acts by disrupting both the acute phase response and delayed-type immune reaction.

DSS reduced cGMP is blocked by treatment with SP

To determine if DSS induced inflammation decreases NOS coupling and thus NO production we assayed the BH4:BH2 ratio following 7 days DSS treatment. Colonic

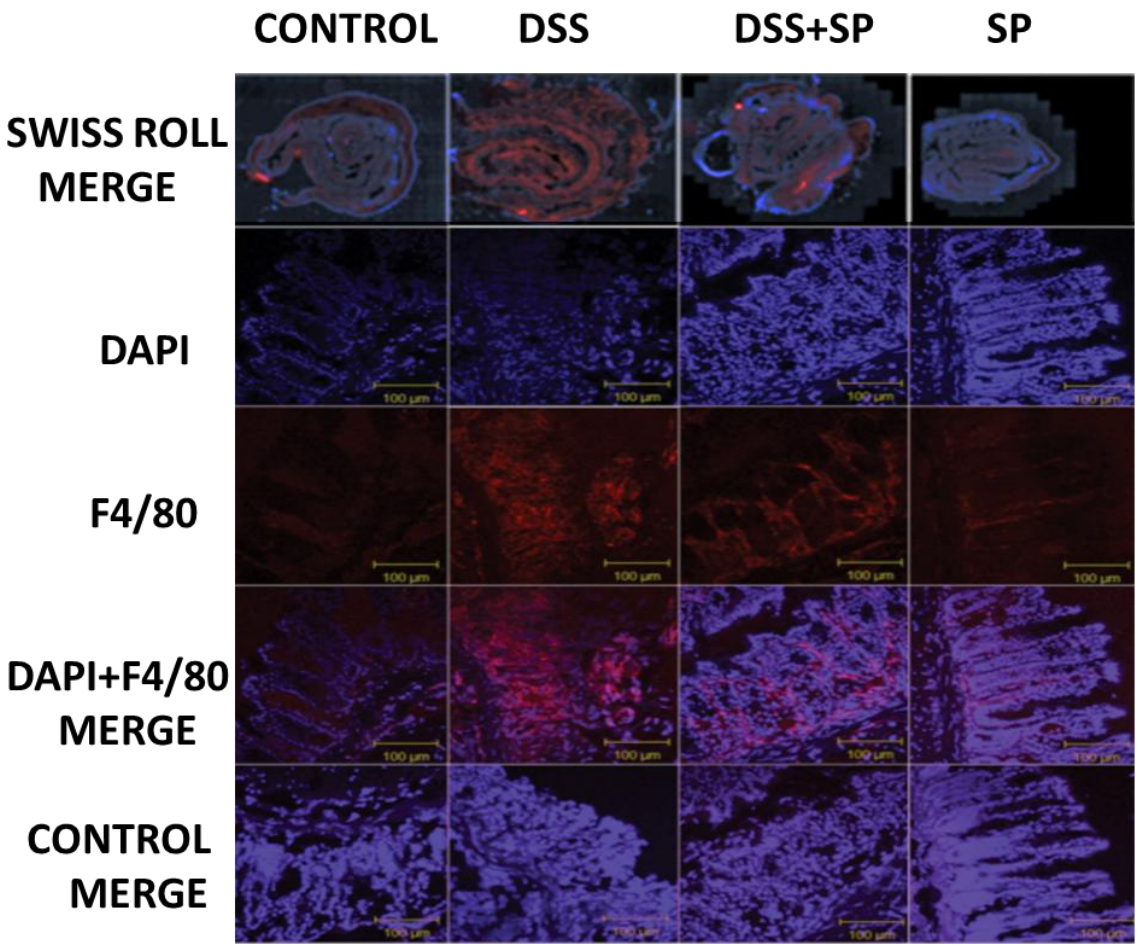

Figure 4.4. Decreased infiltrating macrophages in SP co-treated colons. Cryosections were stained for the macrophage marker F4/80 and analyzed by immunofluorescence.

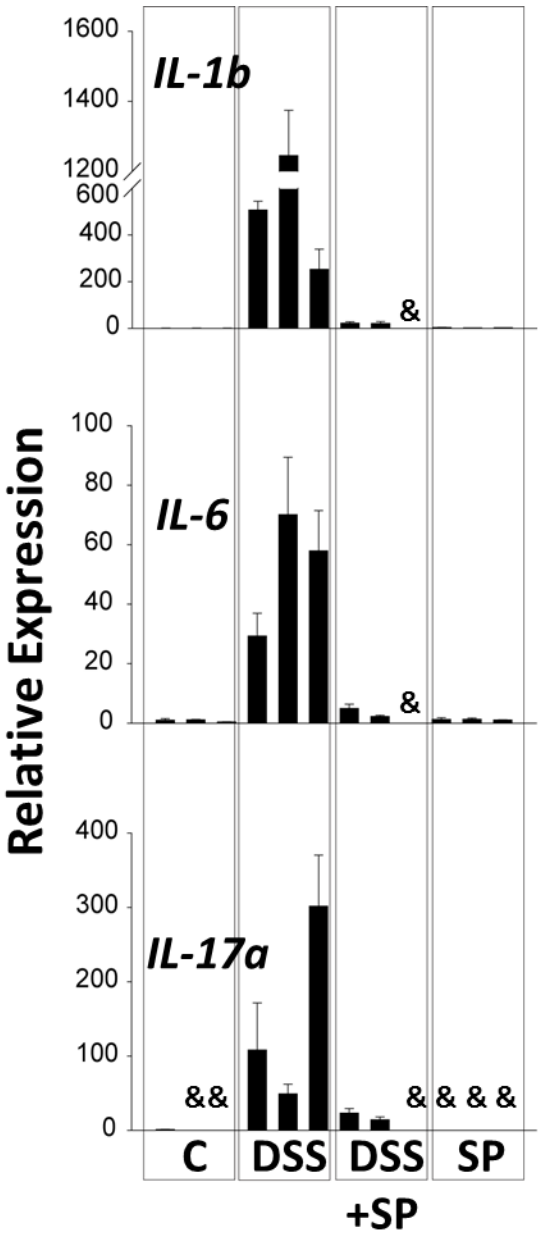

Figure 4.5. Increased pro-inflammatory cytokine expression of diseased colons is reduced by SP treatment. The results represent the average of 3 samples +/-SEM.

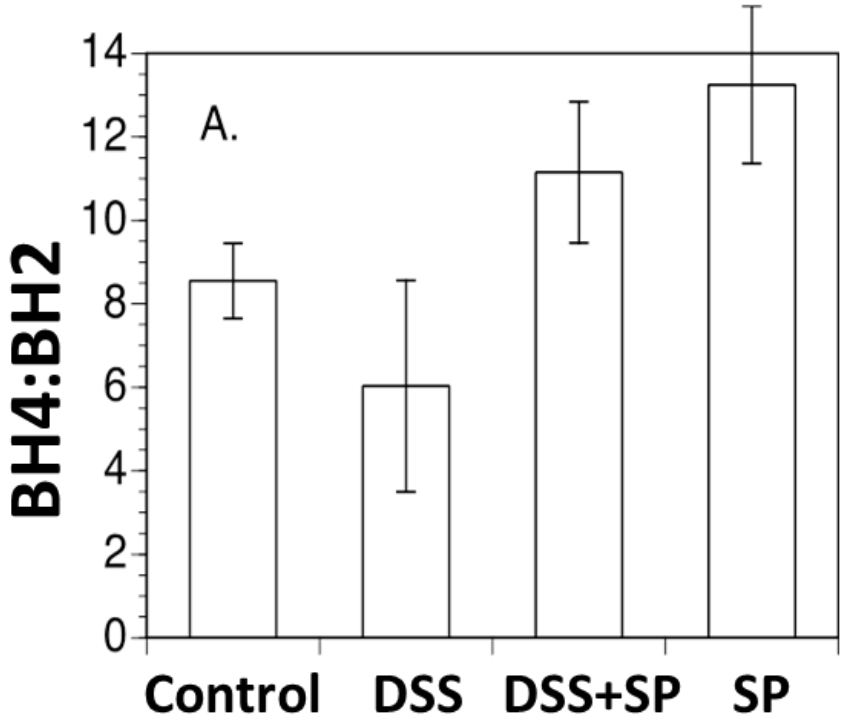

Figure 4.6. BH4:BH2 levels in colons from control and treated mice. A. BH4 and BH2 were measured by HPLC analysis as described in Materials and Methods. Each bar represents the mean +/- SEM of four colons for each treatment.

cGMP levels were also measured at this time as an indirect measure of coupled NOS activity. Figure 4.6 shows the results from one experiment where the BH4:BH2 was measured at day 7 of DSS treatment. While the trend of lower BH4:BH2 with DSS treatment was observed the magnitude of the change never reached statistical significance due to the high variability between samples. SP treatment with or without DSS, however, increased the BH4:BH2. While we were unable to observe any significant change in the BH4/BH2 ratio with DSS treatment, production of cGMP – an indirect measure of NO production – was significantly reduced in DSS treated colons (Figure 4.7B, $P<0.01$). The DSS-induced reduction in levels of cGMP was reversed by SP treatment. SP alone significantly increased cGMP production relative to control animals. That SP treatment reverses the effect of DSS on colon cGMP levels suggests that increased NO generation is required. To further test this mechanism we used the sGC inhibitor, ODQ, which is an irreversible inhibitor of sGC. In these experiments, ODQ was delivered i.p. on a daily basis with changes in the SP-containing water. As shown in Figure 4.7B, ODQ blocked the activity of SP to prevent the decrease in cellular cGMP in the colons of mice treated with DSS. Parallel experiments were performed in which the DAI of the animals were measured. As shown in Figure 4.7A, ODQ also prevented the SP-induced recovery in the DAI of DSS treated animals.

SP inhibits DSS-induced protein tyrosine nitration

Previous investigators have termed uncoupled NOS as a “peroxynitrite synthase”. Thus if uncoupling of NOS occurs with DSS treatment one would expect increased protein Tyr nitration as has been observed in numerous studies with DSS-induced colitis, e.g. (Yasui et al., 2007; Westbrook and Schiestl, 2010). As shown in

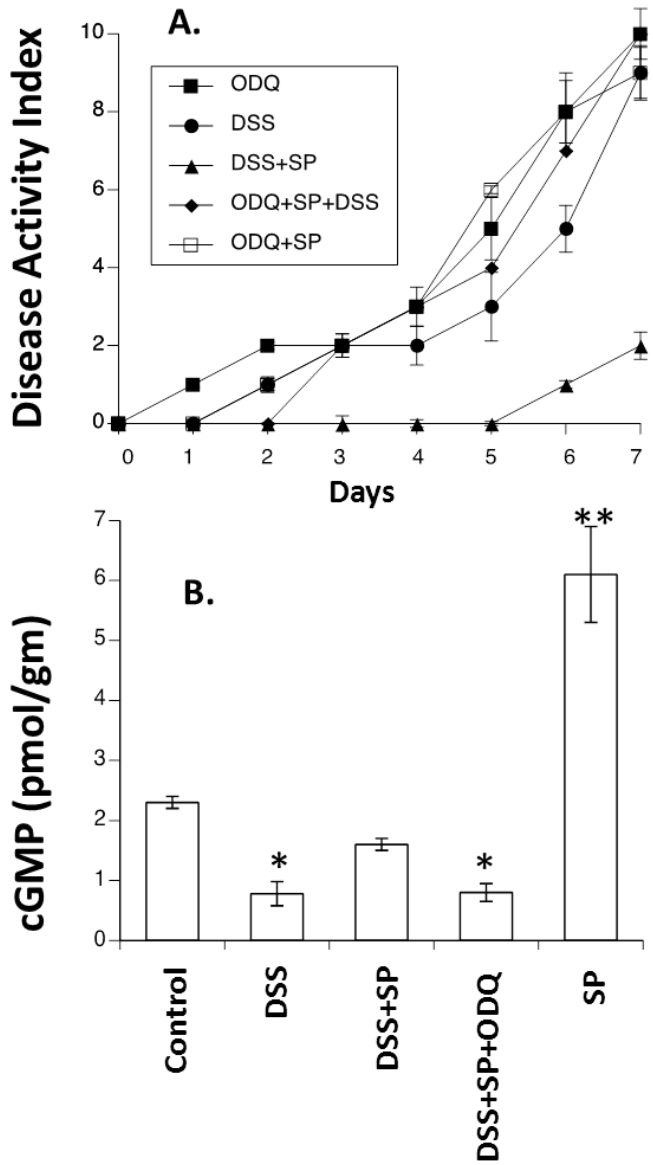

Figure 7. The sGC inhibitor, ODQ, inhibits the SP mitigation of DSS-colitis and blocks SP induced cGMP increases in DSS treated colons. A. DAI was measured as described in Figure 1. B. cGMP assayed by ELISA shows decreased cGMP production in DSS-treated whole colons that is restored when animals also received SP. cGMP is an indirect measure indicating decreased NO production in DSS-treated colons. Data presented as mean ± SEM, 4 colons per treatment group with *P<0.05 for DSS and SP compared to Control or DSS+SP

Figure 4.8, DSS treatment enhances colonic protein Tyr nitration as detected by immunofluorescence and this was abrogated by co-administration of SP. Statistical analysis demonstrated a >5-fold increase in nitro Tyr staining relative to DAPI fluorescence in the colons from DSS treated animals compared to controls and SP+DSS treated animals ($p<0.01$, n=3 animals per treatment group and 3 images per animal). As shown in image N, a magnification of image J, the increased nitro Tyr staining was due not only to infiltrating inflammatory cells but also colonic epithelial cells. This result along with the observed changes in cGMP and their reversibility by treatment with the BH4 precursor, SP, are consistent with uncoupling of NOS in DSS-induced colitis.

SP shows protection against AOM/DSS induced adenocarcinoma

Given that SP protects against the development of DSS-induced colitis we tested the hypothesis that this protection may extend to preventing the development of AOM/DSS induced CRC. Animals received a dose of AOM followed by three one-week courses of DSS with or without SP co-treatment. Following 70-days of treatment, colons were excised and assayed morphologically for tumor development. Individual single treatments with AOM or DSS did not induce cancer formation as previously described (Neufert et al., 2007). As seen in Figure 4.9A, the combined AOM+DSS treatment induced tumor formation that was significantly reduced by co-treatment with SP ($P<0.05$). In the ten animals treated with AOM+DSS as described, the number of tumors per distal colon ranged between 2 and 8. The ten animals in the AOM+DSS+SP group the number of tumors per colon ranged between 0 and 3. The modest increase (15%) in colon length with SP treatment was insufficient to account for the difference observed

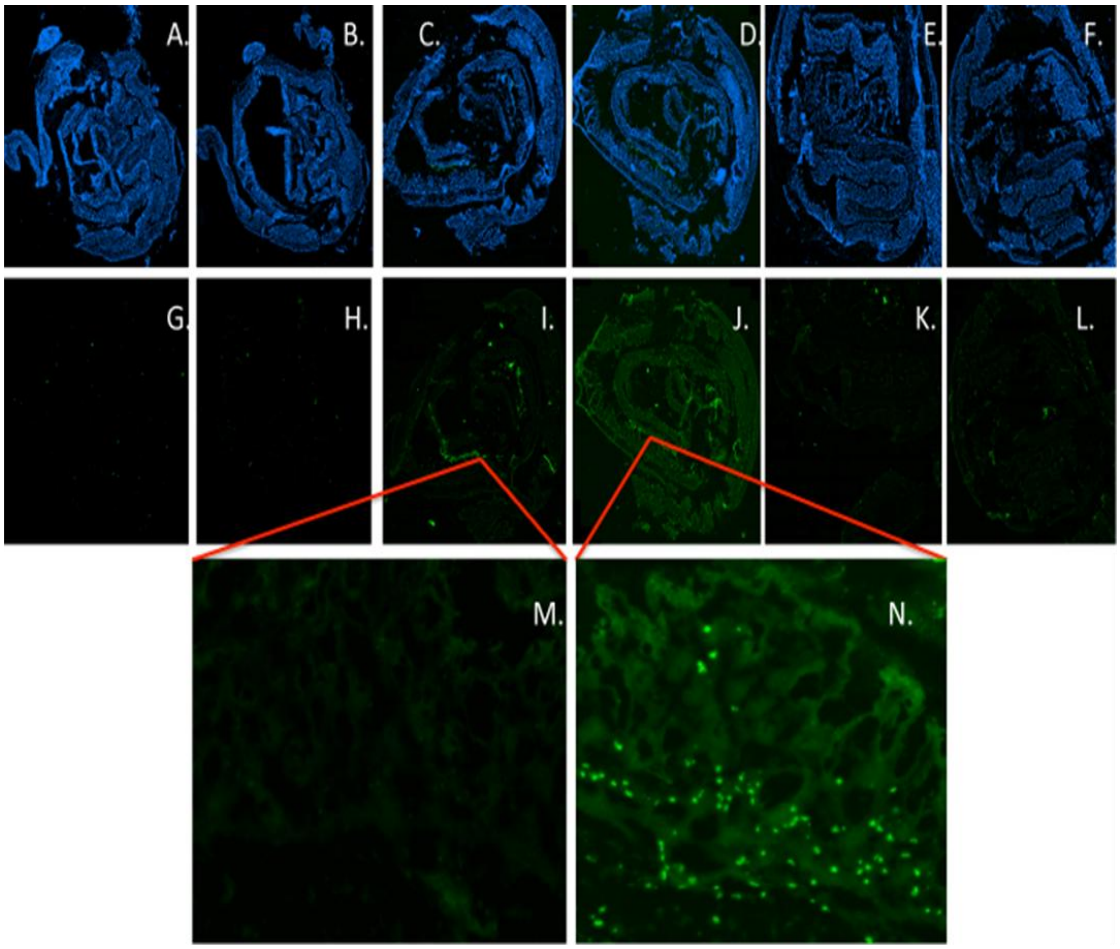

Figure 4.8 NitroTyr staining is increased in diseased colons by a mechanism inhibited by SP. Images A-F are DAPI+fluorescein-Avidin stained Swiss rolls with images G-L the corresponding fluorescein-Avidin stained sections with the blue DAPI fluorescence off. Lanes A+G (no primary anti-nitroTyr) and B+H (+primary anti-nitroTyr) are adjacent cryostat sections from the colons of untreated animals; C+I (no primary anti-nitroTyr) and D+J (+primary antinitroTyr) are adjacent colon sections from DSS treated animals; E+K (no primary anti-nitroTyr) and F+L (+primary anti-nitroTyr) are adjacent sections from the colons of DSS animals rescued with SP. Images M and N are magnifications of sections from the adjacent images I and J showing infiltration of inflammatory cells into the colon of DSS treated animals as well as increased nitroTyr staining of epithelial cells.

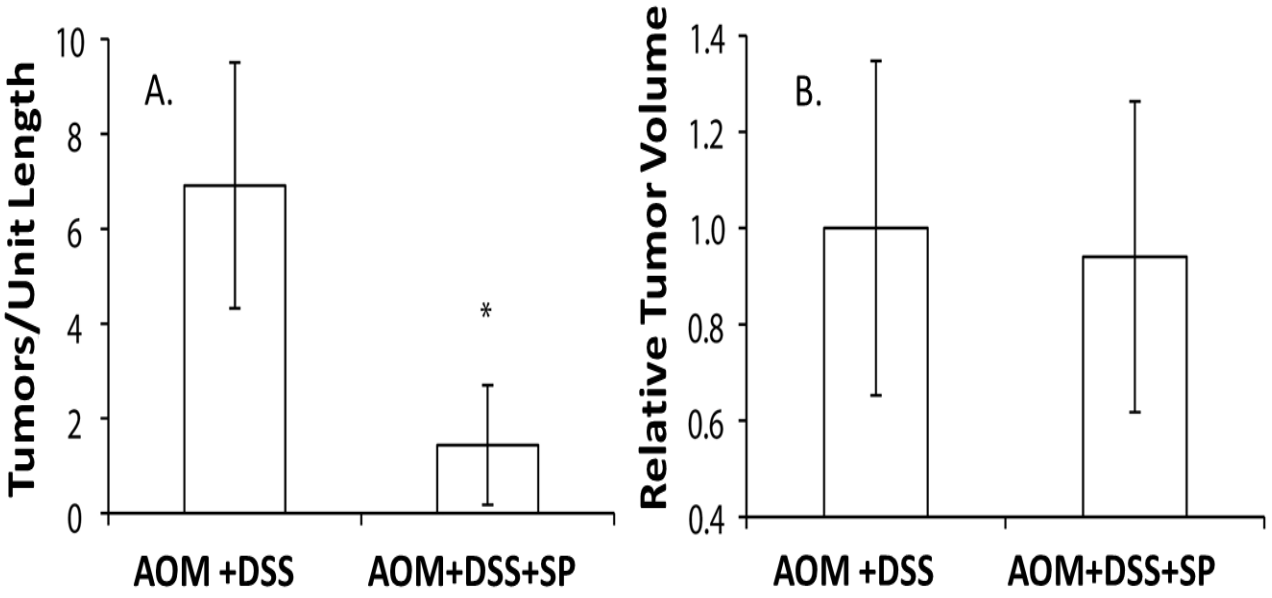

Figure 4.9. Reduced DSS/AOM induced colon tumorigenesis in SP treated animals. A. Number of tumors identified per unit length of colon in Swiss rolls. The results represent the mean plus SEM for n=10 for each treatment group with a *P<0.05. B. Relative size of tumors evaluated digitally from H&E stained sections.

between the two groups. Interestingly, the SP co-treatment did not decrease the average size of those tumors that do develop (Figure 4.9B) suggesting that SP acts to limit tumor initiation rather than restricting tumor progression. However, tumors were harvested at a relatively late time post-initiation and effects of SP on tumor progression would have been missed.

Discussion

By multiple criteria, we have demonstrated that co-treatment of animals with SP counteracts the colitis inducing effects of DSS. Thus SP treatment blocks the increased DAI, the loss of microvilli and crypts, and recovers the Ca2+-induced contractility responses lost as a consequence of DSS treatment. In addition the experimentation demonstrates that SP treatment reduces the inflammatory response measured as either increased numbers of infiltrating inflammatory macrophages and neutrophils or increased expression of pro-inflammatory cytokines IL-1β, IL-6 and IL-17A. Our studies also show that by minimizing inflammation SP also decreased the numbers of tumors formed as a consequence of tumor initiation with the carcinogen AOM.

The initial hypothesis for this study was that DSS treatment would further promote the chronic inflammatory environment characteristic of colitis by reducing the BH4:BH2 ratio and uncoupling NOS activity resulting in the generation of ROS/RNS. However, the observed changes in the colonic BH4:BH2 ratio while consistent with the hypothesis were not statistically significant. Although a significant decrease in the BH4:BH2 was not measured in the colons from DSS-treated animals, the observed changes in cGMP levels and protein Tyr nitration following DSS treatment and their

reversibility with SP are consistent with NOS uncoupling. A previous study demonstrated that DSS-induced colitis is associated with inhibition of colonic sGC activity leading to lower cGMP levels [141, 142]. The underlying mechanism for the inhibition was not established but protein levels and mRNA levels of NOS remained unchanged. These authors argued that the reduced sGC activity was associated with a decreased colonic responsiveness to nitrergic stimuli. More recently a mechanism for the inactivation of sGC in inflammatory conditions has been shown to involve oxidation of the heme cofactor of sGC [143]. Protection of sGC from oxidative inactivation *in vitro* was achieved by culturing cells with BH4 or its precursors BH2 and SP. This latter mechanism can occur without changes in the BH4:BH2 and NOS coupling. Measurements of total BH4:BH2 in the whole distal colon do not necessarily reflect changes in the different cellular compartments of the colon that may have an impact on colitis. For example, DSS-induced NOS uncoupling in nitrergic neurons by disrupting the normal nicotinic-nitrergic communication could by inhibiting cholinergic signaling increase secretion relative to absorption and thereby stimulate diarrhea[144]. The immunofluorescent images of protein Tyr nitration also suggest localized changes in NOS activity with DSS treatment.

Colitis is a consequence of the relative changes in secretory and absorptive functions of the colon that results in changes in gastrointestinal motility. Genetic, environmental, microbial and immunological factors all play a role ultimately resulting in loss of barrier function and the pathological invasion of inflammatory cells into the mucosa and increased expression of inflammatory cytokines. It remains unclear how these different factors relate to one another in initiation and progression of colitis and

where NO signaling and biopterins such as BH4 and SP contribute to the development and prevention of colitis. One mechanism that deserves consideration also involves sGC and its role in inhibiting the recruitment of inflammatory cells to sites of tissue injury [145]. In endothelial cells sGC activity inhibits inflammatory cell recruitment by blocking P-selection expression. Thus besides restoring maintaining barrier function and the normal balance of secretion and absorption, SP by protecting sGC from oxidative inactivation may also mitigate the effects of DSS-induced colitis by preventing the recruitment of inflammatory cells.

The three cytokines examined, IL-1β, IL-6, and IL-17 have all been associated with DSS induced colitis and with colon CRC [146-148]. One unifying feature for all three cytokines is their transcriptional regulation by NF-κB [149]. A relatively specific inhibitor of NF-κB, dehydroxymethylepoxyquinomicin, inhibits the mRNA expression of IL-β, IL-6, TNF-α, IL-12p40, IL-17A and MCP-1 and also suppresses both DSS and TNBS-induced colitis. Our results from studies in Chapter 3 show that SP can inhibit NFκB activation and this is potential mechanism of how macrophage infiltration is decreasing. Our lab showed that low inflammatory levels of RNS result in the nitration Tyr181 of IκBα, the inhibitor protein of NF-κB, dissociating the complex and facilitating translocation of active transcription factor, p65/p50, into the nucleus [25]. SP treatment by increasing the BH4:BH2 recouples NOS activity enhancing NO generation and reducing RNS generation necessary for Tyr nitration as well as s-nitrosylating p65 reducing NFκB activity. Thus recoupling of NOS inhibits NF-κB activity leading to suppression of the inflammatory response critical for colitis and colitis associated carcinogenesis. The mechanism of SP's actions is still to be determined but these

results suggest a potential approach in mitigating colitis and associated CRC by modulating colonic BH4/cGMP metabolism. One potential candidate is a synthetic BH4, Kuvan, currently used for treatment of some types of phenylketonuria. Kuvan is also being examined in Phase 2 trials for treatment of different inflammatory and vascular diseases [150, 151].

Chapter 5

Perspectives

Through the course of this dissertation I have identified NOS as uncoupled in several tumor cell types both *in vitro* and *in vivo*. The experiments and results here have looked at the tumor cell and the inflammatory tumor environment from a new perspective of NOS dysregulation. I have demonstrated that a portion of SP's effects lie in reducing ROS mediated pro-inflammatory signaling in the cell. Depending on the cell type the actual pathways manipulated may be different. I have demonstrated that by reducing the activity of NFκB and STAT3 in MCF-7 cells, SP reduces the pro-survival "inflammation begets inflammation" cycle that tumor cells thrive in. The big question remaining is whether the effects we see are mediated by the stromal cells, by direct effects on tumor cells or both. As TAM's generate large amounts of NO and are more than likely the source of the majority of uncoupled NOS (NOSII) in the tumor environment, the development of an inducible GTP-CH would be critical in understanding the effects of SP. Other considerations are the role that GTP-CH plays in NOS uncoupling and whether SP could be used to remodel vasculature in conjunction with other therapeutics.

Does GTP-CH or SR function as a tumor suppressor gene?

Published results have shown that in some inflammatory disease states, as in diabetes mellitus, proteasome dependent degradation of GTP-CHI causes BH4 deficiencies [152]. We discussed the importance of this previously as the loss of NO bioavailability is a cardinal feature of endothelial function. These researchers suggested that inflammation induced $ONOO^-$ results in nitration of the 26S proteasome resulting in activation. Low GTP-CH has the same effect on NOS as BH4 oxidation to BH2.

Other researchers have suggested that induction of vascular GTP-CH and endogenous BH4 synthesis protect against inflammation induced endothelial dysfunction in atherosclerosis. In this case, BH4 acts a defense mechanism against inflammation induced endothelial dysfunction [153]. In our future studies western blot analysis of GTP-CH and RT-PCR of tumor tissue and normal tissue can be used to determine protein and mRNA levels of GTP-CH.

There is no evidence of SR reduction or induction in the literature as a response to inflammatory stimuli. However, since SR is necessary for the endogenous synthesis of BH4 and for the conversion of exogenous SP to BH4 it may be worth examining in a similar fashion.

SP in vascular normalization or as an adjuvant in treatment

The literature has some reports of pro-survival and pro-angiogenic findings in tumor cells in the presence of exogenous BH4, and has been shown to be mediated through activation of PI3 Kinase [154]. The inhibiting angiogenesis argument stems from angiogenesis enhancing tumor vasculature leading to enhanced tumor blood flow,

promoting tumor growth. Dysregulation of angiogenesis occurs in various pathologies and is one of the hallmarks of cancer. The imbalance of pro- and anti-angiogenic signaling within tumors creates an abnormal vascular network [155]. These abnormalities and the inflammatory microenvironment fuel tumor progression and lead to reduction in the efficacy of chemo, radio, and immunotherapy. The implications of enhancing tumor vasculature are of significant importance for the possible implementation of combination therapeutic strategies. Tumors are known to be poorly vascularized and this can lead to resistance to some chemotherapeutics. Normalizing the function and structure of tumor vasculature will make the tumor more available to drug delivery. Normalizing tumor vasculature increases oxygen delivery to the tumor and as oxygen is a potent radiosensitizer, increases the efficacy of radiotherapy.

Preliminary studies conducted in our laboratory show that SP may lead to enhanced vascularization due to increased presence of blood in the tumor. In figure 5.1 we can see that tumors treated with SP are more vascularized compared to control. Future studies can be undertaken to determine the extent to which SP would enhance the efficacy of current therapeutics.

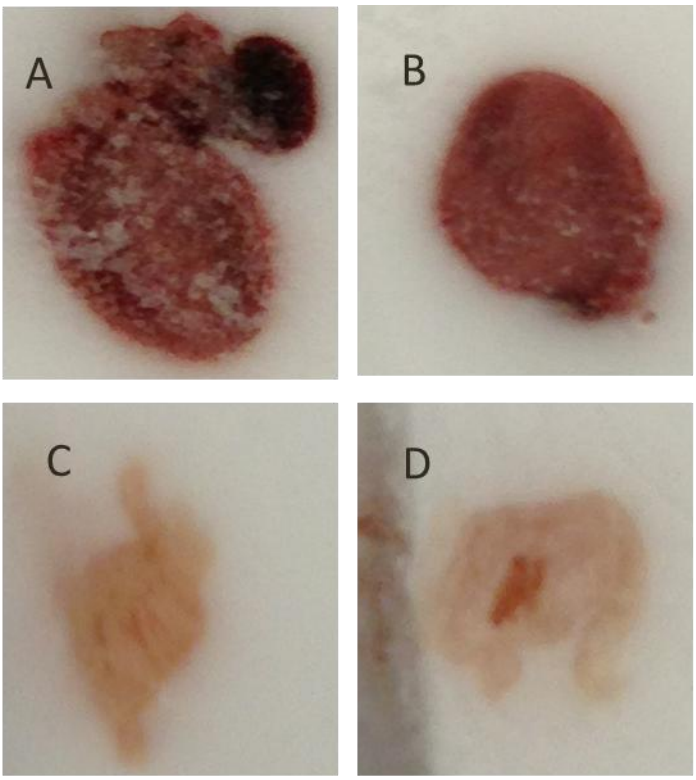

Figure 5.1 Enhanced vascularization of SP treated tumors. MDA 231 flank xenografts were treated with 1mg/kg/ml SP in their drinking water for 72 hours (A and B) or were left untreated (C and D). It can be seen that SP treated tumors show signs of enhanced vascularization as there is enhanced blood flowing through the tumor.

Literature Cited

1. *Balkwill, F. and A. Mantovani, Inflammation and cancer: back to Virchow? Lancet, 2001. 357(9255): p. 539-45.*
2. *Dvorak, H.F., Tumors: wounds that do not heal. Similarities between tumor stroma generation and wound healing. The New England journal of medicine, 1986. 315(26): p. 1650-9.*
3. *Atherton, J.C., The pathogenesis of Helicobacter pylori-induced gastro-duodenal diseases. Annual review of pathology, 2006. 1: p. 63-96.*
4. *Schiffman, M., et al., Human papillomavirus and cervical cancer. Lancet, 2007. 370(9590): p. 890-907.*
5. *Kuper, H., H.O. Adami, and D. Trichopoulos, Infections as a major preventable cause of human cancer. Journal of internal medicine, 2000. 248(3): p. 171-83.*
6. *Maeda, H., T. Okamoto, and T. Akaike, Human matrix metalloprotease activation by insults of bacterial infection involving proteases and free radicals. Biological chemistry, 1998. 379(2): p. 193-200.*
7. *Yakovlev, V.A., Nitric oxide-dependent downregulation of BRCA1 expression promotes genetic instability. Cancer research, 2013. 73(2): p. 706-15.*
8. *Brigati, C., et al., Tumors and inflammatory infiltrates: friends or foes? Clinical & experimental metastasis, 2002. 19(3): p. 247-58.*
9. *Baron, J.A. and R.S. Sandler, Nonsteroidal anti-inflammatory drugs and cancer prevention. Annual review of medicine, 2000. 51: p. 511-23.*
10. *Garcia-Rodriguez, L.A. and C. Huerta-Alvarez, Reduced risk of colorectal cancer among long-term users of aspirin and nonaspirin nonsteroidal antiinflammatory drugs. Epidemiology, 2001. 12(1): p. 88-93.*
11. *Andrew, P.J. and B. Mayer, Enzymatic function of nitric oxide synthases. Cardiovascular research, 1999. 43(3): p. 521-31.*
12. *Knowles, R.G. and S. Moncada, Nitric oxide synthases in mammals. The Biochemical journal, 1994. 298 (Pt 2): p. 249-58.*
13. *Drew, B. and C. Leeuwenburgh, Aging and the role of reactive nitrogen species. Annals of the New York Academy of Sciences, 2002. 959: p. 66-81.*

14. *Nathan, C., Role of iNOS in human host defense. Science, 2006. 312(5782): p. 1874-5; author reply 1874-5.*
15. *Coggins, M.P. and K.D. Bloch, Nitric oxide in the pulmonary vasculature. Arteriosclerosis, thrombosis, and vascular biology, 2007. 27(9): p. 1877-85.*
16. *Ballou, D.P., et al., Revisiting the kinetics of nitric oxide (NO) binding to soluble guanylate cyclase: the simple NO-binding model is incorrect. Proceedings of the National Academy of Sciences of the United States of America, 2002. 99(19): p. 12097-101.*
17. *Bae, Y.S., et al., Regulation of reactive oxygen species generation in cell signaling. Molecules and cells, 2011. 32(6): p. 491-509.*
18. *Toledano, M.B., A.G. Planson, and A. Delaunay-Moisan, Reining in H(2)O(2) for safe signaling. Cell, 2010. 140(4): p. 454-6.*
19. *Bedard, K. and K.H. Krause, The NOX family of ROS-generating NADPH oxidases: physiology and pathophysiology. Physiological reviews, 2007. 87(1): p. 245-313.*
20. *Irani, K., et al., Mitogenic signaling mediated by oxidants in Ras-transformed fibroblasts. Science, 1997. 275(5306): p. 1649-52.*
21. *Beckman, J.S. and W.H. Koppenol, Nitric oxide, superoxide, and peroxynitrite: the good, the bad, and ugly. The American journal of physiology, 1996. 271(5 Pt 1): p. C1424-37.*
22. *Abello, N., et al., Protein tyrosine nitration: selectivity, physicochemical and biological consequences, denitration, and proteomics methods for the identification of tyrosine-nitrated proteins. Journal of proteome research, 2009. 8(7): p. 3222-38.*
23. *Hess, D.T., et al., Protein S-nitrosylation: purview and parameters. Nature reviews. Molecular cell biology, 2005. 6(2): p. 150-66.*
24. *Jaffrey, S.R., et al., Protein S-nitrosylation: a physiological signal for neuronal nitric oxide. Nature cell biology, 2001. 3(2): p. 193-7.*
25. *Yakovlev, V.A., et al., Tyrosine nitration of IkappaBalpha: a novel mechanism for NF-kappaB activation. Biochemistry, 2007. 46(42): p. 11671-83.*
26. *Hausladen, A., A.J. Gow, and J.S. Stamler, Nitrosative stress: metabolic pathway involving the flavohemoglobin. Proceedings of the National Academy of Sciences of the United States of America, 1998. 95(24): p. 14100-5.*
27. *Stamler, J.S. and A. Hausladen, Oxidative modifications in nitrosative stress. Nature structural biology, 1998. 5(4): p. 247-9.*
28. *Corcoran, A. and T.G. Cotter, Redox regulation of protein kinases. The FEBS journal, 2013. 280(9): p. 1944-65.*

29. *Denu, J.M. and K.G. Tanner, Redox regulation of protein tyrosine phosphatases by hydrogen peroxide: detecting sulfenic acid intermediates and examining reversible inactivation. Methods in enzymology, 2002. 348: p. 297-305.*
30. *Rhee, S.G., et al., Hydrogen peroxide: a key messenger that modulates protein phosphorylation through cysteine oxidation. Science's STKE : signal transduction knowledge environment, 2000. 2000(53): p. pe1.*
31. *Meng, T.C., T. Fukada, and N.K. Tonks, Reversible oxidation and inactivation of protein tyrosine phosphatases in vivo. Molecular cell, 2002. 9(2): p. 387-99.*
32. *Barrett, D.M., et al., Inhibition of protein-tyrosine phosphatases by mild oxidative stresses is dependent on S-nitrosylation. The Journal of biological chemistry, 2005. 280(15): p. 14453-61.*
33. *Sturla, L.M., et al., Requirement of Tyr-992 and Tyr-1173 in phosphorylation of the epidermal growth factor receptor by ionizing radiation and modulation by SHP2. The Journal of biological chemistry, 2005. 280(15): p. 14597-604.*
34. *Kim, J.E. and S.R. Tannenbaum, S-Nitrosation regulates the activation of endogenous procaspase-9 in HT-29 human colon carcinoma cells. The Journal of biological chemistry, 2004. 279(11): p. 9758-64.*
35. *Kim, Y.M., et al., Nitric oxide prevents tumor necrosis factor alpha-induced rat hepatocyte apoptosis by the interruption of mitochondrial apoptotic signaling through S-nitrosylation of caspase-8. Hepatology, 2000. 32(4 Pt 1): p. 770-8.*
36. *Torok, N.J., et al., Nitric oxide inhibits apoptosis downstream of cytochrome C release by nitrosylating caspase 9. Cancer research, 2002. 62(6): p. 1648-53.*
37. *Gallo, O., et al., Role of nitric oxide in angiogenesis and tumor progression in head and neck cancer. Journal of the National Cancer Institute, 1998. 90(8): p. 587-96.*
38. *Ridnour, L.A., et al., Molecular mechanisms for discrete nitric oxide levels in cancer. Nitric oxide : biology and chemistry / official journal of the Nitric Oxide Society, 2008. 19(2): p. 73-6.*
39. *Bergers, G. and L.E. Benjamin, Tumorigenesis and the angiogenic switch. Nature reviews. Cancer, 2003. 3(6): p. 401-10.*
40. *Mollace, V., et al., Modulation of prostaglandin biosynthesis by nitric oxide and nitric oxide donors. Pharmacological reviews, 2005. 57(2): p. 217-52.*
41. *Wang, Y., et al., Biological activity of bevacizumab, a humanized anti-VEGF antibody in vitro. Angiogenesis, 2004. 7(4): p. 335-45.*

42. *Patumraj, S., et al., Combined effects of curcumin and vitamin C to protect endothelial dysfunction in the iris tissue of STZ-induced diabetic rats. Clinical hemorheology and microcirculation, 2006. 35(4): p. 481-9.*
43. *Plummer, S.M., et al., Inhibition of cyclo-oxygenase 2 expression in colon cells by the chemopreventive agent curcumin involves inhibition of NF-kappaB activation via the NIK/IKK signalling complex. Oncogene, 1999. 18(44): p. 6013-20.*
44. *Cardnell, R.J. and R.B. Mikkelsen, Nitric oxide synthase inhibition enhances the antitumor effect of radiation in the treatment of squamous carcinoma xenografts. PloS one, 2011. 6(5): p. e20147.*
45. *Hibbs, J.B., Jr., et al., Nitric oxide: a cytotoxic activated macrophage effector molecule. Biochemical and biophysical research communications, 1988. 157(1): p. 87-94.*
46. *Rao, C.V., et al., Nitric oxide-releasing aspirin and indomethacin are potent inhibitors against colon cancer in azoxymethane-treated rats: effects on molecular targets. Molecular cancer therapeutics, 2006. 5(6): p. 1530-8.*
47. *Ouyang, N., J.L. Williams, and B. Rigas, NO-donating aspirin inhibits angiogenesis by suppressing VEGF expression in HT-29 human colon cancer mouse xenografts. Carcinogenesis, 2008. 29(9): p. 1794-8.*
48. *Gao, L. and J.L. Williams, Nitric oxide-donating aspirin induces G2/M phase cell cycle arrest in human cancer cells by regulating phase transition proteins. International journal of oncology, 2012. 41(1): p. 325-30.*
49. *Williams, J.L., et al., NO-donating aspirin inhibits the activation of NF-kappaB in human cancer cell lines and Min mice. Carcinogenesis, 2008. 29(2): p. 390-7.*
50. *Chakrapani, H., et al., Synthesis, nitric oxide release, and anti-leukemic activity of glutathione-activated nitric oxide prodrugs: Structural analogues of PABA/NO, an anti-cancer lead compound. Bioorganic & medicinal chemistry, 2008. 16(5): p. 2657-64.*
51. *Shami, P.J., et al., Antitumor activity of JS-K [O2-(2,4-dinitrophenyl) 1-[(4-ethoxycarbonyl)piperazin-1-yl]diazen-1-ium-1,2-diolate] and related O2-aryl diazeniumdiolates in vitro and in vivo. Journal of medicinal chemistry, 2006. 49(14): p. 4356-66.*
52. *Nath, N., et al., JS-K, a nitric oxide-releasing prodrug, modulates ss-catenin/TCF signaling in leukemic Jurkat cells: evidence of an S-nitrosylated mechanism. Biochemical pharmacology, 2010. 80(11): p. 1641-9.*
53. *Huerta-Yepez, S., et al., Involvement of the TNF-alpha autocrine-paracrine loop, via NF-kappaB and YY1, in the regulation of tumor cell resistance to Fas-induced apoptosis. Clinical immunology, 2006. 120(3): p. 297-309.*

54. *Riganti, C., et al., Nitric oxide reverts the resistance to doxorubicin in human colon cancer cells by inhibiting the drug efflux. Cancer research, 2005. 65(2): p. 516-25.*
55. *Evig, C.B., et al., Endogenous production and exogenous exposure to nitric oxide augment doxorubicin cytotoxicity for breast cancer cells but not cardiac myoblasts. Nitric oxide : biology and chemistry / official journal of the Nitric Oxide Society, 2004. 10(3): p. 119-29.*
56. *Kurimoto, M., et al., Growth inhibition and radiosensitization of cultured glioma cells by nitric oxide generating agents. Journal of neuro-oncology, 1999. 42(1): p. 35-44.*
57. *Verovski, V.N., et al., Low-level doxorubicin resistance in P-glycoprotein-negative human pancreatic tumour PSN1/ADR cells implicates a brefeldin A-sensitive mechanism of drug extrusion. British journal of cancer, 1996. 73(5): p. 596-602.*
58. *Wink, D.A., et al., The reemergence of nitric oxide and cancer. Nitric oxide : biology and chemistry / official journal of the Nitric Oxide Society, 2008. 19(2): p. 65-7.*
59. *Vasquez-Vivar, J., B. Kalyanaraman, and P. Martasek, The role of tetrahydrobiopterin in superoxide generation from eNOS: enzymology and physiological implications. Free radical research, 2003. 37(2): p. 121-7.*
60. *Vasquez-Vivar, J., et al., Superoxide generation by endothelial nitric oxide synthase: the influence of cofactors. Proceedings of the National Academy of Sciences of the United States of America, 1998. 95(16): p. 9220-5.*
61. *Alp, N.J. and K.M. Channon, Regulation of endothelial nitric oxide synthase by tetrahydrobiopterin in vascular disease. Arteriosclerosis, thrombosis, and vascular biology, 2004. 24(3): p. 413-20.*
62. *Mitchell, B.M., A.M. Dorrance, and R.C. Webb, GTP cyclohydrolase 1 downregulation contributes to glucocorticoid hypertension in rats. Hypertension, 2003. 41(3 Pt 2): p. 669-74.*
63. *Zheng, J.S., et al., Gene transfer of human guanosine 5'-triphosphate cyclohydrolase I restores vascular tetrahydrobiopterin level and endothelial function in low renin hypertension. Circulation, 2003. 108(10): p. 1238-45.*
64. *Crabtree, M.J., et al., Ratio of 5,6,7,8-tetrahydrobiopterin to 7,8-dihydrobiopterin in endothelial cells determines glucose-elicited changes in NO vs. superoxide production by eNOS. American journal of physiology. Heart and circulatory physiology, 2008. 294(4): p. H1530-40.*
65. *Longo, D., et al., Influence of the 5-HTTLPR polymorphism and environmental risk factors in a Brazilian sample of patients with autism spectrum disorders. Brain research, 2009. 1267: p. 9-17.*

66. *Hasegawa, H., et al., Delivery of exogenous tetrahydrobiopterin (BH4) to cells of target organs: role of salvage pathway and uptake of its precursor in effective elevation of tissue BH4. Molecular genetics and metabolism, 2005. 86 Suppl 1: p. S2-10.*
67. *Sawabe, K., et al., Cellular accumulation of tetrahydrobiopterin following its administration is mediated by two different processes; direct uptake and indirect uptake mediated by a methotrexate-sensitive process. Molecular genetics and metabolism, 2005. 86 Suppl 1: p. S133-8.*
68. *Zielonka, J., J. Vasquez-Vivar, and B. Kalyanaraman, Detection of 2-hydroxyethidium in cellular systems: a unique marker product of superoxide and hydroethidine. Nature protocols, 2008. 3(1): p. 8-21.*
69. *Paige, J.S. and S.R. Jaffrey, Pharmacologic manipulation of nitric oxide signaling: targeting NOS dimerization and protein-protein interactions. Current topics in medicinal chemistry, 2007. 7(1): p. 97-114.*
70. *Fukumura, D., S. Kashiwagi, and R.K. Jain, The role of nitric oxide in tumour progression. Nature reviews. Cancer, 2006. 6(7): p. 521-34.*
71. *Lim, K.H., et al., Tumour maintenance is mediated by eNOS. Nature, 2008. 452(7187): p. 646-9.*
72. *Jarchau, T., et al., Cloning, expression, and in situ localization of rat intestinal cGMP-dependent protein kinase II. Proceedings of the National Academy of Sciences of the United States of America, 1994. 91(20): p. 9426-30.*
73. *Browning, D.D., et al., Nitric oxide activation of p38 mitogen-activated protein kinase in 293T fibroblasts requires cGMP-dependent protein kinase. The Journal of biological chemistry, 2000. 275(4): p. 2811-6.*
74. *Hood, J. and H.J. Granger, Protein kinase G mediates vascular endothelial growth factor-induced Raf-1 activation and proliferation in human endothelial cells. The Journal of biological chemistry, 1998. 273(36): p. 23504-8.*
75. *Suhasini, M., et al., Cyclic-GMP-dependent protein kinase inhibits the Ras/Mitogen-activated protein kinase pathway. Molecular and cellular biology, 1998. 18(12): p. 6983-94.*
76. *He, B. and G.F. Weber, Phosphorylation of NF-kappaB proteins by cyclic GMP-dependent kinase. A noncanonical pathway to NF-kappaB activation. European journal of biochemistry / FEBS, 2003. 270(10): p. 2174-85.*
77. *Cornwell, T.L., et al., Regulation of the expression of cyclic GMP-dependent protein kinase by cell density in vascular smooth muscle cells. Journal of vascular research, 1994. 31(6): p. 330-7.*
78. *Hou, Y., et al., An anti-tumor role for cGMP-dependent protein kinase. Cancer letters, 2006. 240(1): p. 60-8.*

79. *Deguchi, A., W.J. Thompson, and I.B. Weinstein, Activation of protein kinase G is sufficient to induce apoptosis and inhibit cell migration in colon cancer cells. Cancer research, 2004. 64(11): p. 3966-73.*
80. *Singer, A.L., et al., Cyclic nucleotide phosphodiesterases in neoplastic and nonneoplastic human mammary tissues. Cancer research, 1976. 36(1): p. 60-6.*
81. *Zhu, B., et al., Suppression of cyclic GMP-specific phosphodiesterase 5 promotes apoptosis and inhibits growth in HT29 cells. Journal of cellular biochemistry, 2005. 94(2): p. 336-50.*
82. *Goluboff, E.T., Exisulind, a selective apoptotic antineoplastic drug. Expert opinion on investigational drugs, 2001. 10(10): p. 1875-82.*
83. *Kwon, I.K., et al., Expression of cyclic guanosine monophosphate-dependent protein kinase in metastatic colon carcinoma cells blocks tumor angiogenesis. Cancer, 2008. 112(7): p. 1462-70.*
84. *Thompson, W.J., et al., Exisulind induction of apoptosis involves guanosine 3',5'-cyclic monophosphate phosphodiesterase inhibition, protein kinase G activation, and attenuated beta-catenin. Cancer research, 2000. 60(13): p. 3338-42.*
85. *Soh, J.W., et al., Cyclic GMP mediates apoptosis induced by sulindac derivatives via activation of c-Jun NH2-terminal kinase 1. Clinical cancer research : an official journal of the American Association for Cancer Research, 2000. 6(10): p. 4136-41.*
86. *Soh, J.W. and I.B. Weinstein, Role of COX-independent targets of NSAIDs and related compounds in cancer prevention and treatment. Progress in experimental tumor research, 2003. 37: p. 261-85.*
87. *Karayiannakis, A.J., et al., Expression patterns of beta-catenin in in situ and invasive breast cancer. European journal of surgical oncology : the journal of the European Society of Surgical Oncology and the British Association of Surgical Oncology, 2001. 27(1): p. 31-6.*
88. *Prasad, C.P., et al., Wnt signaling pathway in invasive ductal carcinoma of the breast: relationship between beta-catenin, dishevelled and cyclin D1 expression. Oncology, 2007. 73(1-2): p. 112-7.*
89. *Ozaki, S., et al., Alterations and correlations of the components in the Wnt signaling pathway and its target genes in breast cancer. Oncology reports, 2005. 14(6): p. 1437-43.*
90. *Ryo, A., et al., Pin1 regulates turnover and subcellular localization of beta-catenin by inhibiting its interaction with APC. Nature cell biology, 2001. 3(9): p. 793-801.*

91. Lustig, B. and J. Behrens, The Wnt signaling pathway and its role in tumor development. Journal of cancer research and clinical oncology, 2003. 129(4): p. 199-221.

92. Tsukamoto, A.S., et al., Expression of the int-1 gene in transgenic mice is associated with mammary gland hyperplasia and adenocarcinomas in male and female mice. Cell, 1988. 55(4): p. 619-25.

93. Nusse, R. and H.E. Varmus, Many tumors induced by the mouse mammary tumor virus contain a provirus integrated in the same region of the host genome. Cell, 1982. 31(1): p. 99-109.

94. Lane, T.F. and P. Leder, Wnt-10b directs hypermorphic development and transformation in mammary glands of male and female mice. Oncogene, 1997. 15(18): p. 2133-44.

95. Wong, S.C., et al., Expression of frizzled-related protein and Wnt-signalling molecules in invasive human breast tumours. The Journal of pathology, 2002. 196(2): p. 145-53.

96. Benhaj, K., K.C. Akcali, and M. Ozturk, Redundant expression of canonical Wnt ligands in human breast cancer cell lines. Oncology reports, 2006. 15(3): p. 701-7.

97. Watanabe, O., et al., Expression of twist and wnt in human breast cancer. Anticancer research, 2004. 24(6): p. 3851-6.

98. Nagahata, T., et al., Amplification, up-regulation and over-expression of DVL-1, the human counterpart of the Drosophila disheveled gene, in primary breast cancers. Cancer science, 2003. 94(6): p. 515-8.

99. Giles, R.H., J.H. van Es, and H. Clevers, Caught up in a Wnt storm: Wnt signaling in cancer. Biochimica et biophysica acta, 2003. 1653(1): p. 1-24.

100. Hanson, C.A. and J.R. Miller, Non-traditional roles for the Adenomatous Polyposis Coli (APC) tumor suppressor protein. Gene, 2005. 361: p. 1-12.

101. Zhang, Y.S., et al., Acetyl-11-keto-beta-boswellic acid (AKBA) inhibits human gastric carcinoma growth through modulation of the Wnt/beta-catenin signaling pathway. Biochimica et biophysica acta, 2013. 1830(6): p. 3604-15.

102. Li, H., et al., Naringin inhibits growth potential of human triple-negative breast cancer cells by targeting beta-catenin signaling pathway. Toxicology letters, 2013. 220(3): p. 219-28.

103. Ichim, C.V., Revisiting immunosurveillance and immunostimulation: Implications for cancer immunotherapy. Journal of translational medicine, 2005. 3(1): p. 8.

104. Grumbach, I.M., et al., A negative feedback mechanism involving nitric oxide and nuclear factor kappa-B modulates endothelial nitric oxide

synthase transcription. Journal of molecular and cellular cardiology, 2005. 39(4): p. 595-603.

105. *Park, S.W., et al., Tyrosine nitration on p65: a novel mechanism to rapidly inactivate nuclear factor-kappaB. Molecular & cellular proteomics : MCP, 2005. 4(3): p. 300-9.*
106. *Kelleher, Z.T., et al., NOS2 regulation of NF-kappaB by S-nitrosylation of p65. The Journal of biological chemistry, 2007. 282(42): p. 30667-72.*
107. *Chaturvedi, M.M., et al., NF-kappaB addiction and its role in cancer: 'one size does not fit all'. Oncogene, 2011. 30(14): p. 1615-30.*
108. *Croghan, G.A., et al., A study of paclitaxel, carboplatin, and bortezomib in the treatment of metastatic malignant melanoma: a phase 2 consortium study. Cancer, 2010. 116(14): p. 3463-8.*
109. *Yang, J., et al., Unphosphorylated STAT3 accumulates in response to IL-6 and activates transcription by binding to NFkappaB. Genes & development, 2007. 21(11): p. 1396-408.*
110. *Kunigal, S., et al., Stat3-siRNA induces Fas-mediated apoptosis in vitro and in vivo in breast cancer. International journal of oncology, 2009. 34(5): p. 1209-20.*
111. *Dien, J., et al., Signal transducers and activators of transcription-3 up-regulates tissue inhibitor of metalloproteinase-1 expression and decreases invasiveness of breast cancer. The American journal of pathology, 2006. 169(2): p. 633-42.*
112. *Ling, X. and R.B. Arlinghaus, Knockdown of STAT3 expression by RNA interference inhibits the induction of breast tumors in immunocompetent mice. Cancer research, 2005. 65(7): p. 2532-6.*
113. *Deguchi, A., et al., Vasodilator-stimulated phosphoprotein (VASP) phosphorylation provides a biomarker for the action of exisulind and related agents that activate protein kinase G. Molecular cancer therapeutics, 2002. 1(10): p. 803-9.*
114. *Yadav, V.R., et al., The role of chalcones in suppression of NF-kappaB-mediated inflammation and cancer. International immunopharmacology, 2011. 11(3): p. 295-309.*
115. *Li, H., R. Pamukcu, and W.J. Thompson, beta-Catenin signaling: therapeutic strategies in oncology. Cancer biology & therapy, 2002. 1(6): p. 621-5.*
116. *Thibeault, S., et al., S-nitrosylation of beta-catenin by eNOS-derived NO promotes VEGF-induced endothelial cell permeability. Molecular cell, 2010. 39(3): p. 468-76.*

117. Liu, Y.C., et al., Blockade of JAK2 activity suppressed accumulation of beta-catenin in leukemic cells. Journal of cellular biochemistry, 2010. 111(2): p. 402-11.

118. Di Leonardo, A., et al., DNA damage triggers a prolonged p53-dependent G1 arrest and long-term induction of Cip1 in normal human fibroblasts. Genes & development, 1994. 8(21): p. 2540-51.

119. Aliouat-Denis, C.M., et al., p53-independent regulation of p21Waf1/Cip1 expression and senescence by Chk2. Molecular cancer research : MCR, 2005. 3(11): p. 627-34.

120. Aguero, M.F., et al., Phenoxodiol, a novel isoflavone, induces G1 arrest by specific loss in cyclin-dependent kinase 2 activity by p53-independent induction of p21WAF1/CIP1. Cancer research, 2005. 65(8): p. 3364-73.

121. Munoz-Alonso, M.J., et al., p21Cip1 and p27Kip1 induce distinct cell cycle effects and differentiation programs in myeloid leukemia cells. The Journal of biological chemistry, 2005. 280(18): p. 18120-9.

122. Masgras, I., A. Rasola, and P. Bernardi, Induction of the permeability transition pore in cells depleted of mitochondrial DNA. Biochimica et biophysica acta, 2012. 1817(10): p. 1860-6.

123. Romanov, V.S., et al., p21(Waf1) is required for cellular senescence but not for cell cycle arrest induced by the HDAC inhibitor sodium butyrate. Cell cycle, 2010. 9(19): p. 3945-55.

124. Duhe, R.J., et al., Nitric oxide and thiol redox regulation of Janus kinase activity. Proceedings of the National Academy of Sciences of the United States of America, 1998. 95(1): p. 126-31.

125. Mamoon, N.M., et al., Multiple cysteine residues are implicated in Janus kinase 2-mediated catalysis. Biochemistry, 2007. 46(51): p. 14810-8.

126. Pickert, G., et al., Inhibition of GTP cyclohydrolase attenuates tumor growth by reducing angiogenesis and M2-like polarization of tumor associated macrophages. International journal of cancer. Journal international du cancer, 2013. 132(3): p. 591-604.

127. Chen, L., et al., Roles of tetrahydrobiopterin in promoting tumor angiogenesis. The American journal of pathology, 2010. 177(5): p. 2671-80.

128. Guzik, T.J., et al., Mechanisms of increased vascular superoxide production in human diabetes mellitus: role of NAD(P)H oxidase and endothelial nitric oxide synthase. Circulation, 2002. 105(14): p. 1656-62.

129. Landmesser, U., et al., Oxidation of tetrahydrobiopterin leads to uncoupling of endothelial cell nitric oxide synthase in hypertension. The Journal of clinical investigation, 2003. 111(8): p. 1201-9.

130. *Maier, W., et al., Tetrahydrobiopterin improves endothelial function in patients with coronary artery disease. Journal of cardiovascular pharmacology, 2000. 35(2): p. 173-8.*
131. *Cosentino, F., et al., Chronic treatment with tetrahydrobiopterin reverses endothelial dysfunction and oxidative stress in hypercholesterolaemia. Heart, 2008. 94(4): p. 487-92.*
132. *Porkert, M., et al., Tetrahydrobiopterin: a novel antihypertensive therapy. Journal of human hypertension, 2008. 22(6): p. 401-7.*
133. *Heitzer, T., et al., Tetrahydrobiopterin improves endothelium-dependent vasodilation by increasing nitric oxide activity in patients with Type II diabetes mellitus. Diabetologia, 2000. 43(11): p. 1435-8.*
134. *Hyland, K., et al., Tetrahydrobiopterin and biogenic amine metabolism in the hph-1 mouse. Journal of neurochemistry, 1996. 67(2): p. 752-9.*
135. *Khoo, J.P., et al., Pivotal role for endothelial tetrahydrobiopterin in pulmonary hypertension. Circulation, 2005. 111(16): p. 2126-33.*
136. *Itzkowitz, S.H. and X. Yio, Inflammation and cancer IV. Colorectal cancer in inflammatory bowel disease: the role of inflammation. American journal of physiology. Gastrointestinal and liver physiology, 2004. 287(1): p. G7-17.*
137. *Seril, D.N., J. Liao, and G.Y. Yang, Colorectal carcinoma development in inducible nitric oxide synthase-deficient mice with dextran sulfate sodium-induced ulcerative colitis. Molecular carcinogenesis, 2007. 46(5): p. 341-53.*
138. *Ross, G.R., et al., Nitrotyrosylation of Ca2+ channels prevents c-Src kinase regulation of colonic smooth muscle contractility in experimental colitis. The Journal of pharmacology and experimental therapeutics, 2007. 322(3): p. 948-56.*
139. *Lundberg, J.O. and E. Weitzberg, NO generation from inorganic nitrate and nitrite: Role in physiology, nutrition and therapeutics. Archives of pharmacal research, 2009. 32(8): p. 1119-26.*
140. *McNamee, E.N., et al., Interleukin 37 expression protects mice from colitis. Proceedings of the National Academy of Sciences of the United States of America, 2011. 108(40): p. 16711-6.*
141. *Van Crombruggen, K., et al., Influence of soluble guanylate cyclase inhibition on inflammation and motility disturbances in DSS-induced colitis. European journal of pharmacology, 2008. 579(1-3): p. 337-49.*
142. *Schmidt, K., et al., Tetrahydrobiopterin protects soluble guanylate cyclase against oxidative inactivation. Molecular pharmacology, 2012. 82(3): p. 420-7.*
143. *Fernhoff, N.B., et al., Heme-assisted S-nitrosation desensitizes ferric soluble guanylate cyclase to nitric oxide. The Journal of biological chemistry, 2012. 287(51): p. 43053-62.*

144. Green, C.L., et al., Dextran sodium sulfate-induced colitis reveals nicotinic modulation of ion transport via iNOS-derived NO. American journal of physiology. Gastrointestinal and liver physiology, 2004. 287(3): p. G706-14.
145. Ahluwalia, A., et al., Antiinflammatory activity of soluble guanylate cyclase: cGMP-dependent down-regulation of P-selectin expression and leukocyte recruitment. Proceedings of the National Academy of Sciences of the United States of America, 2004. 101(5): p. 1386-91.
146. Kaler, A., Health interventions and the persistence of rumour: the circulation of sterility stories in African public health campaigns. Social science & medicine, 2009. 68(9): p. 1711-9.
147. Hyun, E., et al., Contribution of bone marrow-derived cells to the pro-inflammatory effects of protease-activated receptor-2 in colitis. Inflammation research : official journal of the European Histamine Research Society ... [et al.], 2010. 59(9): p. 699-709.
148. Waldner, M.J., S. Foersch, and M.F. Neurath, Interleukin-6--a key regulator of colorectal cancer development. International journal of biological sciences, 2012. 8(9): p. 1248-53.
149. Funakoshi, T., et al., A novel NF-kappaB inhibitor, dehydroxymethylepoxyquinomicin, ameliorates inflammatory colonic injury in mice. Journal of Crohn's & colitis, 2012. 6(2): p. 215-25.
150. Burton, B.K., et al., Tetrahydrobiopterin therapy for phenylketonuria in infants and young children. The Journal of pediatrics, 2011. 158(3): p. 410-5.
151. Cunningham, A., et al., Recommendations for the use of sapropterin in phenylketonuria. Molecular genetics and metabolism, 2012. 106(3): p. 269-76.
152. Xu, J., et al., Proteasome-dependent degradation of guanosine 5'-triphosphate cyclohydrolase I causes tetrahydrobiopterin deficiency in diabetes mellitus. Circulation, 2007. 116(8): p. 944-53.
153. Antoniades, C., et al., Induction of vascular GTP-cyclohydrolase I and endogenous tetrahydrobiopterin synthesis protect against inflammation-induced endothelial dysfunction in human atherosclerosis. Circulation, 2011. 124(17): p. 1860-70.
154. Anastasiadis, P.Z., et al., Mitogenic effects of tetrahydrobiopterin in PC12 cells. Molecular pharmacology, 1996. 49(1): p. 149-55.
155. Goel, S., et al., Normalization of the vasculature for treatment of cancer and other diseases. Physiological reviews, 2011. 91(3): p. 1071-121.